TÉCNICO LISBOA

Microfluidic isolation and characterisation of bladder cancer cells from urine for early and non-invasive diagnosis of bladder cancer

Catarina Filipa Matoso Abreu

Thesis to obtain the Master of Science Degree in

Biological Engineering

Supervisor(s): Dr. Marta Isabel Abreu Oliveira
Prof. Susana Isabel Pinheiro Cardoso de Freitas

Examination committee

Chairperson: Prof. Gabriel António Amaro Monteiro

Supervisor: Dr. Marta Isabel Abreu Oliveira

Members of the committee: Dr. Virginia Chu

October 2016

Acknowledgments

Firstly, I would like to thank Dr. Marta Oliveira, from the International Iberian Nanotechnology Laboratory (INL), for introducing and accepting me in this project and in the group. I am very grateful for all the support and guidance through the past months and for constant supervision even when she could not be physically present. For all the advices, not only regarding this project but also concerning my professional future and personal life. I also thank Dr. Lorena Diéguez for supervising my work and supporting me in this project. Even though, in paper, she was not recognised as one of my supervisors, her support was crucial and I learnt a lot under her orientation. In spite of the fact that this master internship has ended, this partnership will still continue.

I would like to express my gratitude to professor Susana Cardoso de Freitas for her support and guidance ever since I attended her classes in Techniques of Micro and Nanofabrication. This course provided me important tools and knowledge in nanotechnology as well as clean-room contact. This experience enhanced my will to pursue in this field through the incorporation of nanotechnology in health, which ultimately brought me in contact with INL.

Also from INL, I would like acknowledge several people who have played an important role in this project and have supported me during the entire process. Manuel Neves for guiding me in the laboratory, particularly in the first months, when I had no previous experience in mammalian cell culture and for all his advice and motivational speeches when things did not work out so well. I would also like to recognise Alexandre Chícharo, Silvina Samy, Joana Carvalho and Elisabete Fernandes, from the microfluidics laboratory, for all the fruitful discussions, good working environment, and friendship above all else. During my project, I came in contact with the clean-room for the fabrication of the microfluidic masters, for which I need to thank Dr. João Gaspar for the help with AutoCAD, as well as all the clean-room staff for guiding me through the entire fabrication process. I also want to acknowledge professor Paulo Freitas, Director-general of INL, for all the help and support provided in this project.

This work was only possible with the collaboration of the department of Urology of Centro Hospitalar do Porto-Hospital Geral de Santo António (CHP-HSA). Within this department, I would like to acknowledge Dr. Avelino Fraga, service director, for establishing the project partnership between CHP-HSA and INL, without his support we could have never performed the validation of our platform without access to clinical samples. I also want to extent thanks to Dr. Manuel Oliveira, for authorising my presence in the operating room for the visualisation of the tumour resections. Without his help, it would not be possible to collect the bladder wash and urine samples and perform the comparison between the medical diagnosis and our results.

I would like to acknowledge my friends, particularly Ana Rita Gomes, Sofia Macedo, Cátia Cardoso and Sofia Marques for all the support over the past months, particularly in hard times. I could always count with them.

I want to thank Diogo Fernandes for encouraging me in complicated times, for the emotional support and helpful discussions, for staying with me at INL when I had to work late and endless other things. This experience would have not been the same without him.

Last but not least, I would like to thank my family for all the support and for enduring all the financial costs associated with my education. Everything I have accomplished in life, I owe it to them, my parents, aunt, sister and grandparents. I could never put in words what they mean to me. This work is dedicated to them, particularly to an important person who is no longer present but always wished to see me achieve this milestone.

Abstract

Bladder cancer has one of the highest recurrence rates among cancers and requires lifelong surveillance. Cystoscopy and urine cytology are the “gold standard” for bladder cancer detection but have well-known limitations. Thus, new methodologies to early identify and characterise various bladder cancers and their true biological potential are urgently needed. In this work, rare tumour-associated cells from body fluids of bladder cancer patients were isolated and characterised, using a microfluidic device. Importantly, cell capture was based on deformability and size, so that all cancer cells were trapped, regardless of their phenotype. Results show that in spiking experiments of HT1376 bladder cancer cells with peripheral blood mononuclear cells, the microfluidic platform reached an isolation efficiency of around 50% and an enrichment ratio of 22. Additionally, bladder wash and urine samples collected from bladder cancer patients subjected to transurethral resection were immunostained in situ with the following identifying markers: pan-cytokeratin (epithelial), vimentin (mesenchymal), survivin (malignancy), DAPI (nucleus) and CD45 (leukocyte). Notably, survivin, pan-cytokeratin and vimentin positive cells were found both in bladder wash and urine samples of a patient diagnosed with high-grade non-invasive papillary urothelial carcinoma (stage Ta). In contrast, for another patient diagnosed with low-grade carcinoma, survivin could not be detected in any sample, and vimentin positive cells were only present in the bladder wash. Overall, our findings revealed the phenotypic diversity of cancer cells in body fluids, likely relevant for patient treatment and follow up and pave the way for the realisation of a liquid biopsy for bladder cancer.

Keywords: Bladder cancer, Microfluidics, Liquid biopsy, Urine, Survivin

Resumo

O cancro da bexiga apresenta uma das maiores taxas de recorrência, requerendo vigilância apertada. Métodos atuais de diagnóstico consistem em cistoscopia e citologia urinária, contudo apresentam severas limitações. Por conseguinte, novas metodologias capazes de identificar precocemente e caracterizar diversos tipos de cancro da bexiga assim como o seu potencial biológico são urgentemente necessários. Neste projeto, células cancerígenas provenientes de fluídos corporais de pacientes com cancro da bexiga foram isoladas e caracterizadas através uma plataforma microfluídica, de acordo com o seu tamanho e deformabilidade, independentemente do seu fenótipo. Resultados mostram que em controlos de populações mistas de células tumorais da bexiga HT1376 e células mononucleares do sangue periférico, a plataforma obteve um rendimento de captura de aproximadamente 50% e um fator de concentração de 22. Adicionalmente, amostras de lavado vesical e urina de pacientes com cancro de bexiga submetidos a ressecção tumoral foram avaliadas por imunocitoquímica na plataforma com os seguintes marcadores: pancitoqueratina (epitelial), vimentina (mesenquimal), survivina (malignidade), DAPI (nuclear) e CD45 (leucócito). Células expressando survivina, pancitoqueratina e vimentina foram detetadas em amostras de lavado vesical e urina de um paciente diagnosticado carcinoma urotelial papilar de alto grau (estadio Ta). Por sua vez, para outro paciente com carcinoma de baixo grau, survivina não foi detetada em nenhuma amostra e vimentina apenas foi expressa em células de lavado vesical. Resumindo, estes resultados revelaram a existência de diversidade fenotípica em células cancerígenas de fluídos corporais, potencialmente relevante para definição de tratamento e monitorização de cancro da bexiga através de biopsia líquida.

Palavras-chave: Cancro da Bexiga, Microfluídica, Biopsia Líquida, Urina, Survivina

Contents

List of Tables

List of Figures

List of Acronyms

µTAS	miniaturized total analysis systems
BSA	Bovine Serum Albumin
CA	Cell aggregate
CIS	Carcinoma *in situ*
CK	Cytokeratin
CSC	Cancer stem cell
CTCs	Circulating tumour cells
DAPI	4',6-Diamidino-2-Phenylindole
DI	Deionized
DRIE	Deep Reactive Ion Etching
ELISA	enzyme-linked immunosorbent assay
EMT	epithelial-to-mesenchymal transition
EpCAM	Epithelial Cell Adhesion Molecule
EtOH	Ethanol
FACS	Fluorescence activated cell sorting
FBS	Fetal Bovine Serum
FDA	Food and Drug Administration
FISH	Fluorescence in Situ Hybridisation
HC	Haematologic cell
hCFHrp	human complement factor-H related protein
ICDC	Irregularly shaped cells with dense cytoplasm
ICTC	Irregularly shaped cells with translucent cytoplasm
IPA	Isopropyl alcohol
MEMS	micro-electromechanical systems
MET	Mesenchymal-to-epithelial transition
MIBC	Muscle invasive bladder cancers
mRNA	messenger RNA
NMIBC	non-muscle invasive bladder cancers
NMP	Nuclear matrix proteins
Pan-CK	Pan-cytokeratin
PBMCs	Peripheral Blood Mononuclear Cells
PBS	Phosphate Buffered Saline
PDMS	Polydimethylsiloxane
PEO	poly-ethylene-oxide
PFS	polytetrafluorofluoroethylene organosilane
PPO	polypropyleneoxide
PR	Photoresist
PUNLMP	papillary urothelial malignancy of low potential
qRT-PCR	quantitative reverse transcriptase-PCR

RCDC	Round cells with defined cytoplasm
SAMs	Self-assembled monolayers
TNM	Tumour-Node-Metastasis
TURBT	transurethral resection of bladder tumour

1. Introduction

1.1. Bladder Cancer: Background and Clinical Practice

1.1.1. Disease Incidence

Bladder cancer is the most common malignancy of the urinary tract. In 2015, it was the 5th most common type of cancer in Europe and in the United States[1]. This year, an estimated 76,960 new cases are expected to be diagnosed in the United States, along with 16,390 deaths[2] (Figure 1.1). Men are nearly three times more affected than women.

	Common Types of Cancer	Estimated New Cases 2016	Estimated Deaths 2016
1.	Breast Cancer (Female)	246,660	40,450
2.	Lung and Bronchus Cancer	224,390	158,080
3.	Prostate Cancer	180,890	26,120
4.	Colon and Rectum Cancer	134,490	49,190
5.	**Bladder Cancer**	**76,960**	**16,390**
6.	Melanoma of the Skin	76,380	10,130
7.	Non-Hodgkin Lymphoma	72,580	20,150
8.	Thyroid Cancer	64,300	1,980
9.	Kidney and Renal Pelvis Cancer	62,700	14,240
10.	Leukemia	60,140	24,400

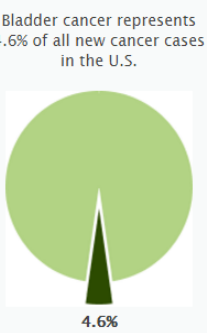

Figure 1.1. Most common types of cancer in the United States and estimated new cases and deaths for 2016 (adapted from seer.cancer.gov)[2]

In Europe and North America, over 90% of bladder cancers are the transitional cell type, also known as urothelial cell carcinoma. This malignant tumour arises from the urothelial (transitional) cells lining the inside of the bladder, which are capable of changing their shape according to the fluid occupancy. The median age at the time of diagnosis is 73 and although 11% of the tumours have already spread to distant sites, the majority (around 85%) are confined to the bladder (Figure 1.2).

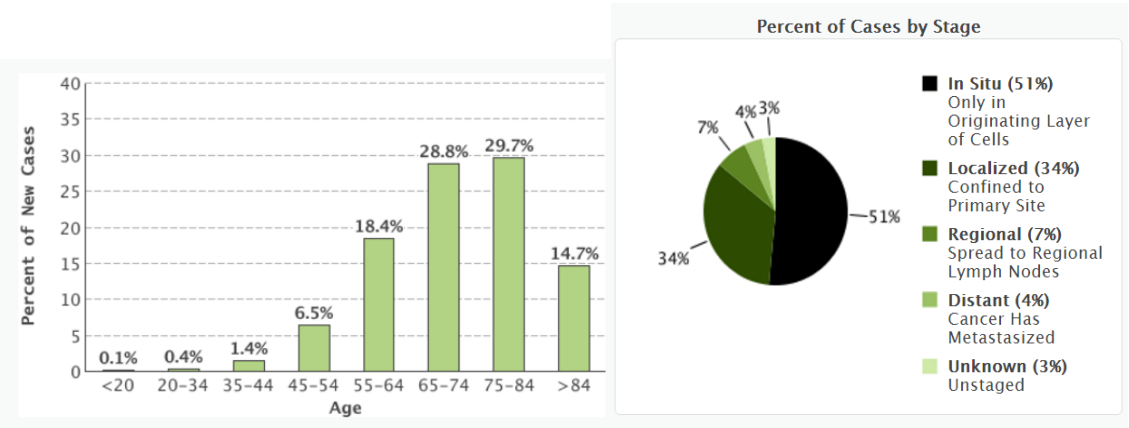

Figure 1.2. Percentage of new cases by age and stage for citizens of the United States in 2015 (adapted from seer.cancer.gov)[2]

1.1.2. Staging and Grading

Urothelial cell carcinomas are staged according to the Tumour-Node-Metastasis (TNM) staging system[3], which assesses tumour aggressiveness in terms of bladder wall invasion extent (T-primary tumour, N-if it has spread to the lymph nodes, M-if it has metastasized). The different stages of bladder cancer classified according to the TNM system are schematically represented in Figure 1.3.a.

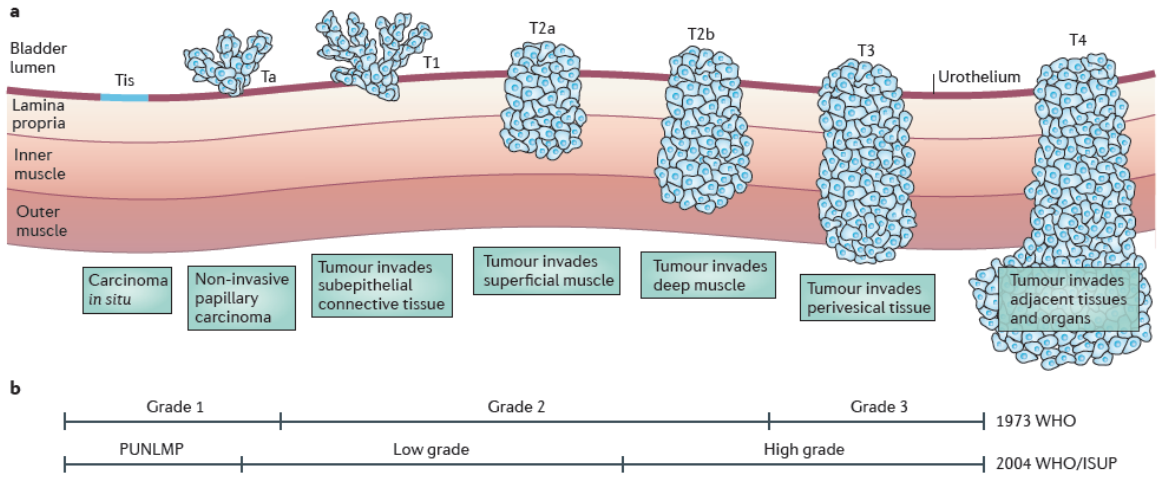

Figure 1.3. Bladder cancer grading and staging (Knowles, 2015)[4].
a) Bladder cancer staging according to the Tumour-Node-Metastasis (TNM) system for primary tumours. **b)** Grading according to the 1973 World Health Organization (WHO) and 2004 WHO/International Society of Urological Pathology (ISUP) criteria. The main difference is in the classification of papillary tumours, which are classified as grades 1,2 and 3 in the 1976 WHO system and as papillary urothelial malignancy of low potential (PUNLMP, equivalent to grade 1), low-grade papillary urothelial carcinoma or high-grade papillary urothelial carcinoma in the WHO/ISUP 2004 classification.

In addition to staging, primary tumours are also graded based on the degree of cellular differentiation and morphology when examined under a microscope. Grading consists in well differentiated (Grade 1), moderately differentiated (Grade 2) and poorly differentiated (Grade 3) according to the 1973 WHO system or papillary urothelial malignancy of low potential (PUNLMP), low-grade and high-grade according to the WHO/ISUP system (Figure 1.3.b). Grading is particularly important for the establishment of prognosis as Grade 3 or high-grade tumours are the most aggressive and most likely to become invasive.

Non-muscle invasive bladder tumours can be restricted to the urothelium or invade the sub-epithelial connective tissue. Within the first, two different stages are defined depending on the type of tumour: papillary carcinoma (stage Ta) and carcinoma *in situ* (CIS, stage Tis). Papillary carcinomas have the appearance of tiny mushrooms while CIS is a flat tumour. At time of diagnosis, the majority of bladder cancers (~60%) are staged as non-muscle invasive papillary tumours of low-grade (stage Ta, low-grade) whereas tumours that have invaded the sub-epithelial connective tissue but have not reached the muscle are mostly of high-grade (stage T1, high-grade). Figure 1.4 presents the approximate probability of the different stages and grades of non-muscle invasive bladder cancers (NMIBC) to recur in 5 years and the likelihood to progress to invasion.

Pathology	Approximate Probability of Recurrence in 5 years	Approximate Probability of Progression to Muscle Invasion
Ta, low grade	50%	Minimal
Ta, high grade	60%	Moderate
T1, low grade (rare)	50%	Moderate
T1, high grade	50%-70%	Moderate-High
Tis	50%-90%	High

.

Figure 1.4. Approximate probability of recurrence and progression for non-muscle invasive bladder cancers (adapted from NCCN guidelines, 2014)[5]

Commonly, NMIBC recur at a rate of 50% - 70% or progress to invasion (10% - 15%) with a five-year survival rate of 90%[4]. Thus, patient lifelong surveillance is required. Of note, carcinoma *in situ* has a higher probability of recurrence and presents high probability of progression to muscle invasion[5]. At diagnosis, only 20% are muscle-invasive bladder cancers (MIBC) and are mostly poorly differentiated (Stage T2-4, high grade). These cancers have a five-year survival rate of less than 50% and commonly progress to metastasis[4].

1.1.3. Early Disease

1.1.3.1. Diagnosis: a major challenge in bladder cancer management

Almost all cases of suspected bladder cancer are associated with haematuria (blood in the urine); other symptoms include increased frequency, urgency and pain or difficulty in the urination (dysuria). The current standard for diagnosis and follow-up of bladder cancer is cystoscopy examination coupled with urinary cytology. Pelvic computed tomography can also be considered in selected cases. The NCCN Clinical Practice Guidelines in Oncology (NCCN Guidelines) standard protocol for clinical evaluation of bladder cancer after clinical presentation is summarised in Figure 1.5. However, these different techniques have well-known limitations. Cystoscopy is invasive and expensive, may cause pain and discomfort and, most importantly, may not detect some flat lesions. On the other hand, cytology has low sensitivity in low-grade papillary tumours. Also, imaging technologies may not detect small tumours, therefore insufficient for early diagnosis. Hence, close monitoring, early detection of all lesions and more accurate methods are key for better management and significant reduction of patient cost, anxiety and morbidity.

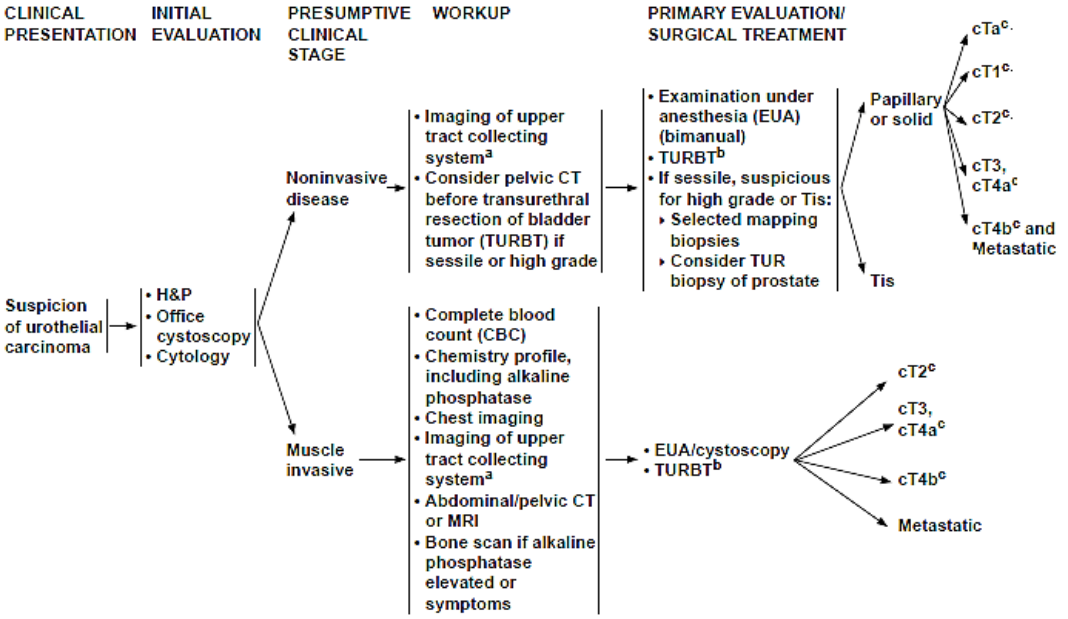

Figure 1.5. Standard protocol defined by the medical community for the diagnosis of bladder cancer (adapted from NCCN guidelines, 2014)[5].

Cystoscopy

Diagnosis is usually established by cystoscopic evaluation, prompted by haematuria or urinary track symptoms. Cystoscopy, which can be done in the doctor's office, consists in the insertion of a cystoscope through the urethra and into the bladder to check for abnormal cell growth. During this procedure, after emptying the bladder, saline buffer is infused through the cystoscope into the bladder to allow a clearer image (Figure 1.6.A). Tumours are usually identified through white light cystoscopy followed by resection of suspicions areas for histopathological diagnosis and local staging. White light cystoscopy has several limitations as referred above, including difficulty in detecting flat neoplasms and differentiating malignant from benign or inflammatory lesions.

Endoscopic treatment with transurethral resection of bladder tumour (TURBT) is the first-line treatment to diagnose, stage, and treat visible tumours. Evidence for a bladder mass previously diagnosed on local cystoscopy is the primary indication for TURBT. This minimally invasive surgical technique consists in the removal, in the operating room, of abnormal tissue and cauterisation of the wound using an instrument with a small wire loop that goes through the cystoscope (Figure 1.6.B). TURBT is not effective for CIS since this disease is often so diffuse and difficult to visualize that surgical removal is not feasible. Therefore, the main role of TURBT is to establish the diagnosis so that appropriate therapy can be defined, either being tumour resection and/or intravesical therapy. In the case of organ-confined MIBCs, which are much more likely to spread, treatment is generally more aggressive, consisting in either radical cystectomy (removal of the entire bladder) and/or radiation and chemotherapy[4].

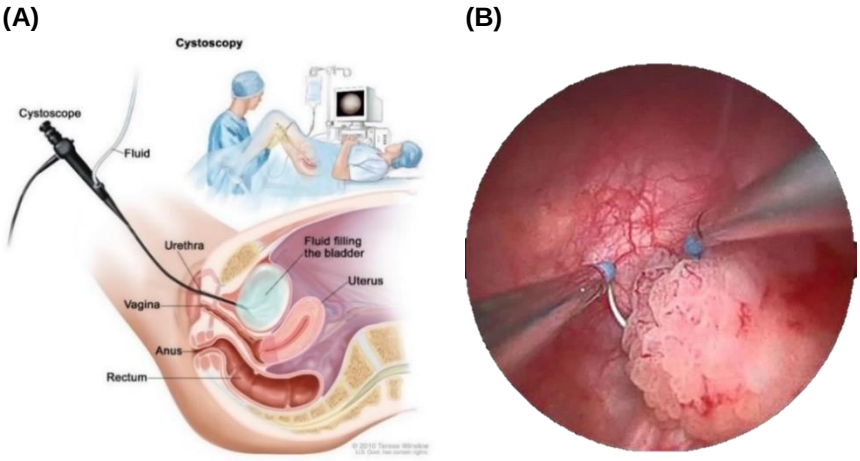

Figure 1.6. Conventional cystoscopy and TURBT procedure for bladder cancer diagnosis and treatment (adapted from www.cancer.gov)[6].

Lifelong surveillance is necessary for patients that have been diagnosed with bladder cancer due to its chronic nature. Even though the majority of bladder cancer patients are diagnosed with non-muscle invasive tumours and these can be completely resected, 50%-70% of these patients will develop tumour recurrence within 5 years, however late recurrence may occur, requiring active surveillance[7]. If the bladder is not removed, current monitoring protocols generally consist of regularly scheduled cystoscopic evaluations combined with urine cytology, performed every 3 months during the first 2 years of follow-up, twice a year during the 3rd and 4th years and annually after this period[8]. Since cystoscopy is a rather expensive and painful procedure, alternative approaches are being explored to improve patient quality of life as well as reducing healthcare costs.

Tumour Biopsy

Biopsies of any suspicious areas are crucial for a complete evaluation. Thus, resected tumours obtained by TURBT or random biopsies (from normal-looking areas) are sent for pathological assessment to help establish the diagnosis and to determine the tumour's extent. Solid tumour biopsy genotypes are often evaluated to add in therapeutic-decision making. However, tumours are highly dynamic and known to acquire mutations or alter their dormant state, especially after drug treatments. Therefore, at the given time point of the treatment scheme, a new biopsy should be collected in order the monitor the patient's response. Corroborating this, studies have shown that 38% of colorectal cancers expressing wild-type Kirsten rat sarcoma viral oncogene homolog (KRAS) develop mutations in response to anti-EGFR therapy, 6 months post-treatment[9]. Yet, multiple and successive tumour resections are not feasible. Also, the area sampled may not be representative of the tumour given its heterogeneous nature. Accordingly, an elegant study by Gerlinger *et al.* in 2012, demonstrated that primary tumours exhibit intra-tumour molecular heterogeneity which may differ from the molecular profile found in a biopsy from a metastatic site[10].

In bladder cancer, directed bladder biopsies to evaluate for the presence of CIS are indicated when no visible tumour is apparent on cystoscopy but urinary cytology is positive. In contrast, random biopsies are controversial. The likelihood of detecting CIS, particularly in low-risk tumours (low-grade papillary tumours and negative cytology), is extremely low (<2%)[11].

The invasive nature of solid tissue biopsy has several drawbacks for patients, such as increased risk of infection, expanded tumour implantation, additional bleeding or bladder perforation. Due to the inherent limitations, this method cannot be used for lifelong surveillance or treatment monitoring. Less invasive methods, such as cytology are more promising for early diagnosis and disease control.

Urine and Bladder Washes Cytology

The collection of voided urine for the search of exfoliated tumour cells is the basis of urocytologic examination and of various molecular assays. Since urine is contained in the bladder and thus in contact with areas of possible malignant neoplasia, detection of putative urologic cancers is favoured in this body fluid than in blood[7]. Voided urine or bladder wash cytology is the most established non-invasive method in the work-up of haematuria and follow-up of patients with bladder cancer history. It is also used as an adjunct to cystoscopy and involves the microscopic evaluation of exfoliated cells based on cytologic criteria using the Papanicolaou stain[7].

Cytology exhibits high specificity (>90%) and sensitivity for high-grade tumours (80% to 90%), however this sensitivity decreases significantly in well-differentiated (low-grade) tumours (20% to 50%)[12]. Several factors contribute for the poor results in urine cytology to detect cancer cells: only a small portion of urine is processed and from this sample only a fraction is used for analysis. Therefore, several cells may be lost during sample processing, reducing the chance of capturing a cancer cell. Second, and most importantly, cells from low-grade tumours are not normally shed due to their cohesive nature and their high cytomorphologic similarity to normal urothelial cells, hindering adequate characterisation.

In voided urine, two main cells types are expected to be found within normal cells: urothelial cells, such as basal, intermediate and superficial (umbrella) cells (Figure 1.7) and/or squamous cells, which shed from the distal urethra, vagina or squamous metaplasia.

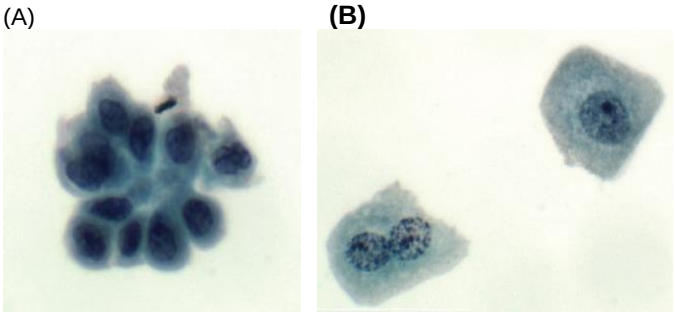

Figure 1.7. Normal urothelial cells present in urine (Sullivan, 2010)[12].
(A) Basal urothelial cells have moderate dense cytoplasm with well-defined borders. Nuclei are centrally-placed with small nucleoli and smooth nuclear contours. **(B)** Superficial urothelial cells (umbrella cells) have abundant granular cytoplasm with rounded and scalloped borders. Nuclei are large, round, frequently multiple, and centrally placed with prominent nucleoli and smooth nuclear borders. (Papanicolaou stain)

Urine samples of low-grade lesions are more cellular than normal, with cohesive or papillary fragments and subtle morphologic changes. This hinders the discrimination between low-grade urothelial neoplasia and hyperplasia (Figure 1.8). Neoplasia is the abnormal growth of tissue leading to as a tumour, whereas hyperplasia corresponds to an increase in cell number which is not associated with malignancy.

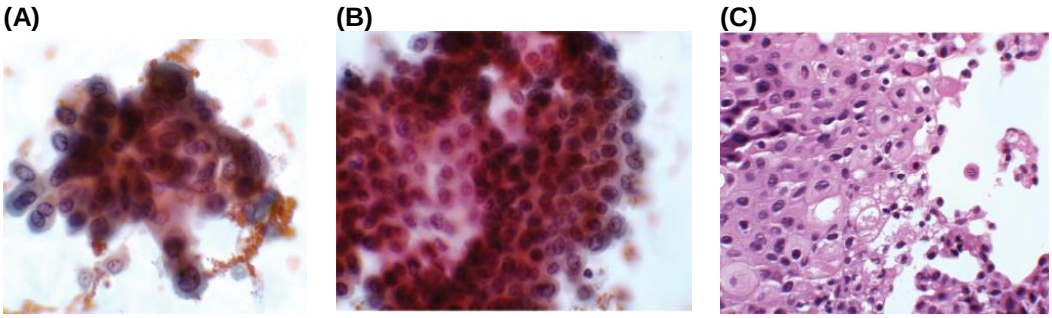

Figure 1.8. Low-grade urothelial neoplasia and hyperplasia (Sullivan, 2010)[12].
The distinction between both entities is difficult, even for an experienced cytopathologist. The nuclear changes in low-grade neoplasms (increased nuclear-to-cytoplasmic ratio, irregular nuclear membranes, visible nucleoli, disorganised growth pattern) may be subtle at a point that it is not possible to discriminate, as it occurs from A -C. (A-B, Papanicolaou stain; C, hematoxylin and eosin stain)

High-grade tumours usually show many atypical cells and loosely cohesive groups. These cells exhibit large nuclei or irregular shape and scant cytoplasm. Due to their obvious characteristics when compared to normal urothelial cells, the sensitivity of cytology is high for these tumours (Figure 1.9).

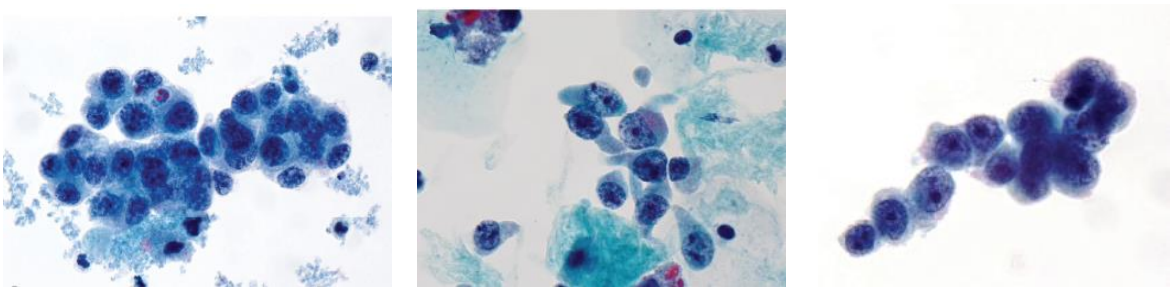

Figure 1.9. High-grade urothelial carcinoma (Sullivan, 2010)[12].
The cytologic changes are more evident in high-grade tumours which include a high nuclear-to-cytoplasmic ratio, dark bristly chromatin, irregular nuclear borders, prominent nucleoli in large single cells. Umbrella cells are typically absent. (Papanicolaou stain)

After urine collection, samples should be processed within 24 hours to avoid cellular degradation. The second morning voided urine is more appropriate for the cytopathological examination (contains enough preserved cells) as compared to first morning urine (contains more cells but viability may be compromised due to prolonged acidic milieu)[13]. One of the major obstacles of cytological evaluation of voided urine is that the origin of malignant cells cannot be identified. Cells may originate from the bladder or any other organ of the urinary tract, namely from the renal pelvis, ureter or urethra. To overcome this, bladder washes can be used since they contain cells solely present in the bladder urothelium.

Bladder washes are obtained during or prior to cystoscopy. First, the bladder should be emptied using a catheter, then 50-100 ml of saline solution is used to wash the bladder and finally recovered. This procedure is usually repeated three times. The bladder washing generally exfoliates large sheets of urothelium therefore, these samples present high cellular content and well preserved cells for analysis[13]. The general criteria for bladder wash cytopathology is summarised in Table 1.1 and is equivalent to urine cytology, as previously described.

Table 1.1. Bladder wash cytomorphologic criteria for bladder cancer diagnosis

Bladder Wash Sample	Cell Morphology	Diagnosis
Normal	Normal urothelial cells	Negative for malignancy
Reactive	Urothelial cells with alterations	
High-grade Urothelial Carcinoma	Loose urothelial cell groups, increased nuclear to cytoplasm ratio, irregular nucleus, hyperchromatic, pleomorphic with prominent nucleoli	High-grade Urothelial Carcinoma
Low-grade Urothelial Carcinoma / Hyperplasia	Papillary clusters with increased nuclear to cytoplasm ratio and atypical nucleus	Urothelial cell hyperplasia or low-grade urothelial carcinoma

Despite its non-invasive nature, current urine cytology has several limitations. As referred above, it is not sensitive for the detection of low-grade tumours and current cytologic criteria are not able to distinguish low-grade urothelial cells from hyperplasia. Moreover, cell characterisation is mainly based in morphological characteristics according to each pathologist evaluation. Thus, more specific and reliable alternatives are required and would be a significant advance. In this context, distinct urinary biomarkers that may assist in the early detection or identification of recurrent disease have been developed and will be discussed below.

1.1.3.2. Urine-based Liquid Biopsy: Non-invasive diagnosis

Liquid biopsy is the sampling and analysis of body fluids for tumourigenic markers to monitor disease progression. It is currently a hot topic in the field of diagnostics. Due to its less invasive nature when compared with solid tumour resection, it has gained the interest of the medical community and is becoming an attractive alternative to conventional diagnostic methods. The use of liquid biopsies offers the possibility of analysing, at different stages, disease evolution or treatment efficacy in a simple and easy way, without the need of a tissue sample. A continuous molecular characterisation of the patient's tumour it is of outmost relevance for disease screening, therapy tailoring and ultimately achieve personalised medicine.

The most common and frequently analysed liquid biopsy is blood. Several studies have shown that circulating tumour cells (CTCs), cell free nucleic acids and exosomes can be found in the blood of a cancer patient. Likewise, other body fluids such as pleural fluids, bone marrow, urine and saliva can also provide valuable information and new insights in resistance mechanisms and disease progression[14]. Since urine may be in contact with bladder neoplasms, many tests using voided urine have been designed to detect molecules that may be associated with primary tumour growth or invasion.

Commercially available biomarkers

Until now, only 6 tumour marker tests in urine have been cleared by the US Food and Drug Administration (FDA) for routine practice in patient care. However, according to the NCCN Clinical Practice Guidelines for bladder cancer, these tests are not recommended for routine diagnosis and clinical management due to the inexistence of prospective clinical trials proving their utility. Table 1.2 summarises the current FDA approved tests as well as their sensitivity and specificity.

Table 1.2. Summary of the current FDA approved markers for diagnosis and follow-up of Bladder cancer (adapted from Smith et al. 2013)[15].

Test	Marker Detected	Assay Type	Sensitivity (%)	Specificity (%)	Material for detection
BTA Stat	protein	Immunoassay	53-83	67-72	Urine
BTA Trak	protein	Sandwich ELISA	66-72	51-75	Urine
NMP22/BladderChek	protein	Sandwich ELISA	47-100	60-90	Urine
ImmunoCyt	protein	Immunocytochemistry	50-100	69-79	Urine exfoliated cells
UroVysion	chromosomal aberrations	FISH	36-100	89-98	Urine exfoliated cells

ELISA – enzyme-linked immunosorbent assay; FISH – Fluorescence in-situ hybridisation

ImmunoCyt

Cell surface mucins are complex glycoproteins expressed on the apical membrane surface of all mucosal epithelial cells. In malignant epithelial cells, including in bladder cancer, they are thought to influence cell adhesion and are clinical targets for tumour immunotherapy and serum tumour marker assays. ImmunoCyt is an immunocytofluorescence test developed in 1997 which detects bladder cancer-associated markers in exfoliated cells from voided urine using a cocktail of three fluorescently labelled monoclonal antibodies. The 19A211 antibody (red) detects the glycosylated form of the carcinoembryonic antigen while M344 and LDQ10 (green) detect mucin glycoproteins which are normally expressed in bladder cancer cells and not in normal cells. M344 appears to be quite sensitive for low stage tumour cells, being expressed in 71% of Ta-T1 tumours, as well as 19A211 which is found in 90% of Ta-T1 tumours[16].

The test takes approximately 2 hours from specimen filtration to slide preparation and samples are evaluated using a fluorescent microscope with dual filter for Fluorescein and Texas Red. A sample is considered positive if cells exhibiting red and/or green fluorescence are present (Figure 1.10)[16].

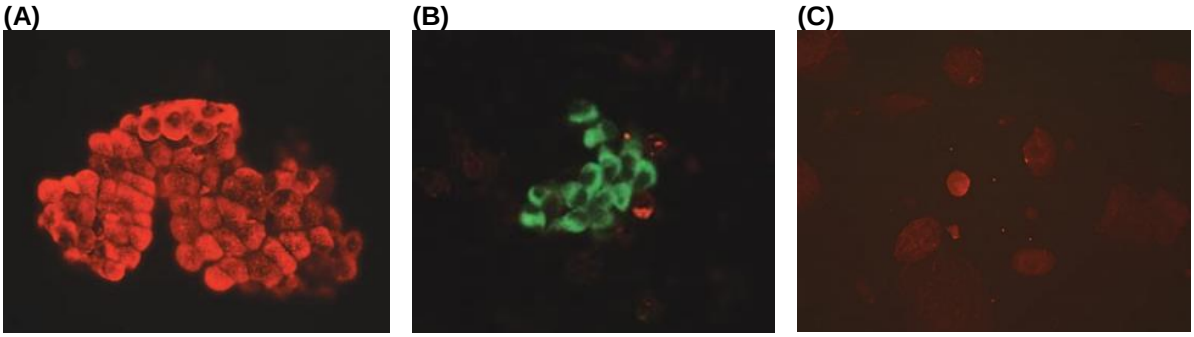

Figure 1.10. Voided urine exfoliated cells analysed with Immunocyt/uCyt+ test (adapted from Greene, 2006)[16].
(A) Positive test for 19A211 antigen exhibiting red fluorescence. **(B)** Positive test for M344 and LDQ10 antigens exhibiting green fluorescence. **(C)** Negative Immunocyt/uCyt+ test.

In a large patient cohort study done in 2005, urine cytology presented an overall specificity of 98% and sensitivity of 29%, whereas immunoCyt had a specificity of 62% and sensitivity of 74%. The

sensitivity of cytology for low malignant potential neoplasms, low and high-grade papillary carcinomas was 6, 18 and 53%, respectively, while when combined with ImmunoCyt reached 71, 79 and 93%. This indicates that the combined use of cytology and immunoCyt can improve the overall sensitivity to 84%. In this study, all carcinomas in situ were found by combining cytology and ImmunoCyt, while 50% had either negative or suspicious urinary cytology[17].

The high negative predictive value of 95% indicates that if the test is negative, patients undergoing a standard cystoscopy for history of bladder cancer are unlikely to have recurrent disease. Thus, in this group, the next control cystoscopy may be postponed. In contrast, the positive predictive value of ImmunoCyt was much lower (26%) than that of cytology (70%), which suggests that such false positivity would lead to unnecessary cystoscopies[17].

Altogether, ImmunoCyt is a useful urine-based adjunct to cytology for the detection of both low and high-grade tumours, including CIS and may be useful in cases with atypia. However, because this test must be interpreted by experienced cytopathologists in conjunction with urine cytology, the test cannot be used on site in the clinic. Also, at least 500 cells without fluorescent signal must be observed on the slide before the test is classified as negative. Low green fluorescent levels or high red background can also compromise the results (Figure 1.10.C)[16,17].

BTA-STAT and TRAK Tests

The BTA *stat* test is a one-step qualitative immunoassay that detects a bladder tumour-associated antigen in human urine and can be performed at point-of-care in 5 min with only five drops of voided urine sample. This antigen has been recognised as human complement factor-H related protein (hCFHrp) and is known to inhibit the complement pathway to cause cell lysis[18].

The assay uses two monoclonal antibodies to specifically detect the presence of hCFHrp. One antibody is conjugated to colloidal gold and serves as the reporter molecule if hCFHrp is present in the specimen, while the other is immobilized on the membrane to capture the protein. If the antigen-conjugate complexes are trapped by the capture antibody, a visible line is formed[19].

In an evaluation of the BTA stat test, out of 501 patients 26.5% had a bladder cancer recurrence at cystoscopy, of which BTA stat Test detected 53.4%. The overall sensitivities and specificities for the BTA stat Test and cytology were 56.0%, 19.2%, 85.7%, and 98.3%, respectively. The main issue regarding this test is the high rate of false positives obtained from urine infection and past BCG instillations. Out of 79 patients with positive BTA stat Test and negative cystoscopy, only 6 (7.6%) had recurrence at next scheduled follow-up cystoscopy. This high false positive rate indicates that the use of BTA stat should only be applied as a complement method to cystoscopy and not used for screening or early detection of bladder tumours. In case of positive test result but negative cystoscopy, urine cytology should be performed in order to evaluate the results. If urine cytology is positive then the patient should be further assessed, whereas patients with negative cytology might wait until the next scheduled cystoscopy[20].

The BTA TRAK is the quantitative enzyme immunoassay equivalent of BTA stat, however the results were not very promising even though it improved slightly the sensitivity of the BTA stat test. One of the main criticisms of the BTA TRAK test is the lack of consistency in the definition of the cut-off point, which varies from study to study[12,16,18].

There aren´t many studies conducted assessing the utilities of these tests, and the ones that exist date from the yearly 2000's, and it has been at downfall ever since. The main reasons are modest sensitivity for low-grade, low-stage tumours for which it merely reaches 50%, when compared to the 78% of cytology. Furthermore, the overall specificity is relatively low, partly because those proteins may be increased in urine of patients with non-neoplastic diseases such as inflammatory conditions[16].

Nuclear Matrix Protein 22 (NMP22) Test

Nuclear matrix proteins (NMP) are responsible for the support of the nuclear shape, DNA organization and coordination of DNA replication, transcription and gene expression. The NMP22 may be detected up to 25-fold greater concentration in tumour cells rather than normal urothelium. This protein is released from the cell nuclei during apoptosis and it can be detected in urine using the NMP22 test[12].

The NMP22 test consists in an enzyme-linked immunoassay that uses two monoclonal antibodies to measure the protein levels in urine. However, because this protein is also released from dead normal urothelial cells and many other non-malignant conditions of the urinary tract, such as stones, inflammation, infection, haematuria and even during cystoscopic evaluation due to handling of the cystoscope, it can lead to high false-positive rates[12,21].

A newer point-of-care version of the NMP22 test, named BladderChek, is an immunochromatographic assay that uses monoclonal antibodies in a lateral flow strip to detect the nuclear matrix protein NMP22 from four drops of freshly voided urine and provides a result within 30 minutes. Two different antibodies are used in the assay, one as a capture antibody and another as a reporter. If NMP22 is present in the urine at a concentration higher than 10 U/ml, it will interact with the primary antibody and can subsequently be visualized by binding to the secondary antibody. In one study, one hundred fresh urine samples were analysed with the BladderCheck test and compared with bladder washing and urine cytology in terms of sensitivity (65%, 76%, and 44%, respectively) and specificity (40%, 62%, and 78%, respectively). The authors concluded that the value of the test is limited by its low specificity, presumably due to frequent positive reaction in benign conditions. Therefore, exact selection of patients is essential to avoid unnecessary further invasive procedures[21].

Because of its low specificity, its use is not recommended by the FDA for primary detection of bladder cancer, only being advised to complement cystoscopic analysis.

UroVysion Test

Fluorescence in Situ Hybridisation (FISH) is a cytogenetic technique that uses fluorescent probes to visualise defined nucleic acid sequences in cellular preparations by hybridisation of complementary probe sequences[22]. In bladder cancer, the loss of the tumour suppressor gene (CDKN2A/p16) located in the 9p21 region is considered a critical event in the progression of the disease. Aneuploidy for chromosome 7 and 17 has been associated with the existence of more aggressive and invasive bladder tumours[23].

The UroVysion test is a multi-target FISH assay that detects aneuploidy of chromosomes 3, 7 and 17, and loss of the 9p21 band in exfoliated cells from urine specimens through fluorescent microscopy. In a study performed in 2002 by Placer *et al.,* FISH test showed great promise in the

detection of low-grade superficial tumours with a sensitivity rate of 53.3% compared to the 25% obtained by cytology in grade 1 tumours. Urovysion was unable to detect seven low-grade Ta stage tumours, however it was able to identify all the high-grade/stage tumours whereas cytology only identified 11% of them. The global specificities of FISH and cytology were very similar (85.3% and 86.1%) and in the five cases that yield false-positive result for FISH, one year after follow-up, recurrence was detected in one of the patients. Moreover, some studies have shown that FISH is able to detect neoplastic cells several months before it is visible by cystoscopy[23].

In a prospective study conducted in 2010, a study population of 216 patients underwent cystoscopy for cancer diagnosis or surveillance and obtained results were compared with the clinical usefulness of the UroVysion assay. In patients with atypical cytology and obvious tumour on cystoscopy the assay was unnecessary, but it was helpful in those with ambivalent or negative cystoscopic assessment (Figure 1.11). In patients with equivocal lesions or negative cystoscopy, the FISH assay was positive in all high-grade tumours with a positive predictive value of 50% and 10%, respectively. In this case there were no false-negative findings. The FISH assay proved to be helpful in detecting urothelial carcinoma in patients with atypical cytology or ambiguous or negative cystoscopy, with a sensitivity of 100% and a specificity that ranged from 60% to 100%[24].

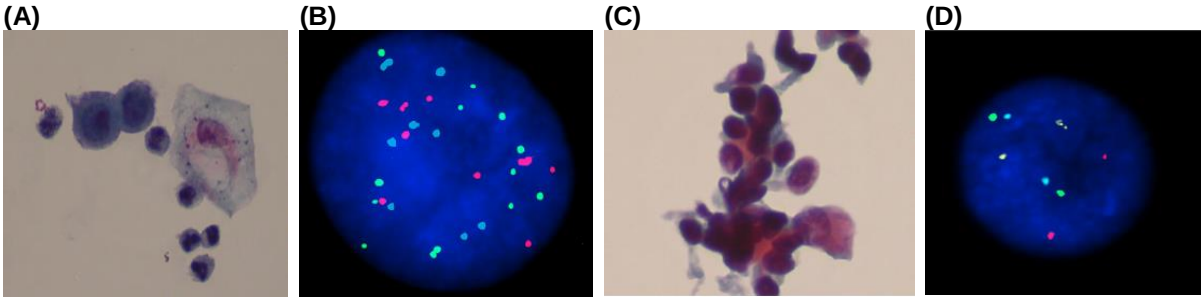

Figure 1.11. Application of the Urovysion test in the analysis of atypical urine cytology (Schlomer *et al. 2010*)[24]
Urovysion test applied in two cases of atypical cytology. Atypical cells present in urine sediment (A) were positive for FISH assay, indicating the presence of tumour cells. Sample (C) was also accessed, however, the multi-target test was negative for the identification of tumour cells.

In summary, the Urovysion test appears to have high specificity for the detection of high-grade tumours and the ability to detect tumour recurrence prior to cystoscopy evaluation. The major limitations of the assay are the lack of consensus on the positive test criteria and the low sensitivity for the detection of low-grade tumours.

Survivin: Promising Biomarker for early diagnosis

Numerous investigations have been developed in the search of novel, more specific, biomarkers[12,15,25]. Among those is survivin, an apoptosis inhibitor protein expressed in the G2/M phase of the cell cycle. Given its tremendous potential for the detection and follow-up of bladder cancer, it will be discussed in detail in this section.

At the beginning of mitosis, survivin binds to the microtubules of the mitotic spindle. The disruption of the interaction between survivin and microtubules results in the loss of the anti-apoptosis function of the protein and increases caspase3 activity leading to cell death during mitosis. This balance in the cell cycle is necessary for the normal cell functioning as the overexpression of survivin inhibits

apoptosis via caspase activation blocking and favours aberrant cell progression[26]. On the other hand, several tumour models have reported that survivin inhibition has been shown to produce defects in chromosome segregation, cytokinesis and ultimately cell division without measurable impact on apoptosis[26,27].

Survivin is one of the most commonly overexpressed genes in cancer, being highly expressed in a variety of solid tumours and haematologic malignancies and absent or underexpressed in normal adult tissue with exception of highly proliferative areas within normal tissues including vascular endothelial, hematopoietic and neural stem cells. Its expression can be detected in all bladder cancer cells but not in normal urothelium and is associated with disease recurrence, stage, progression and mortality[26,28,29]. In addition, survivin is currently being evaluated as a possible therapeutic target to available treatments. In fact, several studies have demonstrated the role of survivin as a chemoresistive agent in both *in-vitro* and *in-vivo* models[27].

In 2004, Shariat *et al.* evaluated the diagnostic potential of urinary survivin in a cohort of 174 patients and compared the results with those obtained for NMP22 and bladder wash cytology. Urinary survivin protein was measured using a Bio-Dot microfiltration detection system in voided urine specimens. The overall specificity of urine survivin, NMP22 and cytology for detecting bladder cancer was 93%, 85% and 91%, respectively. The overall accuracy ratio of urinary survivin, NMP22, and cytology for detecting bladder cancer was 77%, 65% and 71%, respectively. Urinary survivin outperformed cytology in the detection of low stage (Ta or Tis) and/or grade (grades 1 or 2) tumours, whereas urinary cytology had a higher sensitivity and negative predictive value for detecting invasive tumours and/or grade 3 tumours. The authors also found that the diagnostic performance (sensitivity, specificity, positive and negative predictive values) of urinary survivin was superior to that of urinary cytology and NMP22[29].

The detection of mRNA survivin transcripts in exfoliated cells and bladder washes rather than the survivin protein may further improve the detection of bladder cancer. In a study developed in 2006 by Moussa *et al.,* survivin mRNA detection in urine sediment by RT-PCR showed 94% sensitivity and 95% specificity for bladder cancer[28]. However, Cheng *et al.* in 2008 studied the use of survivin and Ki-67 as potential biomarkers for grading non-muscle invasive urothelial carcinoma. In this study, 51 bladder biopsies were graded blindly by 5 experienced general surgical pathologists. Survivin and Ki-76 protein and mRNA expression were evaluated by immunohistochemistry and RT-PCR, respectively. The percentage of urothelial cells with positive survivin nuclear staining was significantly higher in the high-grade than the low-grade group, outperforming Ki-67, a cellular marker for proliferation, showing a significant predictive accuracy for high-grade recurrence than histologic grade. The authors stated that the disagreement of grading by the pathologists could be solved by survivin expression and that survivin mRNA was not more discriminating marker than the immunohistochemical evaluation[26].

Immunomagnetic separation and quantification combined with genetic analysis of bladder cancer CTCs has also been studied for the evaluation of the prognostic significance of survivin-positive CTCs. In a study conducted by Gradilone *et al.,* the group detected CTCs in 24 of 54 patients (44%) with grade 3 T1 bladder cancer and verified among the CTC-positive patients, 92% were survivin-positive, and of these patients, only 82% had survivin-positive primary tumours. In a multivariate

analysis, the authors concluded that CTC+ and survivin+ patients had significantly lower disease free survival, indicating that the expression of this protein in CTCs is a high indicative of a poor prognosis[30]. Despite this, no blood-based biomarker tests are currently in clinical practice for bladder cancer detection or surveillance.

In conclusion, survivin is a very promising marker with good sensitivity and specificity, seems to be predictive for recurrence and can be contribute to reduce the number of unnecessary cystoscopies.

1.2. Epithelial-to-Mesenchymal Transition and Cancer Stem Cells

The epithelial-to-mesenchymal transition (EMT) consists on the transdifferentiation, either partially or fully, of epithelial cells into motile mesenchymal cells. This process is integral in the embryo development, wound healing and stem cell behaviour and has been associated with cancer progression and metastasis[31].

Epithelial cells are characterised by their unequal distribution of proteins between apical side (facing the exterior) and basal side (facing the interior) – apical-basal polarity, interaction between other epithelial cells though cell-cell junctions and with the extracellular matrix (cell-matrix adhesions). During the EMT process (Figure 1.12), the expression of epithelial genes is repressed, alongside with the activation of mesenchymal gene expression. Epithelial cell-cell junctions are disassembled (*e.g.* downregulation of E-cadherin, claudin, β-catenin proteins) and cells lose their apical-basal polarity and acquire front-rear polarity, which is required for migration. This process is balanced by the increased expression of mesenchymal markers, such as neural cadherin (N-cadherin) and reorganization of the cortical actin cytoskeleton to enable dynamic cell elongation, directional motility, increased cell contractility and invasive capacity. Cytoskeletal intermediate filament changes with the repression of cytokeratin and activation of vimentin expression, which enables cell motility, possibly owing to the interaction of vimentin with motor proteins[31]. Because of the drastic change in intermediate filament composition, vimentin is considered a canonical marker of EMT.

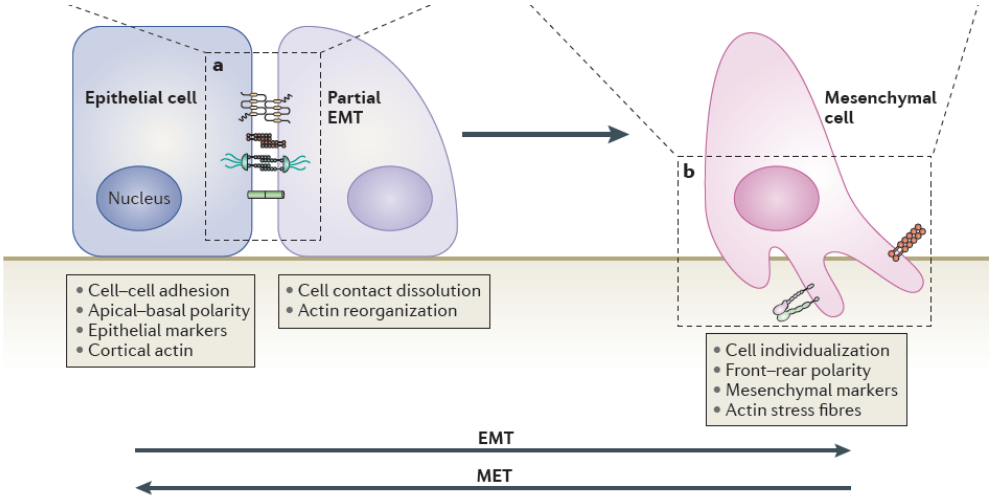

Figure 1.12. Cellular events for epithelial cells undergoing, partially or fully, EMT processes (Lamouille *et al. 2014*)[31]

EMT plays also an important role in the early differentiation of pluripotent embryonic stem cells into the three germ layers, during the embryo development. Therefore, the EMT process has been closely correlated with stemness. Emerging evidence has indicated a subpopulation of stem-like cells within tumours, which exhibit characteristics of both stem cells and cancer cells, known as cancer stem cells (CSCs). Cancer stem cells are tumour cells which possess the capacity of self-renewal, clonal tumour initiation and clonal long term repopulation potential[32].

Expression of cell surface markers such as CD44, CD24, CD29, CD90, CD133, epithelial-specific antigen, and aldehyde dehydrogenase1 has been used to isolate and enrich CSCs from different tumours[33]. One theory (hierarchical model) believes that CSCs arise from normal stem/progenitor cells which obtain the ability to generate tumours when encountering a special genetic mutation or environmental alteration as some CSCs exhibit similarities to normal stem/progenitor cells in cellular property, phenotype, function, and even cell surface markers[33]. An alternative theory (stochastic model) for the origin of CSCs suggests that they arise from normal somatic cells which acquire stem-like characteristics and malignant behaviour through genetic alterations, for instance through EMT[32,33].

1.2.1. EMT and cancer progression

Cancer metastasis is considered a cascade of several steps – invasion, intravasation, systemic transport, extravasation and colonization (Figure 1.13). In response to EMT signals, epithelial cells invade the edge of the tumour while losing some of their epithelial phenotype.

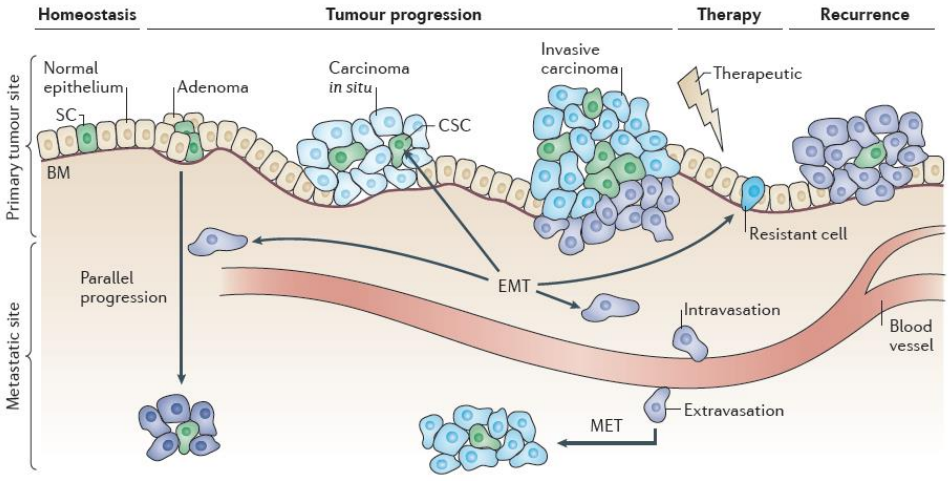

Figure 1.13. Role of EMT in cancer progression (adapted from Craene *et al.* 2013)[34]
In tumour cells, epithelial to mesenchymal transition (EMT) redefines the epithelial status of the cell, potentially — but not necessarily — assigning stem cell (SC) characteristics to dedifferentiated tumour cells, or they may redefine resident genetically altered stem cells to be cancer stem cells (CSCs). The dissemination of tumour cells from the solid tumour and subsequent migration occurs already with a mesenchymal phenotype until it escapes the stream and reverses its phenotype though MET. It is likely that EMT also has a role in parallel progression, in which tumour cells escape early and metastasis progresses in parallel to the primary tumour. MET, mesenchymal to epithelial transition.

These cells start to gain a more mesenchymal phenotype through the EMT signals supplied by the stromal cells. A fully mesenchymal phenotype facilitates intravasation into blood or lymphatic vessels where cancer cells disseminate and exit the stream. When subjected to the appropriate signals, cells are transitioned back to an epithelial state in a distant organ where they proliferate and form

macrometastasis, in a process named mesenchymal-to-epithelial transition (MET). Notably, EMT confers mobility to cancer cells, allowing them to detach from the primary tumour, invade and colonize distant organs and ultimately form metastases with life-threatening consequences. As such, markers of EMT are associated with muscle-invasive bladder cancer, resistance to therapeutic agents and poor outcome[4].

Vimentin has been associated with cancer invasion and poor prognosis in several types of cancers, including melanoma, breast, prostate, and lung cancer and currently poses as potential target for cancer therapy[35]. Furthermore, overexpression of vimentin in a vimentin-negative, non-invasive MCF-7 breast cancer cell line increases integrin traffic, migration and invasiveness. Microinjection of vimentin in the previous cell line, is capable of inducing cell elongation, associated with mesenchymal cell morphology[36].

Several studies have reported that an increase of expression of mesenchymal markers has been associated with increased bladder cancer grade and stage. In a study conducted by Baumgart *et al.* (2007), E-cadherin, plakoglobin, β-catenin, N-cadherin, and vimentin expression was assessed in bladder cancer tissue biopsies by immunohistochemistry[37]. In this study, vimentin was associated with high-grade and invasive tumour stage. However, it was not related with vascular or lymph node invasion. Interestingly, co-expression of epithelial (keratin) and mesenchymal (vimentin) intermediate filaments was observed.

In a recent study conducted by Frazen *et al.* (2015), the authors investigated the ability of bladder cancer-shed exosomes to induce EMT in urothelial cells. To perform this study, messenger RNA (mRNA) was retrieved from primary urothelial cells treated with exosomes derived from MIBC cell lines. The expression of several mesenchymal genes were assessed by quantitative reverse transcriptase-PCR (qRT-PCR). The authors observed an increase in several mRNAs for mesenchymal markers α-smooth muscle actin (α-SMA), vimentin, S100A4, snail and twist while also verifying that varied expression was observed between the exosomes derived from different cell lines. In order to assess if there was also an increase in protein expression, immunostaining was performed for α-SMA in control and exosome-treated conditions, which confirmed increased expression. Concomitantly, expression of epithelial markers E-cadherin and β-catenin was lower compared to control cells treated with phosphate-buffered saline. Interestingly, the presence of exosomes also increased the migration and invasion of urothelial cells[38].

1.3. Rare Cell Isolation from Urine

As previously mentioned, urine is the body fluid of choice for early diagnosis of bladder cancer, as it is in direct contact with the bladder urothelium. However, its cellular content is highly heterogeneous, consisting of various cells of distinct types and sizes. Therefore, a method that could allow the enrichment of exfoliated tumour cells in urine would significantly improve the sensitivity of bladder cancer detection.

Unlike CTC isolation, which has been extensively improved over the years, exfoliated cell isolation from urine still mostly requires benchtop analytical systems. These bulky laboratory equipment demand a large amount (few millilitres) of sample volume (cell suspension) to process. Besides, the

analysis is time consuming and expensive, thus not compatible with point-of-care diagnostics. To overcome some of these limitations inherent to macroscale systems, efforts have been made to develop new methods for rare cell isolation towards point-of-care diagnostics.

In this section, an overview of the conventional exfoliated cell isolation methods from urine are presented as well as the possible application of microfluidics for rare cell isolation from urine.

1.3.1. Conventional Isolation

The conventional methods for exfoliated cell isolation and enrichment are centrifugation and filtration. The ThinPrep™ technique is the standard method for cell isolation used in cytology. In this procedure, cells derived from urine or bladder washes are collected on the polycarbonate membrane filter with 5 µm pores, so predominantly urothelial cells remain on the filter. Cells are then transferred to a glass slide before staining, usually by the Papanicolaou method and examined under a microscope[7].

In a recent work, Per Guldberg's group developed a novel filtration device for on-site collection, storage and shipment of cells from urine. The device consists on a polycarbonate hydrophilic membrane filter with a pore size of 8 µm and a diameter of 25 mm that is able to eliminate over 99% of smaller-sized cells. After the filtration process, the filter cartridge is transferred to a storage cassete which is mounted with a lid containing an appropriate solution for cell preserving or preparing[39]. Nevertheless, this system has been used, by the group, to preserve cell DNA after lysis for mutation and methylation marker analysis. Therefore, even though this work represents a major novelty in exfoliated cell isolation and enrichment, recovery of intact cells for further functional characterisation is still a challenge, as in conventional microfiltration methods.

1.3.2. Microfluidic rare cell isolation

The conceptual idea of microfluidics is that fluids can be processed using a microscale device built with technologies first developed by the semiconductor industry and later expanded by the micro-electromechanical systems (MEMS) field. These devices are commonly named miniaturized total analysis systems (µTAS) or lab-on-chip technologies. Several advantages can arise from passing from macroscale isolation and detection to microscale. Firstly, lower sample or reactant volumes are necessary for processing, which results in faster analysis times and therefore high throughput screening. The implementation of microsystems, allows the possibility of efficient data integration and automation. Due to their relative low cost and easiness of fabrication, microfluidic devices are capable of being single-use, which is seen as a benefit for biomedical applications and point-of-care diagnostics[40].

The idea of using microfluidic devices for liquid biopsy has gain a lot of interest in the last years. Several groups have dedicated their time in the isolation and characterisation of circulating tumour cells from blood of cancerous patients using several methodologies. Nevertheless, identification and enumeration of CTCs has only prognostic and predictive value in metastatic cancer patients, and not in early disease diagnosis. In contrast, bladder washes and urine can be used as the specimen for urinary cancer detection, including low-grade tumours of the bladder wall, which may shed allowing disease targeting at its initial state.

The recent advances in microfluidics applied to medicine may provide new platforms capable of enrichment, enumeration and *in situ* characterisation, aiding in the identification of new drug resistance mechanisms and possible therapeutic targets, either by molecular characterisation of the isolated cells, or their culture for drug screening assays. Even though most of the microfluidic platforms have been designed for isolation of CTCs from blood, the principle of isolation and enrichment can be applied for other target cells in different biological samples, after adjusting the pre-processing sample step.

1.3.2.1. Immunoaffinity Purification – The standard method

Immunoaffinity-based isolation methods are frequently employed due to specific binding between the antibody and the antigens expressed at the surface of cells. By functionalizing the microchannels or microstructures with probes (in this case, specific antibodies) target cells remain bound to the device, while other cell types flow through (positive selection). Negative isolation methodologies have also been employed for the removal of non-target cells. In this case, the surface of the device is functionalised with probes targeting known sample contaminants, for instance CD45 for leukocyte targeting from whole blood, enriching the sample with CTCs.

Nevertheless, immunocapture has drawbacks, such as cells normally flowing in straight streamlines as fluids flow at laminar flow in microchannels. This might reduce the probability of interaction between cells and antibody coated surfaces, decreasing the capture efficiency of the device. To overcome this issue, several micromixing strategies can be implemented including chaotic advection by using passive micromixers such as Herringbone shaped grooves. These structures act as microvortex generators and increase the possibility of collisions between target cells and antibody-coated channels[41]. Also, it is necessary to provide sufficient time for cells to specifically bind to the antibody but not enough time that would allow unspecific binding or would require long term processing. Also, positive selection of cancer cells may be difficult due to their heterogeneity in terms of cancer type, stage, as well as among patients. In addition, the use of antibody-coated devices may be limited since only cells expressing target molecules are captured, and cancer cells are known to vary their cell surface expression levels according to cell phenotype of disease stage. Moreover, immunotrapped cells are difficult to recover and may have altered activation status, compromising further molecular and functional analyses.

1.3.2.2. Microfiltration – Label-free size-based microfluidic isolation

One of the key aspects to consider when designing a microfluidic system for rare cell isolation is the selection of the isolation principle that will be applied in the device. Considering that an ideal platform should target a large variety of cells types at different tumour stages, a label-free isolation method would be a good alternative. Several techniques have been developed, which rely on intrinsic cellular biomechanical (e.g., cell size, density, deformability) or electrical properties. The most common methods are microfiltration, hydrodynamic and dielectrophoresis-based separation. Within the scope of this thesis, only microfiltration microfluidics will be explored in this section.

Size-based enrichment is a standard practice in the conventional cell isolation methods. By adapting the principle to microfluidics it is possible to develop label-free isolation platform with high

throughput. In 2009, Mohamed *et al.* proposed an arrayed microchannel with decreasing widths of 20, 15, 10 and 5 µm to isolate various types of CTCs from whole blood based on differences in size, structure and deformability between normal and cancer cells. This system was tested with two channel heights, 10 and 20 µm, to assess which condition provided better isolation of cells with different sizes and deformabilities. The authors verified that the 20 µm enabled a better discrimination and would be more representative of what to expect in a clinical sample. Subsequently, isolated cells were retrieved by flow reversal or lysed *in situ* for DNA extraction to detect 13 polymorphic markers on different chromosomes. The retrieved cells were cultured and were able to proliferate demonstrating their viability after isolation and recovery[42].

Tan *et al.* (2009) also established a device to isolate breast and colon CTCs from normal cells based on their size and deformability. Normal blood cells transverse the 5 µm gaps of the crescent-shaped structure while cancer cells get trapped. This design also incorporated a pre-filter with gaps of 20 µm to prevent large clumps or debris from clogging the device, improving the isolation purity. Another interesting aspect of this work was the use of pressure differential instead of flow-rates for device operation. In this system, three pressure differentials were tested, 5 kPa, 10 kPa and 15 kPa (equivalent to 50 mbar, 100 mbar and 150 mbar) in which isolation efficiencies of approximately 80%, 60% and 40% were obtained, respectively. The isolation purity remained constant for each pressure condition (approximately 80%). By reversing the flow direction, the captured CTCs were retrieved for cell culture and proliferative assays[43].

Although microfluidic devices allow high throughput, the high flow rates can damage cells and reduce their viability, compromising further analyses. Also due to tumour heterogeneity, cancer cell sizes may overlap with blood cells and consequentially lose some sub-population of target cells or decrease the final purity. In order to overcome these issues, a pre-purification step could be applied to remove some of the contaminants. Red blood cell lysis could be initially used in order to reduce the number of blood cells and associated hindrance, ensuring higher purity and easier isolation of target cells.

1.4. Aims

Cystoscopy adjunct with urine cytology are currently considered the gold standard for initial evaluation of lower urinary tract lesions and detection *of de novo* or recurrent bladder cancer. However, cystoscopy is an invasive and expensive diagnostic procedure with limited sensitivity for flat lesions such as CIS, whereas urine cytology presents low sensitivity for low-grade papillary tumours. Hence, alternative methods able to detect bladder tumour cells both at early stages and during disease progression are urgently required. More importantly, there is an unmet need for novel technologies capable of identifying different cancer cell populations, particularly those most capable of establishing overt metastasis.

Microfluidic devices have been intensively reported over the last years for their applicability in circulating tumour cell isolation from blood. The same principles can likewise be applied for rare cell isolation from other body fluids. Moreover, by targeting rare cells from fluids that have been in direct contact with the primary tumour site, their detection may be facilitated. Cytomorphologic analysis falls short to discriminate between normal urothelial cells and low-grade tumours. In addition, tumour cells have been shown to exhibit distinct intermediate states in the epithelial-mesenchymal axis, which may likely correspond to a higher malignant phenotype and so be prognostically more relevant. Thus, it is crucial to identify different tumour cell subpopulations to better understand their biological and clinical significance.

In this context, the main goal of this thesis was the isolation and characterisation of distinct bladder tumour cells from urine using a microfluidic device. This work was part of a more complex project which envisages the development of a robust, specific and non-invasive point-of-care device for bladder cancer detection, with expected impact on improved clinical management of cancer.

A label-free microfluidic platform consisting of five rows of posts, with increasingly narrower gap widths (50, 20, 15, 10 and 5 µm) was designed by the group to isolate cells according to their size and deformability. Herein, the potential of this platform for the isolation of different bladder cancer cells from bladder washes and urine of bladder cancer patients was assessed as follows:

1. Fabrication of the microfluidic device and evaluation of its performance
2. Selection and evaluation of a panel of biomarkers for adequate phenotypic characterisation using bladder cancer cell lines as model systems.
3. Development and optimisation of a sample pre-processing protocol for both bladder washes and urine specimens.
4. Assessment of the microfluidic platform retention capacity and phenotypic characterisation of captured cells, using clinical samples.

The technical background behind this work is elucidated in Section 1.5. followed by a thoroughly description of all methodologies used and developed during the project (Section 2). Thereupon the achieved results achieved are shown and rigorously examined in Section 3. Finally, future perspectives and conclusions are covered in Section 4.

1.5. Background

1.5.1. Master Fabrication

1.5.1.1. SU-8 photolithography: The Conventional Method

Lithography consists on the transfer of a pattern onto a substrate. Resist lithography uses an irradiation source and a photosensitive polymer to perform the pattern transfer. The radiation exposure initiates a series of photochemical reactions that alter the physical and chemical properties of the polymer, making it susceptible to degradation with an adequate reagent. Most commonly, the polymer is modified by increasing the solubility of the exposed areas (positive photoresist) or by decreasing it through the cross-linking of the chains (negative resist).

The standard method for microfluidic master mould fabrication is through the use of SU-8 photolithography. SU-8 is a negative photoresist, which contains acid-labile groups and a photoacid generator. The exposure of the polymer to radiation will generate a low concentration of a strong acid that will act as a catalyst of the cross-linking reaction. The heating of the polymer activates the cross-linking and regenerates the acid catalyst. This results in a high mechanical and thermally stable lithographic structures after processing (Figure 1.14)[44].

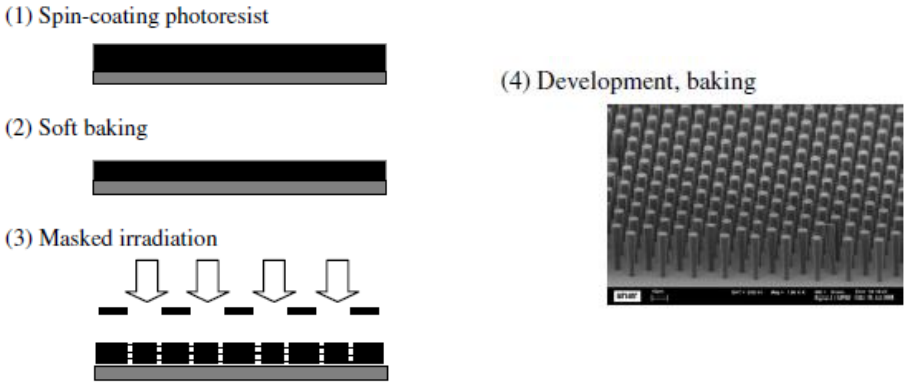

Figure 1.14. Photolithographic steps with the SU-8 negative photoresist (adapted from Campo et al)[44].
(1) The first step of any photolithographic step is the spin-coating of the photoresist at a defined rotation speed and time to ensure proper planarization and right thickness of the resist. **(2)** Soft baking is performed in order to evaporate the solvent and promote adhesion of the polymer to the wafer. **(3)** Exposure is done using a hard mask and UV light to pattern the features on the photoresist. **(4)** After exposure, occurs a hard baking process for the selective cross-linking of the exposed film. The process finishes with the dissolution of unpolymerized SU-8 (development).

Even though SU-8 lithography is vastly used, it presents several issues that make the use of this process undesirable for the fabrication of some master moulds. Firstly, since the SU-8 polymer is very stable, the resist stripping process is very challenging and can result in an incomplete development that will ultimately affect the quality definition of the patterned structures. Secondly, although SU-8 is designed to give rise to planar surfaces after spin coating, planarization defects may occur due to increased viscosity of the solution, unintentional tilt, dirt particles, curvature of the substrate or mask (Figure 1.15.A) Secondly, if the hard mask is in contact with the resist during radiation then the hard mask can gain some defects. On the other hand, if the mask is placed near but not in direct contact, then the resulting air gaps will cause diffraction effects (Figure 1.15.B). This results in pattern edges

being irradiated with higher doses with consequent pattern enlargement at the top of the features, which is particularly problematic in the definition of high aspect features.

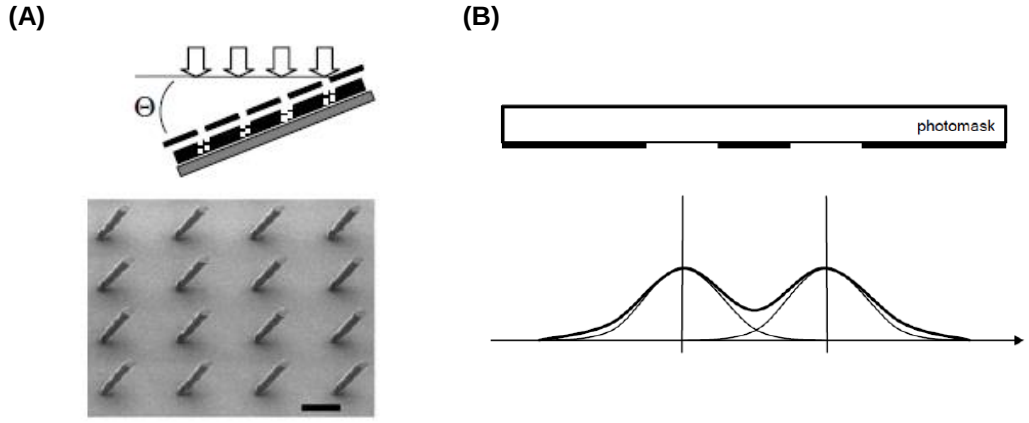

Figure 1.15. SU-8 photolithography drawbacks (adapted from Campo et al)[44].
(A) Tilted SU-8 pillars obtained by tilted UV single exposure. (B) Diffraction effects caused by the patterning with a non-contact mask.

To overcome these issues, patterning can be performed with a focused beam (laser, electron or ion beam lithography) directly into the resist, instead of patterning with hard masks. With Direct Writing Laser (DWL) lithography, a computer controls a focused beam of the used radiation. Software masks designed in AutoCAD are then converted to a digital mask format and processed by DWL lithography. When transferring the mask to the system, the information regarding the regions to expose must be added as the beam is scanned across the entire sample.

Even though the standard method for microfluidic master fabrication is based on the use of SU-8 photolithography, this method only renders a maximum aspect ratio of 20 following the standard protocol and, particularly for thick moulds, is heavily subjected to optical diffraction[44]. In this project, we have used a novel method of microfluidic master fabrication by the use of Silicon Deep Reactive Ion etching, which allows the achievement of very anisotropic high aspect ratio features.

1.5.1.2. Silicon Deep Reactive Ion Etching (DRIE)

Reactive ion etching is a combination of physical and chemical etching processes. In this technique the reactive species generated in an RF plasma react with the material only when the surfaces are activated by the collision of incident ions from the plasma and generate volatile products that are removed from the system (Figure 1.16).

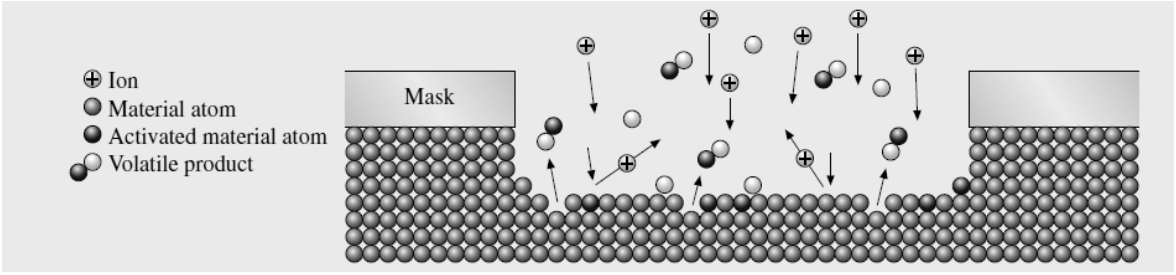

Figure 1.16. RIE principle schematics (adapted from Springer Handbook of Nanotechnology)[45].

The use of silicon deep reactive ion etching dates from 1993 by Robert Bosch GmbH in order to create deep and anisotropic silicon trenches for microelectromechanical systems (MEMS). Since then this process is commonly referred to as the Bosch Process. The process consists in alternating etching and passivation cycles. During the etching step, sulfur hexafluoride (SF_6) plasma is created which isotropically etches silicon. Through the application of a direct current bias to the wafer electrode, the ions bombard the surface of the wafer, reacting with the silicon atoms and creating a volatile product. Due to the direction of the ions, the sidewalls of the trenches are less etched than the surface, however, simply using etching steps would ultimately result in an isotropic process, etching the sidewalls. To prevent sidewall etching, after each etching step, a C_4F_n plasma is created to conformably deposit a few monolayers of PTFE-type fluorocarbon polymer (Teflon-like polymer) across all surfaces exposed to the plasma. The process is then switched to the etching cycle. Due to the cyclic nature of the process, the sidewalls of the etched features show a periodic wave-shape roughness (Figure 1.17).

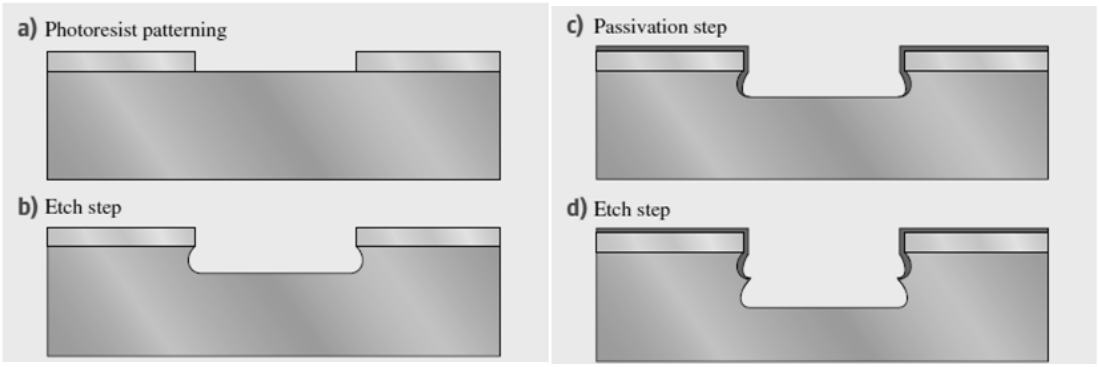

Figure 1.17. DRIE process cycle (adapted from Springer Handbook of Nanotechnology)[45]
a) Photoresist patterning. **b)** Etching step performed with an SF_6 plasma to isotropically etch silicon. **c)** Passivation step with C_4F_n type plasma to protect the exposed silicon areas that are not meant to be etched. **d)** Etching step (Cycle repeat).

1.5.1.3. Master Hydrophobization

To increase the durability of the masters and to aid the removal of the PDMS replica, the master was hydrophobized using a silanization process. Silanization is the generic term applied for the formation of an organosilane monolayer onto a substrate, which depending on its functional group can be used to modify the properties of the surface, such as surface hydrophobization, protein or biomolecule immobilization or to prevent unwanted protein adsorption. Self-assembled monolayers (SAMs) are formed by linear morphology molecules with a reactive group at one end that has a high affinity for a particular surface, and a functional group at the other end that varies according to the application of the SAM. The organosilane SAMs react with trace amounts of water to form intermediate silanol groups which in turn react with free hydroxyl groups on the surface forming covalent bonds (Figure 1.18).

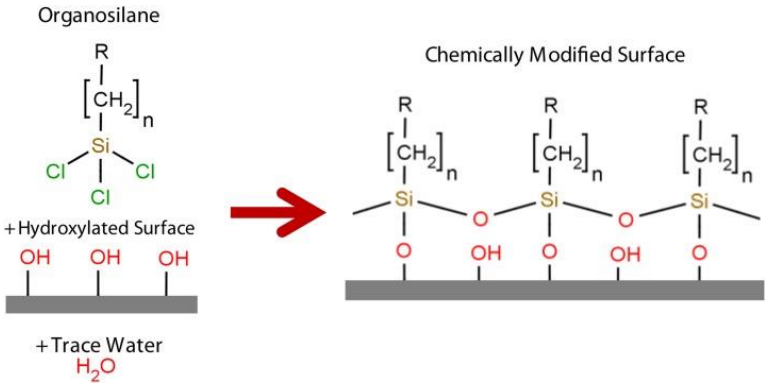

Figure 1.18. Organosilane self-assembled monolayer reaction on a hydroxylated surface (adapted from Glass 2011)[46].
When a hydroxylated surface is exposed to an organosilane in the presence of trace amounts of water, the reactive end bonds to the surface while the tail end becomes the dominant surface chemical species.

In this project, the hydrophobization process was done with trichloro(1H,1H,2H,2H-perfluorooctyl)silane. This polytetrafluorofluoroethylene organosilane (PFS) produces surface fluoride groups that create hydrophobic surfaces which protect the silicon wafer master. The organosilane deposition was performed by chemical vapour deposition. By increasing the percent partial pressure of the organosilane within a closed system, either by heating a closed container or by lowering the base pressure with vacuum, the compound is deposited by chemisorption.

1.5.2. Microfluidics

1.5.2.1. Soft lithography

Soft lithography typically refers to the moulding of a two-part polymer (elastomer and curing agent), named polydimethylsiloxane (PDMS) using a master mould. PDMS is widely used for rapid prototyping of microfluidic devices via soft lithography (Figure 1.19). It is optically transparent, gas and vapour permeable, biocompatible, relatively easy and cheap fabrication are only a few of the advantages of the incorporation of this polymer in microfluidics.

The features defined by the PDMS replica are only limited by the minimum feature that can be achieved in the fabrication of the master. For this reason, when designing microfluidic platforms with high aspect ratio structures, the technology used in MEMS fabrication allows the creation of more complex masters, when compared to SU-8 photolithography.

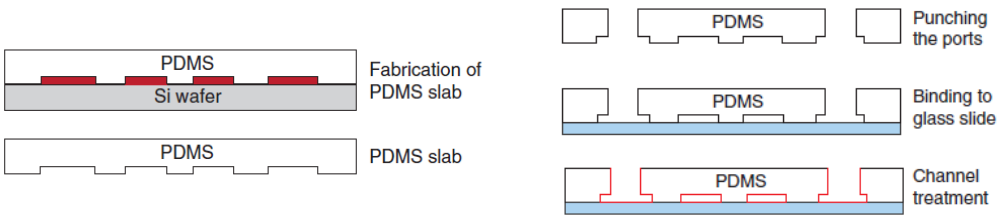

Figure 1.19. Soft lithography to fabricate microfluidic devices in PDMS (adapted from Mazutis, 2013)[47]
Once the master is fabricated, conventionally through SU-8 photolithography, PDMS is poured onto the master, degassed in a desiccator and cured in the oven. After peeling the PDMS off the master, fluidic ports are punctured. Irreversible bond of the PDMS to the glass slide is achieved by oxygen plasma treatment. Finally, the microfluidic channels are functionalised.

1.5.2.2. Surface Oxidation and Bonding

In order to produce microfluidic devices for biomedical applications, it is necessary to consider certain properties such as fabrication reproducibility, cost, biocompatibility and optical transparency for microscope analysis. Considering these aspects, the irreversible bonding between PDMS and glass can offer a great advantage since glass is optical transparent and presents high thermal and structural stability. For the bonding to occur, the PDMS and glass have to be exposed to an oxygen plasma environment in order to activate the bonding surfaces through the creation of silanol groups (Si-OH). When in contact, these groups condense and form Si-O-Si irreversible bonds that can be further enhanced by heat activation (Figure 1.20).

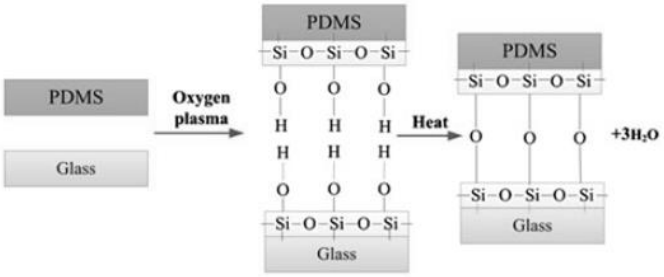

Figure 1.20. Irreversible bonding process between PDMS and glass through oxygen plasma activation (adapted from Xiong 2014)[48].

The bonding efficiency depends on a number of factors such as RF power, oxygen flow, plasma exposure time. Each condition should be optimised for the desired application and design of the microfluidic platform. For instance, higher exposure time might not improve the bonding since the plasma could start to act as an etching agent and possibly damage the design of the PDMS replica.

1.5.2.3. Surface Passivation

The passivation process is extremely important to remove any unspecific interactions between cell surface proteins and PDMS surface. For this, poly-ethylene-oxide (PEO) based surfactants attach to the PDMS surface where their hydrophobic tails will form a brush-like structure that will prevent proteins from adsorbing. Pluronic F-127 is a non-ionic bi-functional copolymer surfactant with two 96-unit hydrophilic PEO chains surrounding one 69-unit hydrophobic polypropyleneoxide (PPO) chain (Figure 1.21.).

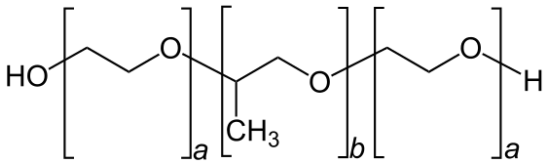

Figure 1.21. General chemical structure of poloxamers (a=96 and b=69 for Pluronic F-127).

Since Pluronic F-127 has a large hydrophobic domain and PDMS is naturally hydrophobic, the PPO chain of the polymer will preferentially interact with the surface resulting in a tangled structure due to the two hydrophilic domains. For this reason, in order to achieve a packed brush-like conformation, passivation should be done right after the plasma activation of the PDMS-glass surface while they still

remain hydrophilic. In order to increase the wettability, ethanol can be flown through the channels and then rinsed with PBS before the passivation process.

1.5.2.4. Flow control

Syringe pumps are the most commonly used flow control systems in microfluidics due to its fast setup and ease to use. These systems allow precise flow control at high flow rates and good reproducibility. However most of the syringe pumps are based on a syringe driven by a motor and a rotary screw, which create cyclic variations and flow pulses. This is particularly problematic for low flow rate systems and very low responsiveness which can vary from seconds to hours.

Another main issue of this system is a possible increase (due to channel clogging for example) of the fluidic resistance and consequently of the internal pressure of the device, leading to device destruction. On the other hand, when using this system, one must consider the ideal syringe volume. The minimal injected volume is proportional to the syringe diameter and a smaller diameter improves the flow rate stability but limits the volume processed.

As an alternative, pressure controllers can be used to control the flow. In this case, a reservoir containing the fluid to be processed is pressurised with compressed air. As fluids are incompressible, this system allows a smooth injection in the microfluidic device. These systems are relevant since allow fast response times and do not limit the amount of volume processed. However, flow rate varies with fluidic resistance, meaning that for a higher flow resistance at constant pressure, the flow rate will decrease (Figure 1.22.)

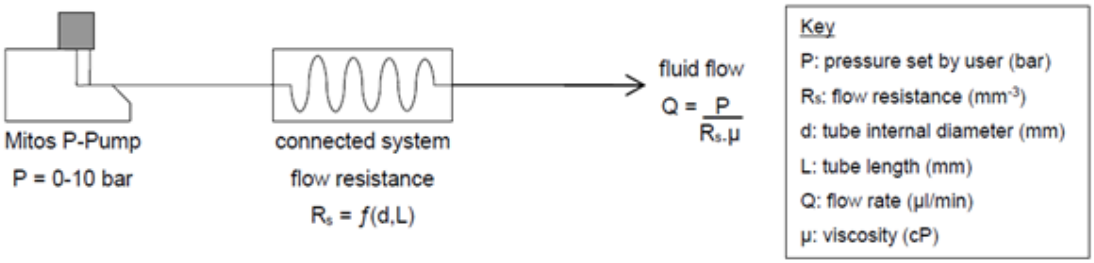

Figure 1.22. Microfluidic pressure control system.

In this project, as cells were trapped in the microposts, the flow resistance in the channels increased with time and therefore the flow rate diminished for a constant pressure process. However, if the flow rate was kept constant, the pressure inside the channels would increase dramatically during sample flowing, so that channels or even cells would eventually disrupt (sample leaking). For this reason, a maximum of 300 mbar was used, as this was the highest working pressure possible without the risk of device leaking.

1.5.3. Immunofluorescence

1.5.3.1. Fluorescence Microscopy

Unlike conventional light microscopy, which relies on specimen-dependent properties, fluorescence microscopy allows the visualisation of fluorescently-labelled target molecules that emit light upon excitation by a light source. Hence, using this technique it is possible to study, among others, the distribution and dynamics of a large variety of macromolecules and metabolites.

Fluorescence results from the emission of photons by atoms or molecules whose electrons are transiently excited to a higher energy state by radiant energy source with the appropriate wavelength, returning almost immediately to their minimal energy state (the ground state). The process can be explained graphically by the Jablonski diagram (Figure 1.23.A), which depicts the increasing energy states with their sublevels of energy. Once an electron is excited to a higher energy state, usually the excited singlet state, it collapses to the ground state emitting energy (Fluorescence), with the absorption and emission phenomena occurring with an interval of 10^{-9} – 10^{-12} seconds. Alternatively, energy can be lost through thermal energy (internal conversion), in which case no photon is emitted. During the excitation process, an electron can also enter the triplet excited state through a process named intersystem crossing. This is associated with high chemical reactivity and can lead to both photobleaching and production of damaging free radicals. In this case, the period between absorption and emission can range from 10^{-2} – 10^{2} seconds, in a process called phosphofluorescence[49].

(A) **(B)**

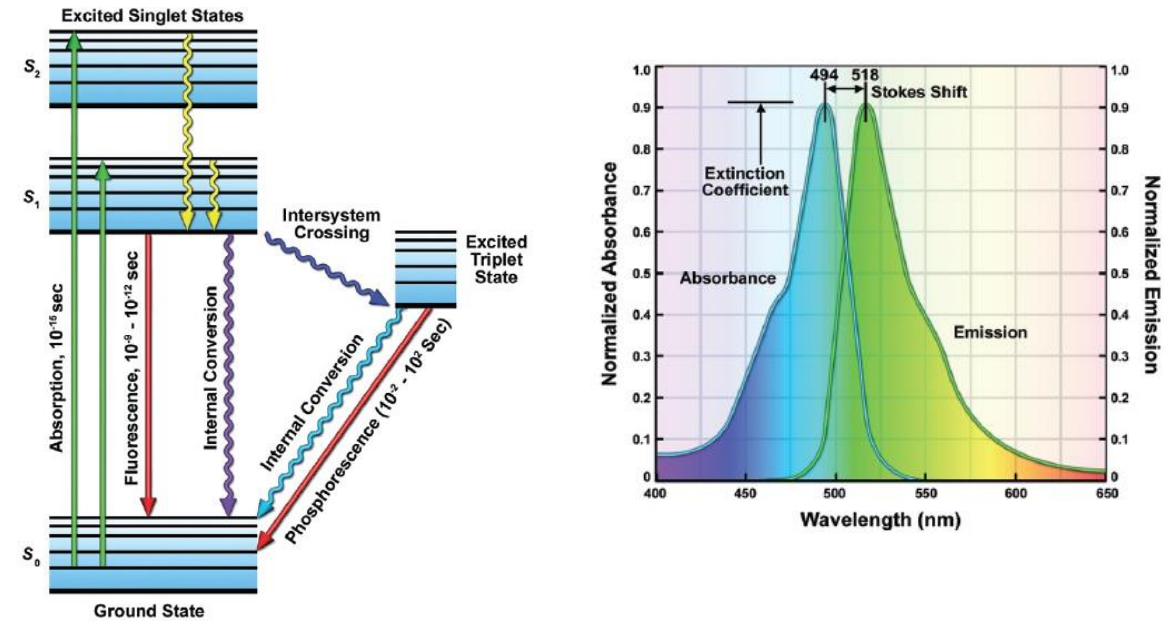

Figure 1.23. (A) Jablonski diagram showing energy levels occupied by an excited electron within a fluorescent molecule (chlorophyll a). (B) Normalized absorption and fluorescence emission spectra of fluorescein conjugated to IgG. (adapted from Fundamentals of Light Microscopy and Electronic Imaging)[49]

Molecules that are capable of fluorescing are called fluorescent molecules, dyes or fluorochromes. Fluorochromes possess distinct excitation and emission spectrums that depend on their structure and properties. These molecules absorb and emit light over a range of wavelengths, i.e. the

excitation and emission spectra respectively. The difference in wavelength between the absorption and emission spectra peaks corresponds to the Stokes Shift (Figure 1.23.B). During the process of decay, the photon loses energy due to vibrational relaxation. This results in the emission of a fluorescent photon with lower frequency of vibration and longer wavelength than the excitatory photon observed. Dyes exhibiting a large Stokes shift are advantageous in fluorescence microscopy, because the bands of excitation and fluorescence wavelengths are easier to isolate using interference filters.

In this project, a Nikon Eclipse MA200 microscope was used. This inverted materials' microscope with long working distance objective lenses, is ideal for the analysis of microfluidic devices as these are sustained in 1mm thick glass slides. The microscope is designed for Bright and Dark field microscopy (white lamp as light source), as well as Epi-Fluorescence microscopy (epi-illuminator with a 75 Watt Xenon arc lamp-Lambda LS Shutter, 320 to 700 nm output range) via liquid light guide transmission (Figure 1.24).

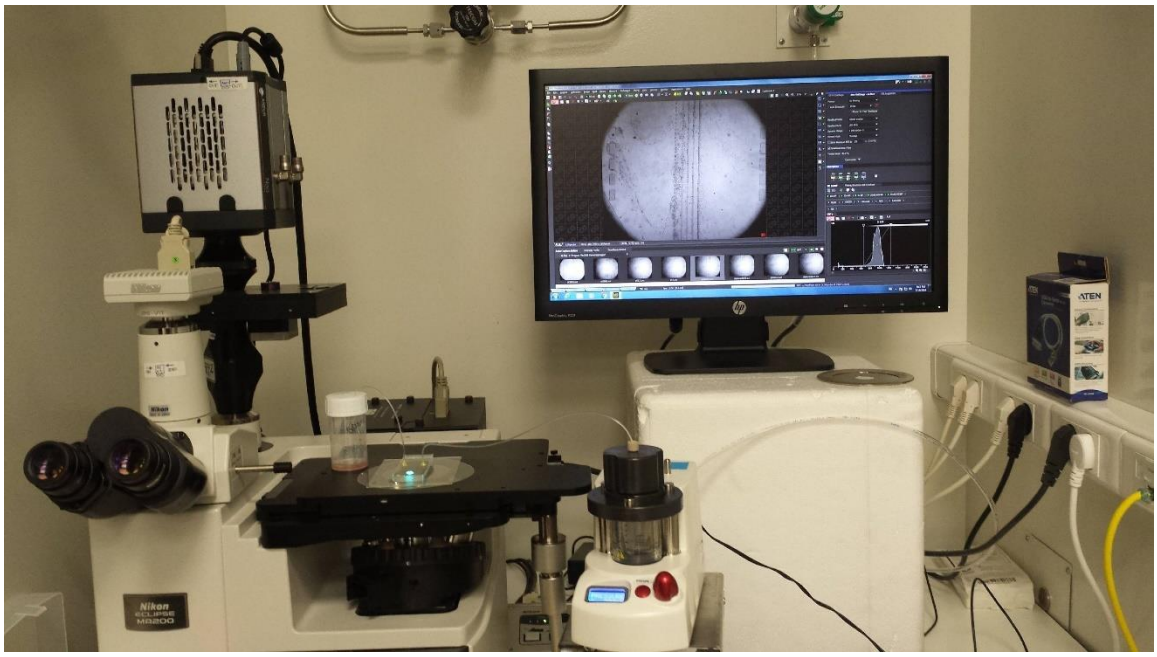

Figure 1.24. Experimental setup comprising the Nikon Eclipse MA200 microscope, Epi-illuminator, CCD and CMOS camera connected to a computer with NIS-Elements Microscope Imaging Software.

The microscope was customized to integrate 5 multi-channels: Blue, Green, Orange, Red and Far red, using a penta-band set designed for high-speed and sequential imaging (BrightLine® Sedat filter set, optimised for DAPI, FITC, TRITC, Cy5 & Cy7). The set is comprised of a penta-band beamsplitter (dichromatic mirror) with five single-band emitters and five single-band exciters which are positioned in the optical path between the epi-illuminator and the objective.

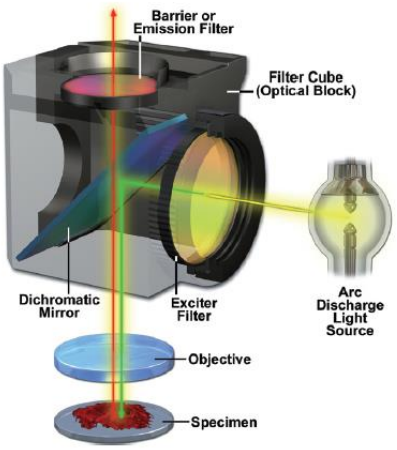

Figure 1.25. Filter arrangement in a fluorescence filter cube (adapted from Fundamentals of Light Microscopy and Electronic Imaging)[49].
The diagram shows the orientation of filters in a filter cube in an epi-illuminator for an upright microscope. The excitation beam (yellow line) passes through the exciter and is reflected by the dichromatic mirror and directed toward the specimen (green line). The return beam of emitted fluorescence wavelengths (red line) passes through the dichromatic mirror and the emission filter to the eye or camera. Excitation wavelengths back-reflected or scattered at the specimen are again reflected by the dichromatic mirror back toward the light source. Excitation wavelengths that manage to pass through the dichromatic mirror are blocked by the barrier (emission) filter.

The excitation and emission filters are optimised for the detection of the following fluorophores: DAPI, FITC, TRITC, Cy5 and Cy7. If a different fluorophore is needed, the transmission profile of the filter set must be taken into consideration to ensure that its excitation and emission bands are comprised within the bands of the filter set (Figure 1.26). Table 1.3 comprises the fluorophores recommended for the filter set as well as other fluorophores used for this project (Alexa Fluor® 488, eFluor® 570 and DyLight® 755).

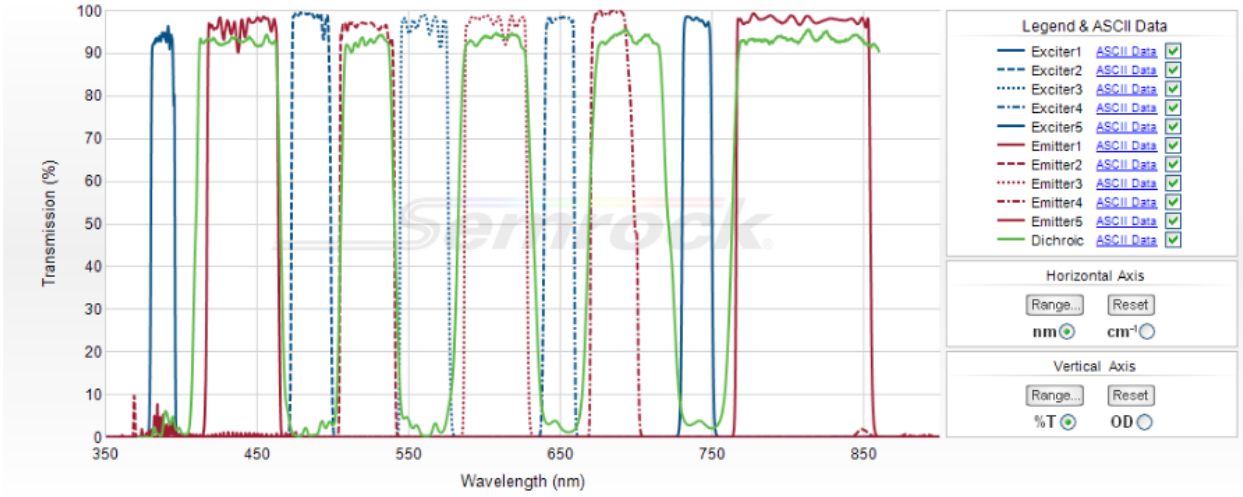

Figure 1.26. Transmission profile for the filter set incorporated in the Nikon Eclipse MA200 microscope (Adapted from Semrock)[50].

Table 1.3. List of recommended and used Fluorophores according to the microscope filter set and respective peaks of excitation and emission as well as compatibility with the filters (adapted from Semrock)[50].

Fluorescence Colour	Fluorophore	Peak Excitation Wavelength (nm)	Peak Emission Wavelength (nm)	Compatibility
Blue	DAPI	359	461	★★★★★
Green	FITC (Fluorescein)	495	519	★★★★★
	Alexa Fluor® 488	499	520	★★★
Orange	TRITC (Tetramethylrhodamine)	552	578	★★★★★
	eFluor® 570	555	570	Not available
Red	Cy5™	649	666	★★★★★
Deep Red	Cy7™	753	775	★★★★★
	DyLight® 755	756	794	Not available

The microscope is coupled with a CCD (Nikon DS-Vi1) and CMOS (Neo Andor Technology) digital cameras for Bright/Dark field and Fluorescence detection respectively. These cameras are connected to a computer with NIS-Elements Microscope Imaging Software.

1.5.3.2. Immunocytochemistry

Immunocytochemistry is a common laboratory technique used to investigate the expression and/or localization of a specific protein or antigen of interest in a cell through the binding of an antigen-specific antibody. The detection antibody may be already conjugated with a fluorochrome and thus only one binding step of the specimen needs to be performed before fluorescent microscopy analysis (Figure 1.27). On the other hand, an indirect labelling may be required if the primary antibody is unlabelled. In this case, the specimen is first stained with the primary antibody for antigen-antibody binding. Then, a secondary antibody conjugated with a fluorochrome is added and will bind to the primary antibody. The label is used to indirectly detect the antigen.

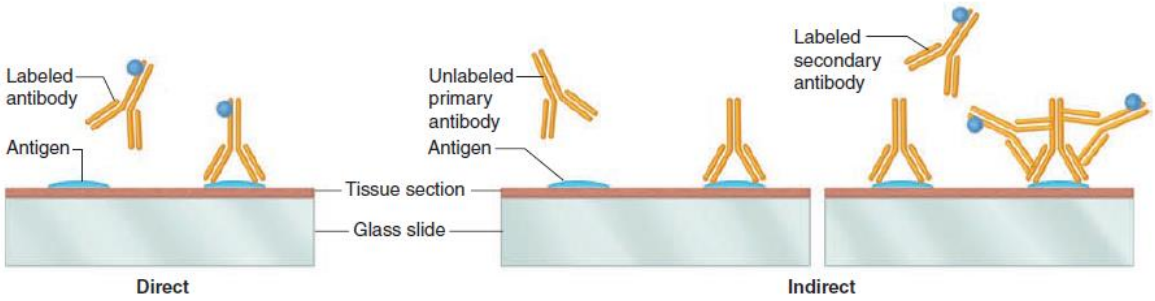

Figure 1.27. Direct and Indirect immunostaining methods (Adapted from Junqueiras Basic Histology Text and Atlas)[51]

2. Materials and Methods

This chapter will focus on the different methodologies used and developed for this project and is divided in three parts: 1) Protocols used for master and microfluidic device fabrication (section 2.1 and 2.2); 2) Protocols developed and optimised for sample processing (section 2.3) and control experiments implemented for the microdevice cell retention (section 2.4); 3) Clinical samples analysis, where the protocols relative to sample collection (section 2.5), processing (section 2.6) and immunofluorescence analysis (section 2.7) will be explored.

2.1. Master Fabrication

The microfluidic master was previously designed by the group in AutoCAD software (Figure 2.1).

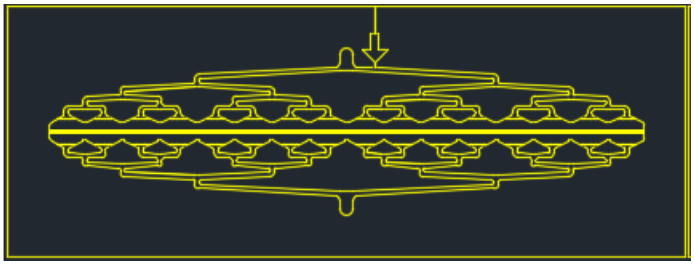

Figure 2.1. AutoCAD design of the microfluidic master.

For the fabrication, a 200 mm diameter and 725±25µm thickness crystalline silicon wafer (P/Boron, <100>, Siegert Wafer) was rinsed with deionized (DI) water in the optical tracks to remove any organic molecules present in the surface of the wafer. Before the photoresist coating, the wafer was dehydrated at 150ºC and exposed to hexamethyldisilazane (HDMS) vapour prime to improve the adhesion of the photoresist to the sample (Figure 2.2.A). The wafers were spin coated with 2.2µm of AZP4110 positive resist (Microchemicals GmbH, Germany), deposited using a SUS MicroTec optical track (Figure 2.2.B). The pattern was transferred onto the coated wafer using a Direct Write Laser system (DWL 2.0 Heidelberg, Germany) with a Hg laser energy of 95% and focus -50 (Figure 2.2.C). After a post bake, exposed PR was developed with AZ400K (Microchemicals GmbH, Germany). The developer dissolves the exposed regions, while the non-exposed areas remain intact. Afterwards, the sample was washed with water and dried by high speed spinning (Figure 2.2.D).

Once the PR was developed, the pattern was etched by Silicon Deep Reactive Ion Etching (STPS Pegasus, United Kingdom) with sulfur hexafluoride (SF_6) and passivation with octafluorocyclobutane (C_4F_8). Trench depth was measured in between steps using an optical profilometer (OPM profilometer) until the desired depth of 20 µm was reached. Once the etching finished, the photoresist and Teflon residues were stripped using oxygen plasma in the STPS Pegasus machine. The master was characterised by means of Scanning Electron Microscopy (Quanta SEM, FEI, United States of America). Finally, the wafer was diced into the individual masters using a DAD 3350 Dicing Saw (Disco, Japan) and cleaned with Isopropyl alcohol (IPA), rinsed with water and dried at 150ºC on a hot plate.

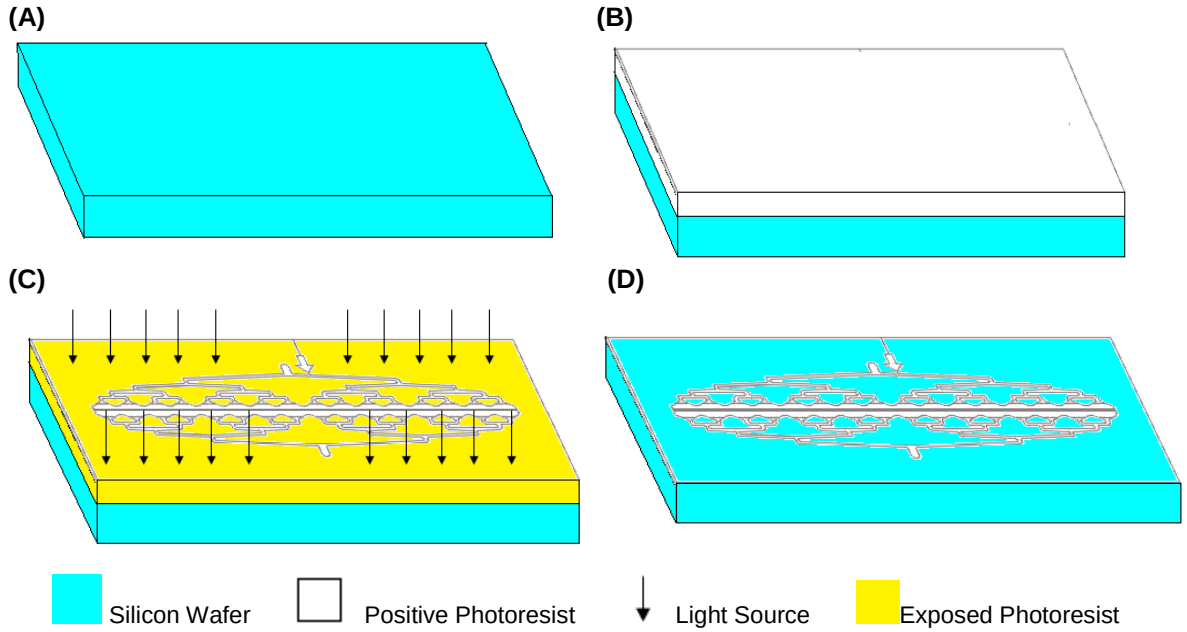

Figure 2.2. Photolithographic master fabrication steps.
A clean silicon wafer (A) is primed with HDMS to enhance the photoresist adherence. A positive photoresist is spin-coated onto the silicon wafer with a thickness of 2.2 µm (B). Direct Write Laser lithography is used to pattern the design on the photoresist (C). After development, the exposed photoresist is removed and the pattern cured onto the silicon wafer (D).

To hydrophobize the master, a glass coverslip was placed inside the vacuum desiccator present inside a fume hood and one drop of trichloro(1H,1H,2H,2H-perfluorooctyl)silane (97%, Sigma Aldrich) was placed on the coverslip. Using tweezers, the masters were placed inside the desiccator and the air was evacuated. Once vacuum was formed, the desiccator valve was closed and disconnected from the vacuum line and placed in the oven at 65ºC for 1 hour. After this period, the contaminated glass coverslip was disposed in the appropriate container and the masters rinsed with ethanol (EtOH) and dried with the Nitrogen (N_2) gun.

2.2. Microfluidic Device Fabrication

PDMS was prepared as a two-part system with mix ratio of 10:1 (w/w) base/curing agent (Sylgard 184 Silicon Elastomer kit, Dow Corning). Polymer solution was centrifuged at 3000xg for 5 minutes to remove any bubbles. PDMS was poured over the master until and degassed using a desiccator. The curing process of PDMS occurred at 65ºC for 2 hours.

Replica was cut with the aid of a scalpel and inlet and outlet ports were made using a 1.5mm biopsy punch (Miltex). Any PDMS debris that may have been present on the master pattern or replica were removed to ensure good binding with the glass surface.

2.2.1. Surface Oxidation and Bonding

For an efficient bonding, 76x100x1.0 mm glass slides (Knittel Glass) were immersed in Hellmanex III 1% (v/v) solution (Hellma Analytics) overnight. Hellmanex III is an alkaline liquid concentrate which must simply be mixed with water to yield an effective cleaning solution for quartz or

glass cells. In this study, this solution removed any contaminant such as grease from the glass slides, since a clear surface is required for an efficient oxidizing process.

Glass slides were then washed with DI water and dried with an N_2 gun. PDMS replicas were cleaned with EtOH to remove any surface debris such as residual PDMS or fibres and also rinsed with DI water and dried with the N_2 gun.

For the surface oxidizing procedure, the glass slides and PDMS replica were placed active side up on the chamber of the plasma cleaner (PDC-002-CE, Harrick Plasma). Oxygen plasma was generated at 800 mTorr, exposing the surfaces for 15 seconds. The active surface of the PDMS replica and glass slide were brought in contact to perform bonding. Theoretically, the bonding should occur naturally, however, since the replica contains high aspect ratio features such as the posts, some pressure needs to be carefully applied with tweezers over these structures with visual control on the optical microscope since bonding may not occur (Figure 2.3).

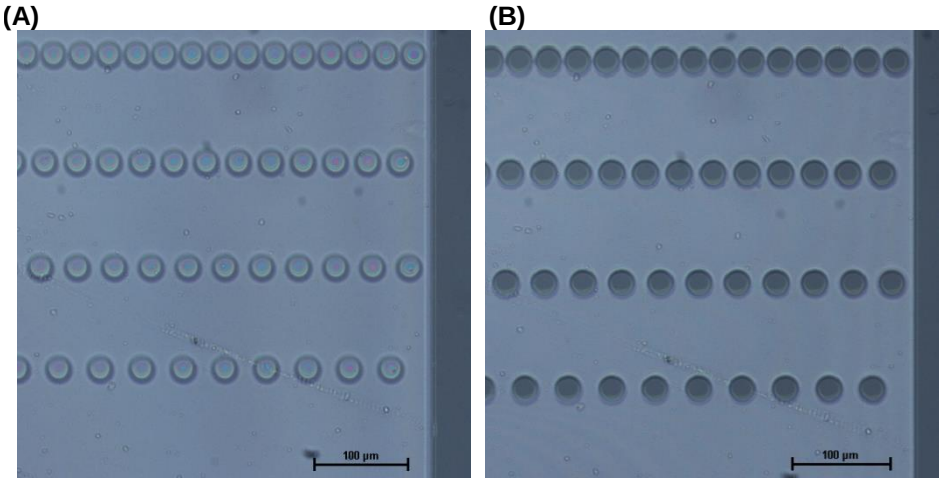

Figure 2.3. Visual inspection of the microposts on the device under the optical microscope before applying pressure (A) and after (B).

Following visual inspection, devices were placed upside-down at 65ºC for 30-60 min to reinforce the bonding without collapsing. Microfluidic platforms were left to cool down to room temperature before the tubing was placed.

Tubing (35cm and 15 cm length for inlet and outlet, respectively) was performed with 0.51x1.52 mm microtube Ethyl-Vynil-Acetate (Cole Parmer Instruments) and inserted with the aid of tweezers and an epoxy polymer (Araldite) at a mix ratio of 1:1.

2.2.2. Passivation

To increase the wettability of the channels, 250 µl of ethanol 70% (v/v) was pumped at 100 mbar using a pressure pump (Mitos P-pump range, dolomite). Channels were rinsed with 250 µl of Phosphate Buffered Saline (PBS) (Phosphate Buffered Saline tablet, 10 mM, pH 7.4, Sigma Aldrich) at 200 mbar. The surface was passivated with 250 µl 1% (w/v) Pluronic F-127 (Sigma Aldrich) in PBS at 300 mbar and devices incubated overnight at 4ºC with parafilm-sealed tubing and under tab water since PDMS is highly gas permeable.

2.3. Cell Culture and Sample Preparation

2.3.1. Model System for Bladder Cancer

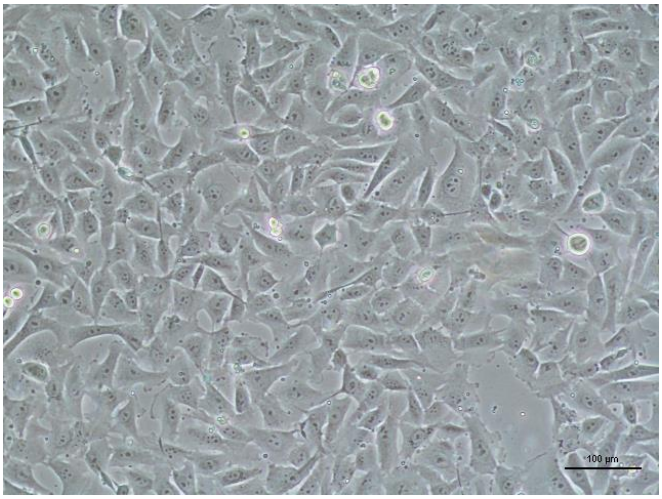

Figure 2.4. Bladder cancer cell line (HT1376) used as positive control for cell retention in the microfluidic device (10x). Scale bar: 100 µm.

HT1376 bladder carcinoma cells (Kindly provided by Dr. Alexandre Ferreira, IPO, Porto) were cultured in T-25 cell culture flasks (working volume of 5 ml) in complete Gibco RPMI 1640 Medium (1X) + GlutaMAX™ (ThermoFisher Scientific) supplemented with 10% (v/v) Heat-inactivated Fetal Bovine Serum (FBS) (Gibco) and 1% (v/v) Penicillin Streptomycin (Pen Strep, Gibco) and incubated in a humidified 37ºC/5% CO_2 chamber (Binder) until 80% confluent (around 3.00×10^6 cells). Cells were then harvested and either used for the experiments or maintained in culture. For sub-culturing, cells were washed with 5 ml of PBS pH 7.4 (1X) (Gibco) and incubated with 10% (v/v) of 0.25% Trypsin-EDTA (1X) (Gibco) in a humidified 37ºC/5% CO_2 incubator for 5 minutes for cell detachment. Cells were then checked under an inverted optical microscope (Nikon Eclipse TS100) and when in suspension, they appeared rounded and refractive. Residual cell clusters or adherent cells were dissociated by gentle agitation. Trypsin was inactivated by adding 5 ml of complete growth medium and gentle washing was performed in order to remove any remaining cells from the growth surface of the flask. Finally, cells were counted in a Neubauer chamber using the Trypan blue dye (Sigma)-exclusion assay, and used in subsequent experiments.

2.3.2. Peripheral Blood Mononuclear Cells Isolation

Human peripheral blood mononuclear cells (PBMCs) were obtained from blood collected on the day of the experiment from healthy volunteers, by density gradient centrifugation. Briefly, one unit of blood sample (3 ml) was carefully layered over one unit of pre-warmed Histopaque-1077 (Sigma Aldrich) without mixing the two solutions. The sample was then centrifuged (Centrifuge 5810 R, Eppendorf) at 650xg for 10 minutes without brake to avoid instantaneous mixing of the two layers. The PBMC layer was collected with a 15 ml plastic Pasteur pipette, transferred to a new 15 ml falcon tube, washed (Figure 2.5) with 5 ml of PBS-2%BSA and centrifuged again at 300xg for 10 min. After discarding the supernatant, cells were resuspended in 1 ml of PBS-2%BSA. For PBMC counting, Tuerk solution (Fluka

Analytical) was used. Tuerk contains 1-2% acetic acid, which lyses red blood cells and a nuclear stain that highlights in purple the nuclei of white blood cells. Cells were diluted at a ratio of 1:10 of Tuerk and a 10 µl aliquot counted in neubauer chamber.

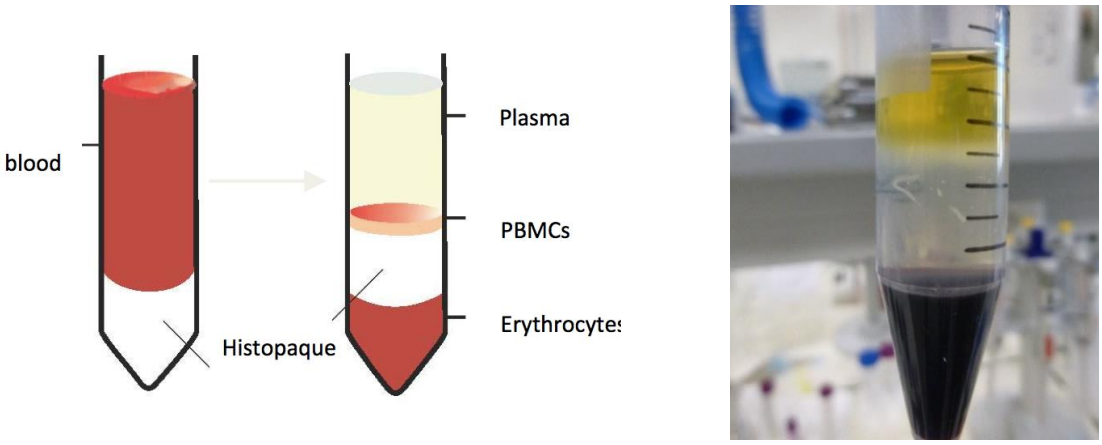

Figure 2.5. Density gradient centrifugation of whole blood.
Schematic representation of the process before (left) and after (middle) centrifugation and image of final separated state (right).

2.4. Microfluidic Device Performance

2.4.1. Capture Efficiency (Positive Control)

For positive control experiments, HT1376 cells were harvested as described above and stained with the cell-permeable dye Calcein AM (Sigma Aldrich) in order to visually count the cells under the fluorescence microscope. In live cells, the non-fluorescent calcein is converted to a green-fluorescent calcein after acetoxymethyl ester hydrolysis by intracellular esterases, so only viable cells will be fluorescent. Approximately $1x10^6$ cells in 800 µl of PBS were mixed with 1µl of 4µM calcein and incubated in a humidified chamber 37ºC/ 5% CO_2 for 20 minutes followed by 3 washing steps at 1000xg for 5 min with PBS. The supernatant was discarded and cells resuspended in a final volume of 1 ml of PBS, to achieve a cellular concentration of $1x10^6$ cells/ mL.

Next, serial dilutions were prepared so that a cell suspension of approximately 1000 HT1376 cells in 500 µL of PBS was obtained. This solution was then run in the microfluidic device at either 200 or 300 mbar using a pressure pump while monitored under the inverted optical fluorescence microscope (Nikon Eclipse MA200). To avoid any sudden increases in pressure and consequentially flow rate, pressure was gradually increased at 50 mbar intervals. At the end of the process, the microfluidic device was washed with 500 µL of PBS and cells fixed during 20 min with 250 µL of 4% (w/v) formaldehyde solution (Formalin, Sigma). A final washing step was performed to remove the fixative from the channels. Capturing efficiency of the microfluidic platform was determined by counting fluorescent entrapped cells.

2.4.2. PBMC retention (Negative Control)

PBMCs were obtained following the sample preparation protocol (section 2.3.2) and similarly to bladder cancer cells, were stained with Calcein-AM as described above to enable accurate detection of enrichment yields. For the negative control experiments, serial dilutions were prepared so that a cell suspension of approximately 10,000 PBMCs in 500 µL of PBS was obtained. The cells suspension was then run under the inverted optical fluorescence microscope by the same protocol as described in section 2.4.1. PBMC retention was determined by counting stained cells trapped on the microposts under the fluorescence microscope.

2.4.3. Spiking Experiments

In order to determine isolation efficiency, purity and enrichment ratio of the device, HT1376 bladder cancer cells (1000 cells) pre-stained with calcein were spiked to unlabelled PBMCs (10,000 cells) in a total volume of 500 µl of PBS. Cell suspension was then processed through the device at 200 mbar, and cells washed with 500µl of PBS, fixed with 250 µl of formalin for 20 min and finally washed again with 500 µL of PBS. Finally, the microfluidic platform was extensively examined and the number of labelled and unlabelled cells counted and registered.

2.5. Clinical Samples

Bladder washes and urine samples were collected at Centro Hospitalar do Porto-Hospital Geral de Santo António (CHP-HSA), from patients who previously underwent diagnostic or follow-up cystoscopy. Patients aged <18 years or patients who had received previous treatment with local or systemic chemotherapy or immunotherapy were excluded from this study.

Catheterized urine samples were collected immediately before surgery and transferred into 50 ml plastic falcons pre-filled with 5 ml of FBS. Bladder washes were collected in parallel, as a part of the TURBT protocol. After the cystoscope was inserted through the urethra into the bladder, saline buffer was irrigated within the bladder and 45 ml were collected into 50 ml plastic falcons pre-filled with 5 ml of FBS. Samples were processed on the same day of collection at the International Iberian Nanotechnology Laboratory (INL) in Braga. This study was approved by the Ethics Committee of the Hospital and sample collection performed after written informed consent was obtained from all subjects.

2.6. Clinical Sample Processing

2.6.1. Bladder Washes Pre-processing

Samples were pelleted by centrifugation (1000xg for 5 min) and resuspended in 1 ml of PBS-2%BSA. Red blood cell lysis was performed through the addition of 2 ml of lysis buffer (145mM Ammonium chloride (NH_4Cl), 10mM Potassium chloride (KCl) and 0.1mM EDTA) and after a 5 min incubation at RT, cells were centrifuged for 5 min at 300xg. Cells were then resuspended in 1 ml of TrypLE™ Select enzyme solution (ThermoFisher Scientific) and incubated for 5 min at RT to promote dissociation of possible cell aggregates present. Enzyme inactivation was performed by diluting cells in 1 ml of PBS-2%BSA.

Bladder washes were then pelleted via centrifugation (1000xg for 5 min), resuspended in a final volume of 10 ml of PBS-2%BSA and filtered through cell strainers (first 70 µm and then 40 µm) to remove any cell aggregates that might clog the device. In order to concentrate the sample, the filtered cell suspension was centrifuged at 1000xg for 5 min and cell pellet resuspended in 1 ml of PBS-2%BSA.

2.6.1. Urine Pre-processing

Non-voided urine samples were pre-processed as the bladder washes, including cell filtration using strainers with different pore sizes (70 and 40 µm). The final cell suspension was centrifuged at 1000xg for 5 min, and the pellet resuspended in 1 ml of RPMI complete medium with 10% DMSO and immediately frozen at -80ºC until further use. At the time of analysis, cells were thawed, resuspended in 5 ml of PBS-2%BSA, centrifuged at 1000xg for 5 min, resuspended again in 3 ml of PBS-2%BSA and passed through the 40 µm cell strainer. Finally, the sample was concentrated by centrifugation at 1000xg for 5 min and pellet resuspended in 1 ml PBS-2%BSA to run in the device.

2.6.2. Cell Isolation in the Microfluidic Device

All samples were visually monitored by microscopy during the microfluidic isolation to ensure no clogging of the device and also to analyse cell behaviour and distribution throughout the separation process. Processed bladder washes or urine samples were flown through the device at 200 mbar, and washed with 500 µl of PBS. Prior to sample fixation, and if necessary, 250 µl of TrypLE™ reagent was pumped into the device to dissociate cell aggregates and left to incubate for 5 minutes. Samples were washed with 250 µl of PBS and then fixed with 250 µl of Formalin solution during 20 minutes before a final washing step. Tubing tips were sealed with parafilm and devices immersed in water for storage at 4ºC until the immunostaining analysis.

2.7. Immunocytochemistry

2.7.1. Survivin Primary Antibody Conjugation

Anti-Survivin monoclonal antibody (Clone 9H18L32, ThermoFisher Scientific) was concentrated from 0.5 mg/ml to 1mg/ml using the AbSelect™ Antibody Concentration & Clean-up Kit (InnovaBiosciences) and labelled with DyLight® 755 (Lightning-Link® Rapid Conjugation System, InnovaBiosciences), a far red fluorescence emitting fluorophore.

2.7.2. Antibodies for Immunocytochemistry

Anti-cytokeratin-pan-FITC (1:100, Clone C-11, Sigma) and anti-CD326-Alexa Fluor 488 (EpCAM) (1:50, Clone 9C4, Biolegend) to identify epithelial cells, anti-CD45-cy5 (1:25, Clone HI30, Abcam) to identify white blood, anti-vimentin-eFluor 570 (1:50, Clone V9, eBioscience) for mesenchymal-like cells, and anti-survivin-Dylight 755 (1:25, Clone 9H18L32, Invitrogen, InnovaBiosciences) as a tumour cell identifying marker. 4',6-Diamidino-2-Phenylindole (DAPI) (1:1000 in ethanol, Sigma) was used as nucleus marker.

2.7.3. Immunocytochemistry in Tissue Culture Wells

Glass coverslips for tissue culture 24 microwell plates (13mm diameter, Deckglaser) were washed with 70% ethanol, rinsed with PBS inside the laminar flow hood to avoid contamination of the surface and then air-dried placed in a microwell plate. Approximately 100,000 HT1376 cells or PBMCs were harvested and spun down at 2500 rpm for 3 minutes (5810R, eppendorf) onto the coverslips. For spiking experiments, a ratio of 1:10 (HT1376:PBMCs) was used, for a total of 110,000 cells. After 4h-6h of incubation at 37ºC to promote adhesion, cells were washed twice with PBS and fixed with Formalin for 20 min at RT and stored in PBS at 4ºC until further use. For the immunostaining, cells were firstly permeabilised with 500 µl of 0.25% Triton X-100 (Sigma Aldrich) for 15 minutes, washed with PBS and incubated with 500 µl of PBS-2%BSA for 30 minutes to block unspecific binding of antibodies. For the immunostaining, anti-cytokeratin-pan-FITC, anti-CD326-Alexa Fluor 488 (EpCAM), anti-CD45-cy5, anti-vimentin-eFluor 570, anti-survivin-Dylight 755 antibodies and DAPI were incubated at RT for 1 hour. Cells were finally washed three times with PBS and kept in 1ml of PBS at 4ºC until imaged.

2.7.4. Immunocytochemistry in Microfluidic Devices

Firstly, permeabilization of fixed cells retained in the device was induced by pumping 250 µl of 0.5% Triton X-100 in PBS into the microfluidic platform and incubating for 15 minutes at RT. Channels were rinsed with 250 µl of PBS and non-specific antibody binding blocked with 250 µl of PBS-2%BSA for 30 min. Entrapped cells were stained using a cocktail of antibodies and nuclear marker (anti-cytokeratin-pan-FITC, anti-CD45-cy5, anti-vimentin-eFluor 570, anti-survivin-Dylight 755 and DAPI) in total volume of 250 µl of PBS-2%BSA. Both ends of tubing were sealed with parafilm and devices stored at 4ºC immersed in water and protected from light until imaging analysis by fluorescence microscopy.

3. Results and Discussion

In this section, the results obtained regarding: 1) device characterisation, 2) the capture efficiency and isolation purity of tumour cells in the microfluidic device, 3) the development and optimisation of a protocol for clinical sample processing and 4) the phenotypic characterisation of cells isolated from body fluids (bladder washouts and urine) of two bladder cancer patients will be described. A critical assessment of the results and platform objectives and utilities will also be presented in the end of this chapter.

3.1. Device Characterisation

In order to produce a non-invasive point-of-care device for early detection of bladder cancer, prior cancer cell isolation and enrichment must be performed. Moreover, for the development of a robust and specific assay, multiple biomarkers should be analysed to perform an accurate characterisation of the cancer cells present in the body fluid of interest.

In this project, a label-free microfluidic platform was designed, by the group, for size-based isolation and enrichment of cancer cells (Figure 3.1) as cancer cells are generally larger than their normal counterparts and those with higher metastatic potential are more deformable. The design consists in five rows of posts, with increasingly narrower gap widths (50, 20, 15, 10 and 5 µm) to separate cells according to their size and deformability, as it was proved effective by Mohamed *et al.* (2009)[42].

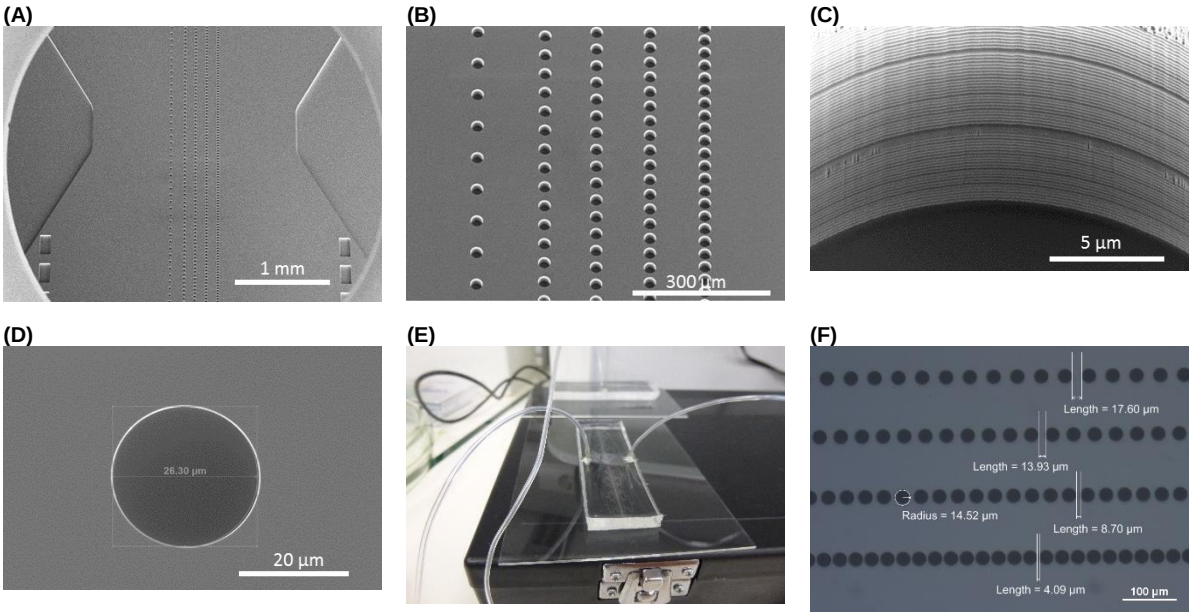

Figure 3.1. Master SEM inspection and microfluidic device characterisation.
(A) Overview of the master design and structure. **(B)** Close-up view of the five rows of gaps that will give rise to the posts in the microfluidic device. **(C)** Steep features and wave-shape roughness are obtained for each gap in the master as a consequence of the DRIE process. **(D)** Diameter measurement of one of the gaps. **(E)** Photograph of the microfluidic device after fabrication. **(F)** Visual inspection of the posts under the optical microscope.

Note that due to the large distribution of sizes that are inherent to bladder epithelial cells[12,39], a row of 50 µm spacing posts was added, which was not present in the work of previously mentioned article. Additionally, square posts were incorporated in the design for structural support of the channels as well as pre-filtering system to prevent debris and large cell clusters from flowing through. The

microfluidic master was designed to fabricate posts with 20 µm height, as it was considered the ideal height that did not allow cells to simply squeeze through and it was not low enough that would cause cells to be unspecifically retained.

3.2. Microfluidic Device Performance

Prior to the analysis of clinical samples in the microfluidic platform, the optimal cancer cell isolation conditions (efficiency) while retaining the minimum false positive cells (noise), were investigated using bladder cancer cell lines as a model.

Since high capture efficiencies and reduced sample processing times are desired, particularly when dealing with high sample volumes, several pressure conditions were previously tested by the group. From this analysis, two pressure conditions were selected for further assessment: 300 and 200 mbar. At 300 mbar cells were still viable and no device leaking was observed, whereas at 200 mbar cells squeezing between posts was prevented.

For these assays, at least three sets of independent experiments were conducted for each pressure condition, and the average percentage and standard deviation determined. The data regarding the number of isolated cells for each experiment can be found in Appendix A.

3.2.1. Cancer Cell Capture Efficiency

To evaluate the capture efficiency of tumour cells in the microfluidic device, experiments using a low number of HT1376 cells (1000 cells per 500 µl of PBS) were performed. PBS, commonly used in various cell culture applications, was used as a vehicle solution as it also closely mimics the saline buffer used to collect bladder washings during cystoscopy. Bladder cancer cells were pre-labelled with calcein as described in Material and Methods section and cell suspensions run at constant pressure differentials (200 or 300 mbar). Cells trapped on the microposts were counted by observation using fluorescence microscopy, and capture efficiency was determined using Equation 1.

$$Capture\ efficiency\ (\%) = \frac{(HT1376\ cells)_{trapped}}{(HT1376\ cells)_{inlet}} \times 100 \quad (1)$$

As illustrated in Figure 3.2, HT1376 bladder cancer cells were successfully captured at 200 mbar (Figure 3.2.A) and 300 mbar (Figure 3.2.B). However, a quantitative analysis over 3 independent experiments (Figure 3.3) indicates higher cell retention (37%) at 200 mbar, while only 16% of cells were captured at 300 mbar input pressure. This discrepancy can be explained by increased hydrodynamic forces acting on the cells trapped on the posts at higher pressure values, which causes cells to deform and squeeze through the posts (Figure 3.2.B). If the inlet pressure were too high, it would ultimately result in unspecific separation regardless of the size or deformability and the cells would flow though the device, with minimal retention.

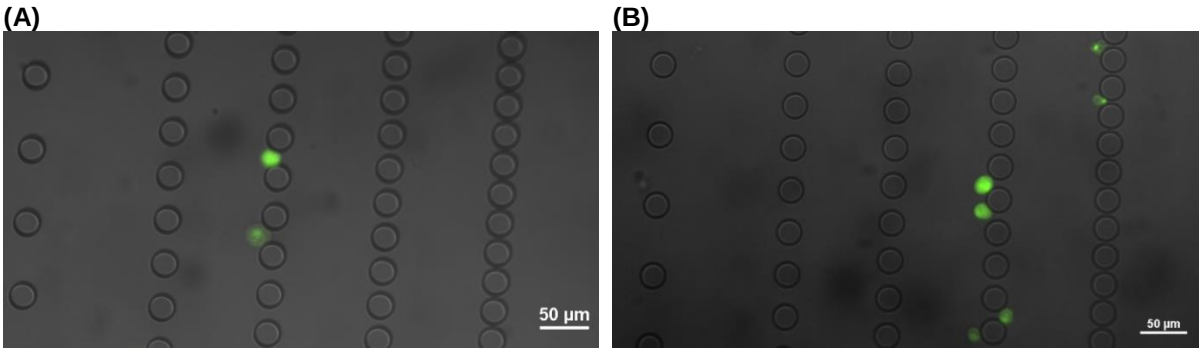

Figure 3.2. HT1376 bladder cancer cells captured in the microfluidic device.
Fluorescence photomicrograph of isolated bladder cancer cells pre-labelled with calcein (green) and run at 200 mbar (A) or 300 mbar (B) in the microfluidic device.

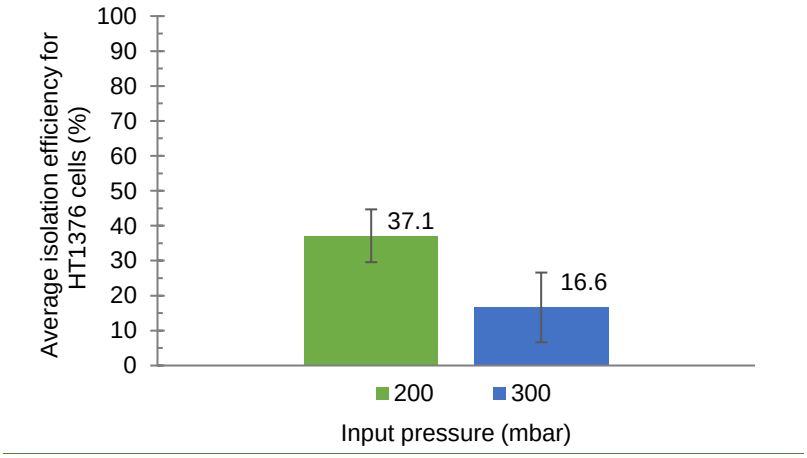

Figure 3.3. Quantification (%) of H1376 bladder cancer cell capture at two different inlet pressures (mbar).
Average isolation efficiency of three different experiments conducted at 200 mbar and 300 mbar. Error bars represent standard deviation.

3.2.2. PBMC retention

Since bladder cancer is associated with haematuria (blood in the urine) and inflammation other cell types, namely white and red blood cells, are expected to be present in bladder washes or urine of patients. Therefore, the retention of unwanted blood cells in the device was also ascertained. To address this, PBMCs were isolated from peripheral blood of healthy donors and 10,000 cells pre-labelled with calcein in 500 µl of PBS were run through the microfluidic device. Figure 3.4 shows examples of trapped cells analysed by bright field and fluorescence microscopy. PBMCs, which comprise lymphocytes and monocytes range between 7 and 15 µm in diameter and are highly deformable cells[52]. Hence, at high pressure conditions, the majority is expected to escape from the microposts.

Figure 3.5 shows that the average PBMC retention, determined using Equation 2, was indeed residual in both conditions. Thus, taking into consideration the better capture efficiency data obtained was at 200 mbar, this was selected as optimal input pressure and therefore used in all subsequent experiments.

$$Noise\ (\%) = \frac{(PBMCs)_{trapped}}{(PBMCs)_{inlet}} \times 100 \qquad (2)$$

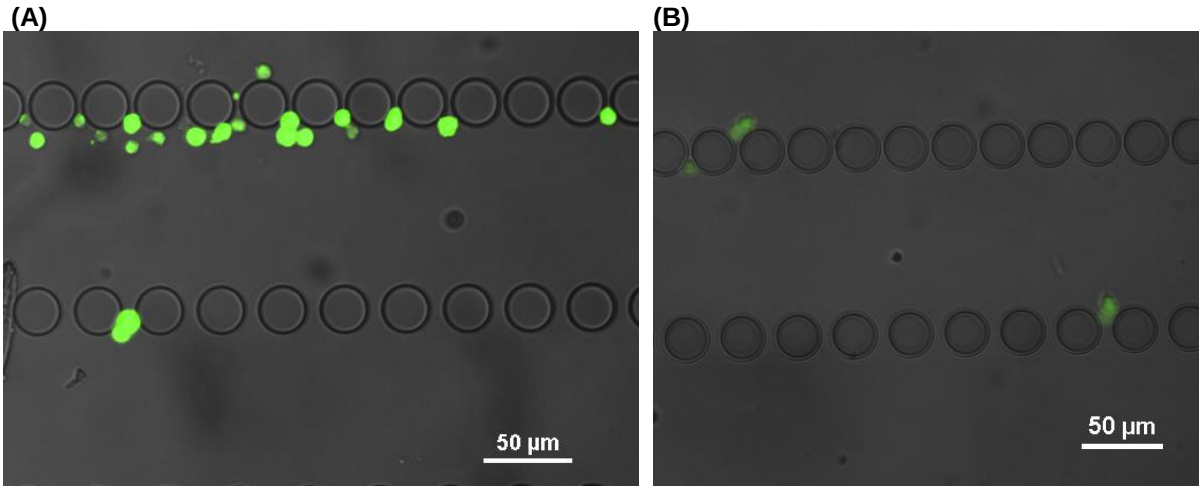

Figure 3.4. PBMC isolation in the microfluidic device.
(A) Negative control experiment performed at 200 mbar. The PBMCs, stained in green, are preferably trapped on the 5 µm gap row of posts. **(B)** Negative control experiments conducted at 300 mbar. Scant number of cells remain captured on the last row of posts since they are capable of squeezing through the gaps likely due to the high applied inlet pressure. The remaining cells are removed on the washing step.

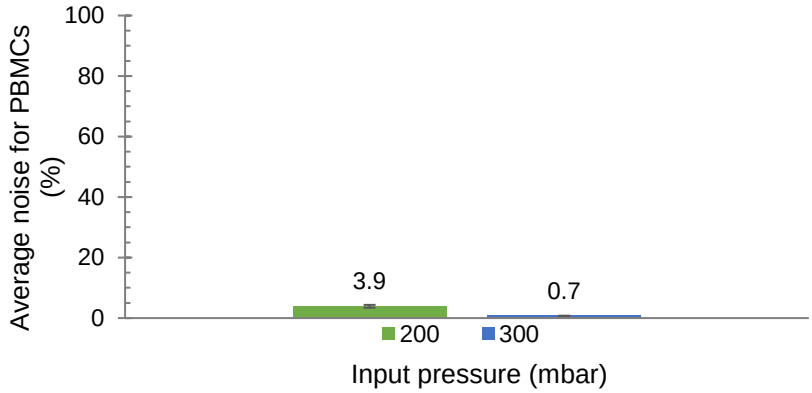

Figure 3.5. Quantification (%) of PBMC retention in function of the input pressure (mbar).
Average isolation efficiency of three different experiments conducted at 200 mbar and 300 mbar. Error bars represent standard deviation.

3.2.3. Spiking Experiments

To evaluate the performance of the device in terms of cancer cell capture purity, 1000 HT1376 cancer cells pre-labelled with calcein were spiked in 10,000 of unstained PBMCs, in a total volume of 500 µl of PBS, loaded and run in the microfluidic platform (Figure 3.6.). Results show that, for spiking experiments, the average percentage of leukocytes retained in the system remains around 4%. Importantly however, the average cancer cell retention percentage increased up to 50% (Figure 3.7.) in comparison to unmixed HT1376 cells (Figure 3.3), possibly due to hindrance caused by leukocytes. More importantly, an average purity of 62% was achieved as determined by Equation 3. Also, the system allowed the concentration of cancer cells in the system in comparison to the initial spiked sample by a factor of 22, determined by Equation 4.

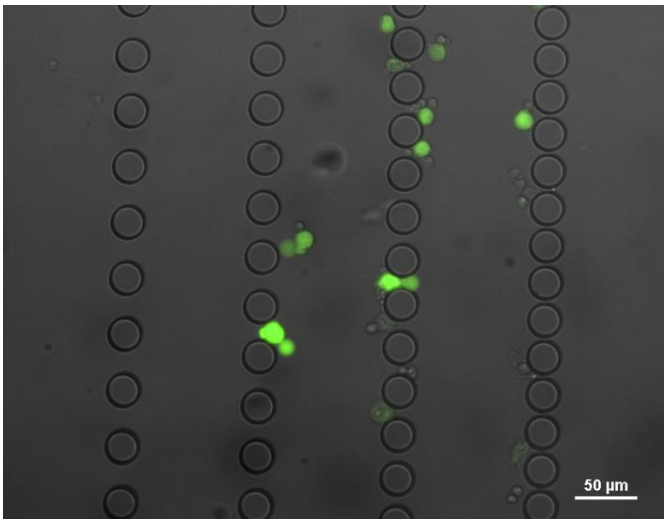

Figure 3.6. HT1376 cancer cells (green) spiked in PBMCs to determine the isolation purity and enrichment ratio.
1000 HT1376 cancer cells, stained in green, were spiked in 500 µl of PBS solution containing 10,000 PBMCs and run in the device at 200 mbar in order to evaluate the isolation purity.

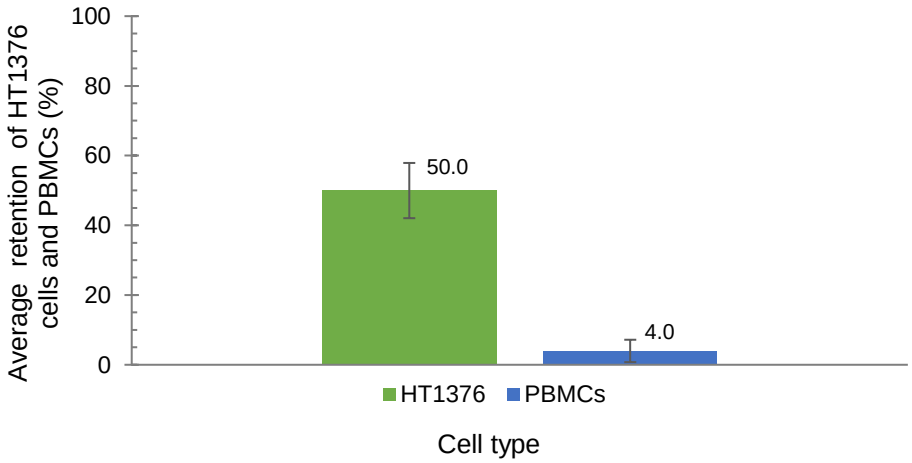

Figure 3.7. Quantification (%) of the retention of H1376 cancer cells and PBMCs at 200 mbar input pressure.
Average isolation efficiency of three different experiments conducted at 200 mbar. Error bars represent standard deviation.

$$Purity\ (\%) = \frac{(HT1376\ cells)_{trapped}}{(HT1376\ cells)_{trapped} + (PBMCs)_{trapped}} \times 100 \quad (3)$$

$$Enrichment\ ratio = \frac{(HT1376\ cells)_{trapped}/(PBMCs)_{trapped}}{(HT1376\ cells)_{inlet}/(PBMCs)_{inlet}} \quad (4)$$

3.3. Phenotypic characterisation of HT1376 bladder cancer cells

In order to identify rare tumour-associated cells in clinical samples, and more importantly, their different phenotypes (epithelial, mesenchymal or stem cell-like), specific tumour cell markers need to be used and their cellular expression investigated. Hence, we started by characterising cells of the bladder HT1376 line for the expression of the following markers: EpCAM and cytokeratins (CK) as epithelial, N-cadherin and vimentin, as mesenchymal and CD44 and CD133 as stem-cell like markers. In parallel, the hematopoietic marker CD45 was also included as a negative control.

Fluorescence activated cell sorting (FACS) was previously performed in the group in order to assess the level of expression of the different biomarkers (data not shown). The FACS analysis revealed that, in HT1376 cells, EpCAM expression was negligible. However high expression of pan-cytokeratin (pan-CK) at the cell surface was detected. Regarding the mesenchymal markers, no significant expression of N-cadherin was observed, contrarily to vimentin which was highly expressed. Within the panel of stem cell-like markers, it was found that this cell line did not express CD133 but had substantial expression of CD44.

Since the goal of this project is to phenotypically characterise cancer cells isolated from clinical samples in the microfluidic device, envisaging a potential diagnosis method, the chosen biomarkers should enable an adequate and accurate characterisation of the cells retained in the microdevice. Such characterisation, performed by fluorescence microscopy, was based on four different biomarkers. To provide a reliable assessment, the nuclear marker DAPI was necessary to ensure that the fluorescence signal was derived from a nucleated cell and not from unspecific debris or PDMS autofluorescence. As epithelial and mesenchymal markers are required for adequate cell phenotype characterisation, and indicative of tumour aggressiveness, pan-cytokeratin and vimentin fluorescently labelled antibodies were included in the biomarker panel. Finally, CD45 was used to identify blood cells that might be present in the sample. Since lymphocytes also express vimentin, only cells lacking CD45 expression were considered cancer cells. This prevented false-positive results for $DAPI^{+}$, $Vimentin^{+}$, CK^{-} cancer cells, which do not express CD45.

The next step consisted on the validation of the selected biomarker panel in the control samples. For that, HT1376 cells and PBMCs were platted alone or in combination and stained by immunocytochemistry according to section 2.7.3. Representative images of spiked tumour cells and PBMCs are illustrated in Figure 3.8 As previously verified by flow cytometry, HT1376 cells do not express EpCAM (Figure 3.8.A). However, these cells are $pan\text{-}cytokeratin^{+}$, $CD45^{-}$ (Figure 3.8.B) and $Vimentin^{+}$ (Figure 3.8.C).

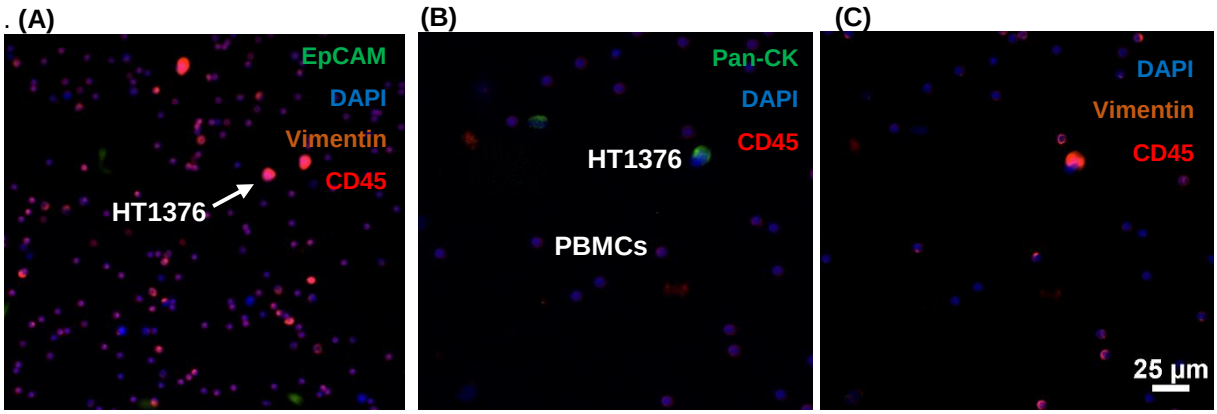

Figure 3.8. HT1376 bladder cancer cells spiked in PBMCs stained with a panel of biomarkers for phenotypic characterisation. Scale bar: 25 µm
Immunocytochemical evaluation of the expression of distinct biomarkers, evidencing the lack of EpCAM on HT1376 cells (A), in contrast to pan-cytokeratin (B) Vimentin is expressed in both cell types, with higher expression for the HT1376 cell (C).

Having confirmed immunofluorescence detection of the selected biomarkers in the bladder cancer cell line HT1376 and human PBMCs in microwell plates, we next investigated whether the same could be observed when cells are trapped inside the microfluidic device. Immunostaining inside the platform allows the evaluation of distinct biomarkers in each cell, which is essential to accurately define various cell types present in the sample as well as identify different cancer cell populations regarding their epithelial/mesenchymal phenotype.

Figure 3.9. shows a photomicrograph of a control spiking experiment, in which the retained cells were immunostained *in situ* with DAPI, pan-cytokeratin, vimentin and CD45 according to section 2.7.4. This analysis led us to some important findings: firstly, as it can be observed in Figure 3.9.A, the two distinct cell populations can be accurately characterised and distinguished by immunocytochemistry inside the device. The HT1376 cells are shown to express pan-cytokeratin^{+}, vimentin^{+}, DAPI^{+} and CD45^{-} whereas human PBMCs are pan-cytokeratin^{-}, vimentin^{+}, DAPI^{+} and CD45^{+}. This finding is extremely important since a clear visualisation of the several biomarkers is required for phenotype characterisation and cell type discrimination. Secondly, a cell distribution pattern can be identified. The PBMCs that remain trapped on the device are scant and when present remain on the 5 µm gap row of posts. On the other hand, HT1376 cells are isolated on previous rows, mainly on the 15 µm or 10 µm gap rows.

Even though the selected biomarker panel allowed the identification of different cell types in control samples, and is commonly used to identify circulating tumour cells in blood of cancer patients, analysis of other body fluids such as bladder washes or urine poses additional challenges. In bladder washes or urine, a larger number of cell types are expected to be present, particularly normal urothelial cells, which exhibit an epithelial phenotype, and shed from the bladder wall during the washing step of the cystoscopic evaluation. Hence, it is imperative to include an additional biomarker to distinguish normal from malignant bladder cells, and more importantly, discern their different phenotypes, as summarised in

Table 3.1.

In contrast, when analysing blood samples, only malignant epithelial cells are expected so all epithelial positive cells should originate from the primary tumour.

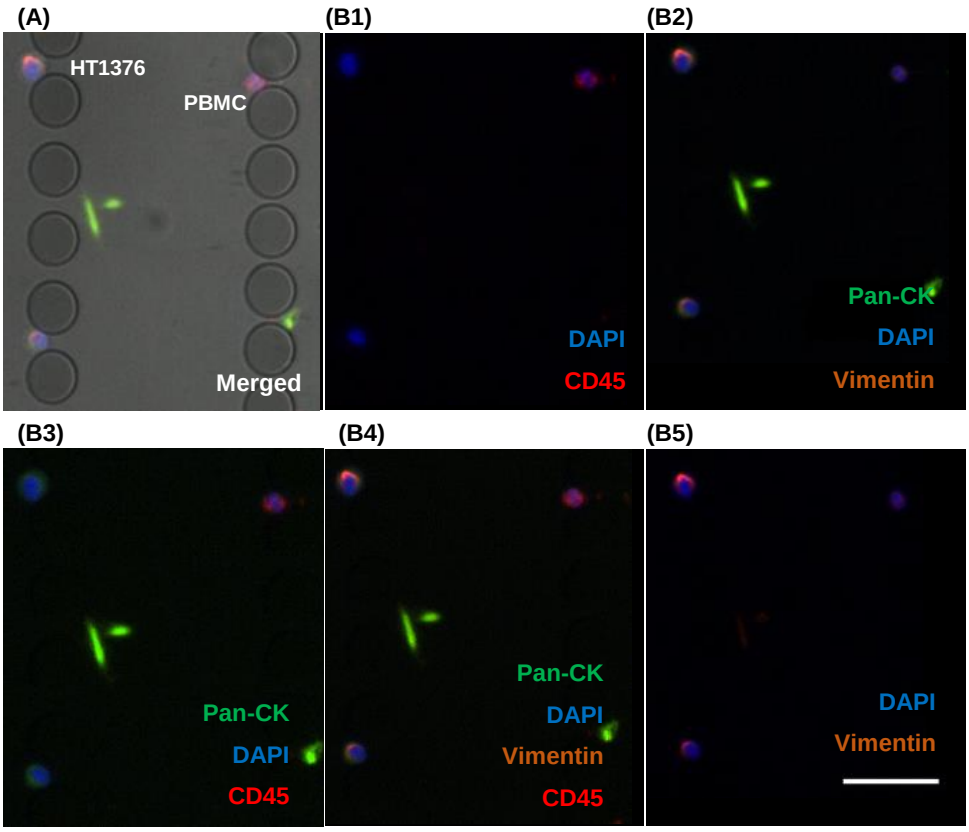

Figure 3.9. Immunocytochemistry performed inside the microfluidic device for retained HT1376 cancer cells and PBMCs. Scale bar: 50 µm
(A) Photomicrograph in Bright Field and Fluorescence channels for the retained HT1376 cells and PBMCs in one section of the device after immunostaining. **(B)** Split of the different fluorescent multi-channels for clearer visualisation of the expression of the different biomarkers. **(B1)** CD45 is only expressed by PBMCs; **(B2)** pan-cytokeratin is solely expressed in HT1376 cells while vimentin is expressed in both cell types, with higher expression in the cancer cells; **(B3)** Clear distinction between cancer cells and PBMCs, though the expression of epithelial and Leukocyte markers; **(B4)** Expression of the four biomarkers in both cell lines; **(B5)** Intense expression of vimentin in the HT1376 cells and mild expression in PBMCs.

Table 3.1. Distinct cellular populations possibly present in bladder washes and urine samples and expected biomarker expression

Cell type	DAPI	Cytokeratin	Vimentin	CD45	Tumourigenic biomarker
Haematopoietic cell	+	-	+	+	-
Normal Urothelial cells	+	+	-	-	-
Cancer cell with an epithelial phenotype	+	+	-	-	+
Cancer cell in EMT	+	+	+	-	+
Cancer cell with a mesenchymal phenotype	+	-	+	-	+

Survivin, an apoptosis inhibitor, is highly expressed in a large variety of solid tumours and haematologic malignancies and is absent or under expressed in normal adult tissues. In bladder cancer, it has been reported in a large number of studies as a potential diagnostic biomarker, particularly in the detection of early stage and low-grade tumours, which is the main limitation of urine cytology[12,26,27]. Thus, it was selected and included in our biomarker panel to specifically detect bladder cells of malignant origin.

Prior to assessing clinical samples, the expression levels of the survivin were evaluated on control HT1376 cells. Figure 3.10.A represents a photomicrograph of the HT1376 cell line stained for both survivin and DAPI.

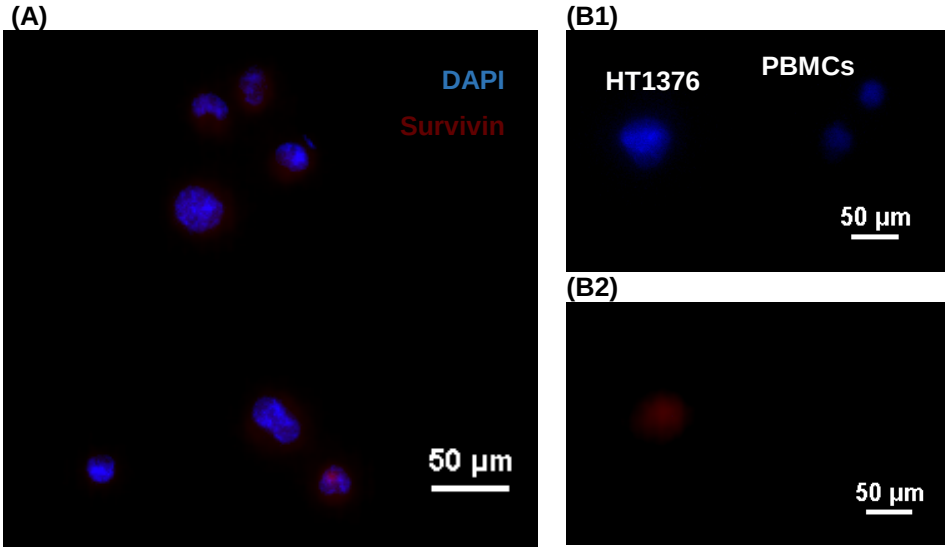

Figure 3.10. Survivin immunostaining of the HT1376 bladder cancer cells and PBMCs in tissue culture wells. **(A)** HT1376 bladder cancer cells stained for DAPI (blue) and Survivin (far red). **(B)** HT1376 bladder cancer cells spiked in PBMCs for survivin expression. **(B1)** Nuclear staining with DAPI (blue) of the HT1376 cancer cells and PBMCs. **(B2)** Survivin staining of cells from Figure B1. Mild intensity is obtained for HT1376 cells while no visible expression is detected in PBMCs.

As illustrated in Figure 3.10.B, positive survivin expression was observed in spiked HT1376 cells when compared to white blood cells. This result was of extreme importance for the project progression. Considering that the antibody-fluorophore conjugate was done in the laboratory and that the microscope was not originally optimised for far red observation, the presence of far red fluorescence indicates that the conjugation step was successful. More importantly, high survivin expression was observed in HT1376 cancer cells whereas no expression was visible in PBMCs. This result validates the phenotypic characterisation described in Table 3.1.

Prompt by these great results, we then moved to clinical sample analysis using this panel of five biomarkers. Identification of cancer cells ($Survivin^{+}/CD45^{-}$) as well as their phenotypic characterisation (pan-cytokeratin and vimentin) was pursued.

3.4. Clinical Sample Pre-Processing

Clinical samples were collected at the hospital during TURBT and analysed in the same day in the laboratory, as described in section 2.6. The pre-processing protocol was applied equally to both bladder washes and urine samples. However, since the specimens had to be processed in the same day to ensure sample quality, bladder washes were prepared for microfluidic analysis in that same day while urine samples were frozen at -80ºC with 10% DMSO after pre-processing until further used.

Since the purpose of this project is to isolate and characterise bladder tumour cells for early diagnosis using microfluidics the samples must be as clean as possible. Noteworthy, bladder washes and urine are incredibly complex matrixes that require a demanding pre-sample processing.

These specimens contain a large variety cells of different sizes, aggregates and debris[12] that can potentially clog the microchannels and interrupt the flow, therefore filtrations are compulsory for the first processing steps. Another main requirement of sample pre-processing for microfluidics is the volume reduction of the initial sample. In this work, around 50 ml of biological fluids were collected at the hospital. This would require several days to process in the microfluidic device and without a continuous flow cells would sediment and form aggregates, obstructing the tubing. In order to avoid this, target cells could be concentrated to a smaller volume or alternatively only a limited volume of the initial sample (for instance the capacity of the system) could be analysed. Herein, the first option (sample concentration from 50 ml to 1 ml) was considered so that all cellular information derived from the specimens was evaluated. This way minimal rare cell loss was ensured, which is critical when searching for such scarce events.

Taking into consideration the previous aspects, the initial pre-processing protocol incorporated a small number of steps, based on the study of Covey *et al.* [53] from 2013. Firstly, a centrifugation step was performed to remove the FBS present in the specimen, which was added in order to improve cell viability by providing a growth factors. This step was also applied to exchange the buffer solution to PSB-2%BSA. Afterwards, a filtration step was performed with a 70 µm cell strainer to remove large cell aggregates and debris. Lastly, the sample was concentrated by centrifugation to a final volume of 1 ml (Figure 3.11).

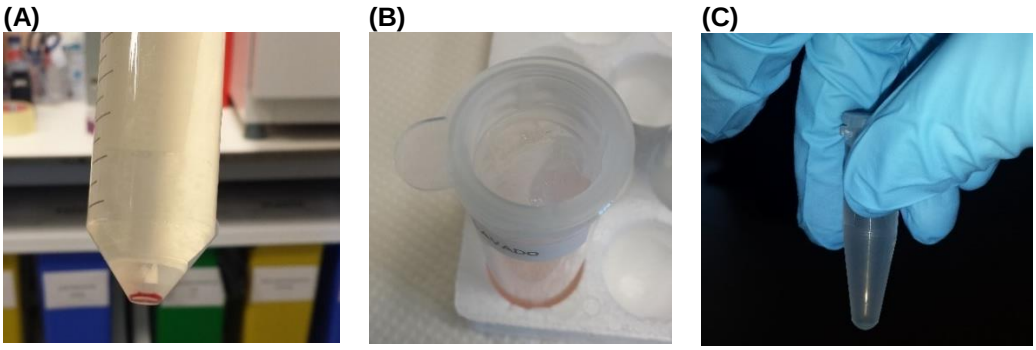

Figure 3.11. Initial pre-processing protocol of the bladder washes and urine.
(A) Centrifugation of the bladder wash at 1000xg for 5 min to remove the FBS present in the sample and perform a washing step with 10 ml of PBS-2%BSA **(B)** Filtration step with a 70 µm cell strainer to remove the main cell aggregates and debris **(C)** Concentration of the sample to a final volume of 1 ml to run in the microfluidic platform.

However, this initial protocol had to be adapted and improved according to technical challenges faced at the time of sample pre-processing. Thus, the protocol varied slightly among patient samples (Table 3.2) until an optimal and final protocol was achieved.

Initially, in the pre-filtration step, only the 70 µm cell strainer was used, however after processing the bladder wash of patient 1, high level of debris which obstructed the line of posts as well as the pre-filters was observed in Figure 3.12.A. This issue severely compromised the imaging and diminishes quality of detection of a cell or even the evaluation of its phenotype. To overcome this issue, another filtration step with a 40 µm cell strainer was introduced in the protocol (Step 2 Table 3.2).

Even though the 40 µm cell strainer helped diminish the device clogging, it was insufficient due to the formation of cell clusters and debris aggregation for patient 2. Adding to the filtration step, it was necessary to incorporate a step that would disable or avoid the formation of cell clusters. In a first attempt, the sample was vortexed to help dissociate cell clusters while being as minimally invasive as possible (Step 3 Table 3.2). Nevertheless, this step failed short to dissociate the aggregates as the sample reached the same condition after a few minutes in the pressure pump.

Since the mechanical dissociation did not achieve the desired results for cell cluster separation, a chemical dissociation method was implemented at this stage. Trypsin is frequently used in the laboratories, particularly in cell culture, for cell dissociation and detachment from the matrix. As this protease might potentially degrade surface proteins of interest in an immunocytochemical evaluation, other alternatives were searched that could produce the same effect and diminish the risk of degradation. TrypLE™ reagent contains recombinant cell-dissociation enzymes that replace porcine trypsin and is aimed to protect cell surface proteins. Also, when developing a sample processing protocol, the aim is to develop a fast and easy process with just key steps. This solution can be stored at room temperature, so it is ready to use and the inactivation of the enzyme is done by dilution, so trypsin inhibitors (like FBS) are not required. The enzyme solution proved to be more effective than the applied vortex as it allowed cell dissociation without compromising its integrity and the disruption of the larger cell debris (Figure 3.12.B1-2). This step became essential in the processing protocol and was incorporated for the samples once it was validated (Step 4 Table 3.2).

Table 3.2. Implemented sample processing steps for each patient and sample analysed.

	Patient ID	1		2		3		4		5		6	
	Sample	BW	U	BW	U	BW	U	BW	U	BW	U	BW	U
Step	Sample processing												
1	Pre-processing	x	x	x	x	x	x	x	x	x	x	x	x
2	40 µm cell strainer		x	x	x	x	x	x	x	x	x	x	x
3	Vortex					x							
4	TryPLE in solution		x		x		x	x	x	x	x	x	x
5	Red blood cell lysis								x	x	x	x	x
6	Dilution								x				
7	Volume analysed (ml)	1	0.5	1	0.5	1	0.5	0.5	0.5	0.5	0.5	0.5	0.5
8	TryPLE in the device		x				x	x		x		x	

Nonetheless, while running the sample in the device, if the cell pellet to process was very dense, the device would get clogged rapidly. At this point, the TrypLE™ reagent was flown in the device to provide single cell isolation and remove, at the same time, obstructing cell debris. The incorporation of the reagent proved to be effective to prevent clogging of the first rows and helped dissociate some cell

clusters. However, in the cases where the device had an extended degree of debris or cell content trapped on the pre-filters, these would not be removed from the device and would accumulate on the first rows (Figure 3.12.B3). Considering the previous scenario, the enzyme solution should only be flown through the device if cell clusters or debris were located in the first rows (Step 8 Table 3.2.).

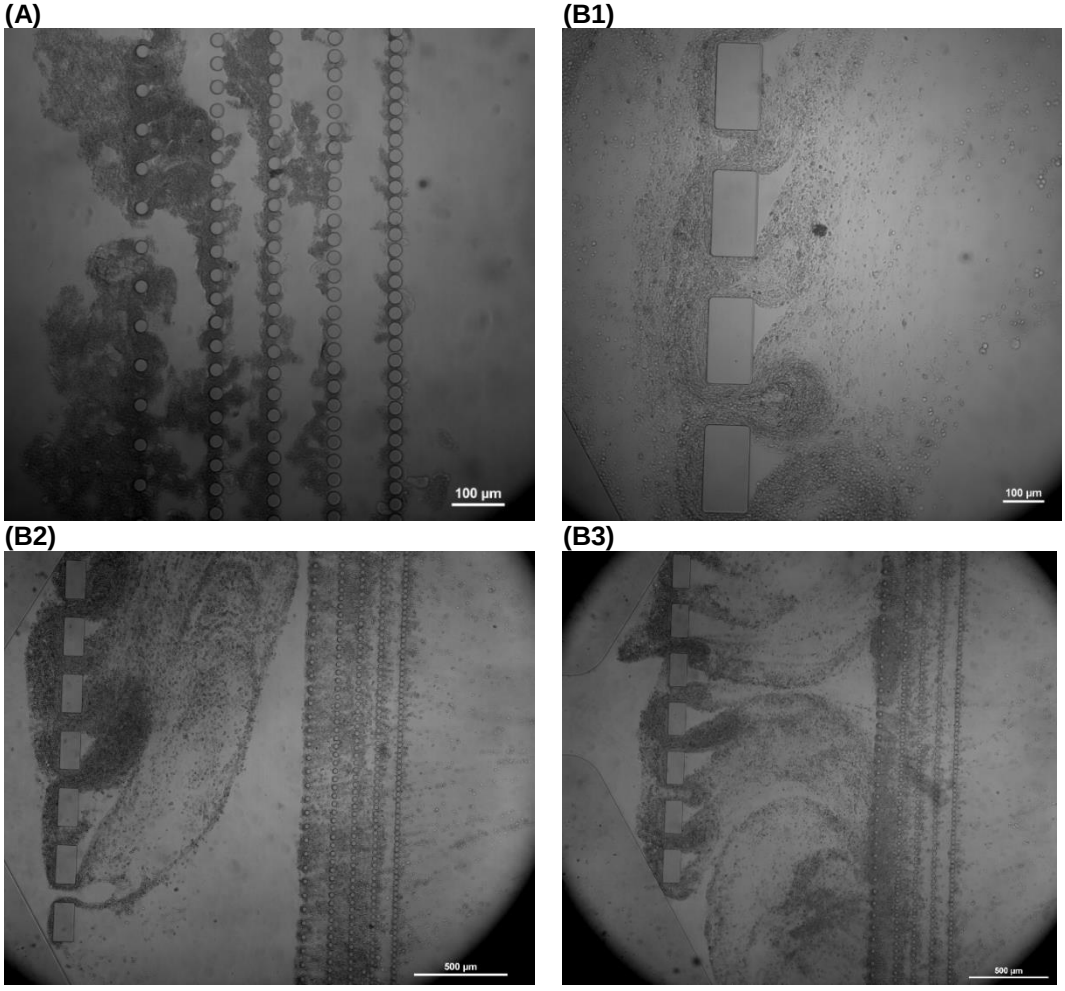

Figure 3.12. Device status during the sample processing protocol optimisation.
(A) Obstruction of the first line of posts due to the entrapment of debris from the bladder wash from patient 1 **(B1)** Initial formation of cell clusters and cell-matrix aggregates **(B2)** Clear obstruction of the 50 µm gap posts. **(B3)** Cell and aggregate dissociation by TryPLE reagent addition in patient's 4 bladder wash sample.

Red blood cells in the sample would not cause clogging of the system per se but could potentially cause hindrance and block the passage to other cells. Hence, red blood cell lysis was incorporated in the sample processing protocol (Step 5 Table 3.2). Still, the posts remained clogged or with high cell or debris density, possibly due to the existence of a large number of cells in a very small volume. Thus, the processed volume was further reduced by half (Step 7 Table 3.2.).

Despite all efforts, in a particular case, additional mechanic cell dissociation was still required to efficiently run it in the device. After pre-processing the urine of patient 4, the elevated cell density interrupted the flow and obstructed the microchannels (Figure 3.13.A). At that point, the experiment had to be interrupted and after a few minutes a large cell pellet was formed in the eppendorf (Figure 3.13.B), which indicated that the sample required further pre-processing and that the analysis had to be performed with a less concentrated sample. For that, the eppendorf was vortexed at 800 rpm for 30 seconds to slightly dissociate the cell pellet and the solution was agitated at 500 rpm for 3 minutes to

promote dissociation (Figure 3.13.C), 500 µl of supernatant were collected and diluted 1:2 in PBS-2%BSA and from this stock, only 500 µl were processed on the device. The implementation of this step permitted cell isolation in the system without the compromising the integrity of the device.

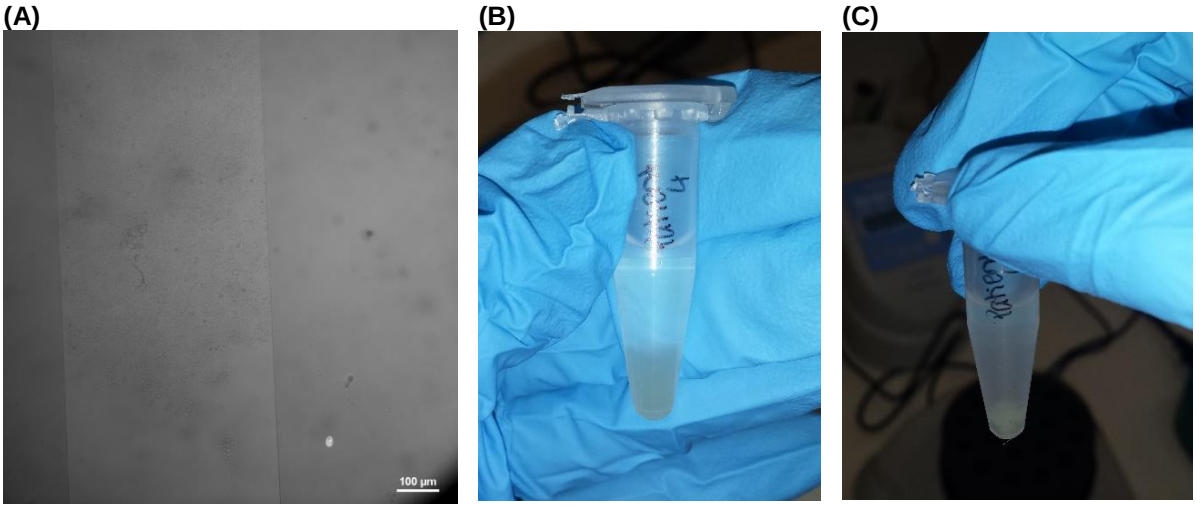

Figure 3.13. Urine processing of patient 4 and device clogging.
(A) Photomicrograph showing the inlet clogging of the microfluidic device used to run the cell pellet from the urine of patient 4. **(B)** Visible high density pellet formation after the flow on the device was interrupted due to the obstruction of the channels and tubing. **(C)** Same tubing as presented in (B) after the vortex of the cell suspension at 800 rpm for 30 seconds to slightly dissociate the cell pellet.

One of the objectives of this project was the development of a pre-processing protocol that would allow an efficient isolation of rare cells in the platform. Given the complexity of clinical samples as compared to control cell lines, adjustments to the initial protocol have been performed. Further improvements are expected to result in the creation of a standard operating procedure.

3.5. Bladder cancer cell detection and phenotypic analysis

Bladder washes and urine samples from 6 patients were processed and immunostained in the microfluidic device. However, due to time and technical constrains, not all could be fully analysed at the time of submission of this thesis. The results obtained for both bladder washes and urine samples from patients 1 and 6 will be thoroughly described and discussed below. Data regarding other patient samples will also be commented in this section, yet the photomicrographs of the remaining patients will be present in Appendix B since the phenotypic analysis was not performed at the time.

3.5.1. Bladder Wash analysis

The processed bladder wash samples contained a diverse variety of cell types. By the visual inspection of the various patients, five main cell morphologies were observed:

- Irregularly shaped cells with a translucent cytoplasm and small nucleus (ICTC)
- Cells with a round and defined membrane and with a dense cytoplasm (RCDC)
- Large and irregular cells with a dense cytoplasm (ICDC)
- Cell aggregates (CA)
- Haematologic cells (HC)

Despite this morphological diversity, cells displaying the same morphology varied incredibly in size, thus it was impossible to establish a direct correlation between the different cell types and their location in the microfluidic filter. Nevertheless, it was possible to establish cell behaviour patterns under the microscope, as discussed below.

Irregular translucent cells are highly deformable and are able to squeeze through the first line of posts (50 µm). Due to their larger size, these cells are normally isolated in the first two rows (50 and 20 µm, respectively).

The second type of cells are possibly the main type of cells isolated in the system. These cells exhibit a considerable size range and therefore are trapped on the different rows. Generally, these cells appear to be quite rigid and are normally retained due to their size, nevertheless some cells appear to have the capacity to squeeze through the posts, suggesting that two different sub-populations co-exist within this category.

Large and irregular cells with dense cytoplasm are very similar with the previous in terms of behaviour but the cell contour does not present a round form.

Cell aggregates can be present in many different forms and sizes. In some patients, particularly in the first set, some cells appeared to be trapped in a matrix of debris or possible extracellular matrix. Other aggregates consisted solely on cell clusters nearly impossible to individualise, even increasing the number of steps in the pre-processing. While the cell-matrix aggregates are isolated preferentially in the 50 and 20 µm rows, due to the dense cell-matrix network, the cell clusters are nearly impossible to establish a pattern at this stage. Firstly, these cell aggregates vary deeply in size due to the number and dimension of each cell present in the cluster and also, some cells appear to be more deformable than others, possibly squeezing through the posts and reaching further rows.

Haematologic cells are a scant population present in the device. Although these cells are present in some extent in the specimens, the majority is eliminated during the pre-processing and the remainder are eliminated in the system. If present, these cells are expected to be retained in the last two rows of posts.

Samples from patient 6 were the first subjected to phenotypic analysis, as at this stage the pre-processing protocol was relatively optimised. Also, during the entire pre-processing, both bladder wash and urine specimens, were relatively clean, without any extensive cell pellet or red blood cells. Figure 3.14 represents two different sections of the microfluidic device at the end of the experiment.

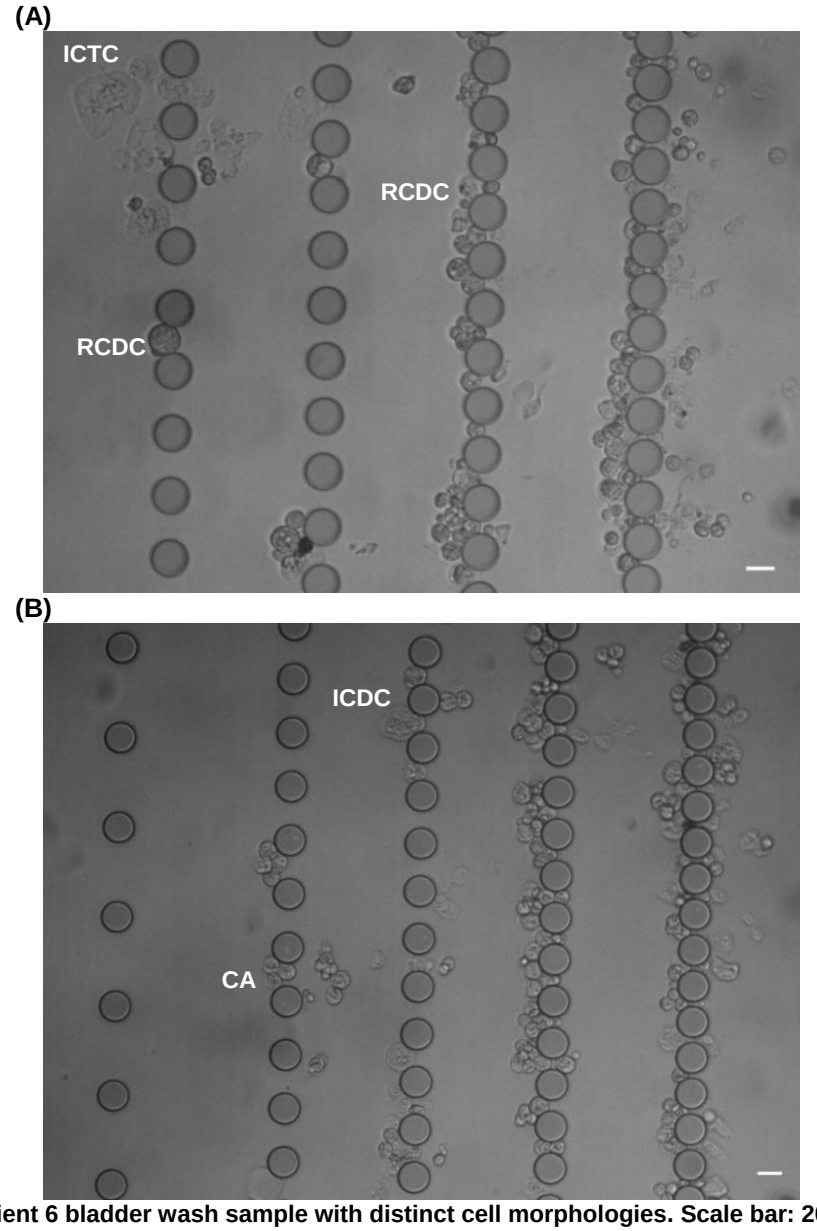

Figure 3.14. Patient 6 bladder wash sample with distinct cell morphologies. Scale bar: 20 µm
(A) Photomicrograph of one region of the bladder wash microdevice where irregular shaped cells with translucent cytoplasm (ICTC) are isolated in the first rows. Round cells with defined membrane and dense cytoplasm and various sizes (RCDC) represent the majority of the isolated cells. **(B)** Different region of the same device, in which it is visible the isolation of cell aggregates (CA) and irregular shaped cells with dense cytoplasm (ICDC).

In the 20 µm row of posts in Figure 3.14.A, it is possible to visualise the presence of two different cell types: round with defined membrane and dense cytoplasm (RCDC), with sizes equal or superior to 20 µm, and translucent irregular cells (ICTC). Regarding the latter, it is clear that these cells are highly

deformable and are able to squeeze until the following row (15 µm gaps). Different photomicrographs of the same device were taken to investigate a possible pattern of cell separation in the system. Figure 3.14.B represents a different section in which no cells were entrapped on the 50 µm gap row and only clusters and cells with a dense cytoplasm were retained. As it is evident, the majority of cell clusters are isolated in the 15 µm and 10 µm gap rows. The same can be verified for patient 1, still it is impossible to make a better assessment due to the submerging extent of debris (Figure 3.15).

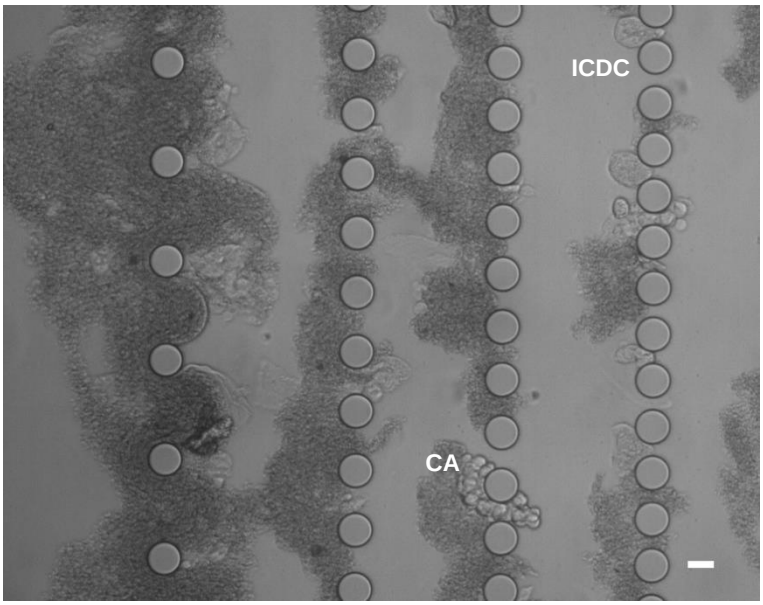

Figure 3.15. Bladder wash of patient 1 where debris and different cell morphologies are explicit. Scale bar: 20 µm

Even experienced cytopathologists may have several difficulties in distinguishing cells simply by cytomorphologic criteria, particularly normal urothelial from potential tumourigenic cells. Moreover, the classification criteria of atypical cells is not consensual in the field. On the other hand, therapeutic tailoring depends on the aggressiveness and metastatic potential of cancer cells, more than their enumeration. Therefore, immunocytochemistry *in situ* with the optimised panel of biomarkers, tested in control samples (DAPI, pan-CK, vimentin, survivin and CD45), was incorporated to perform phenotypical analysis (Figure 3.16).

The observation of Figure 3.16.A indicates the presence of a significant cell number retained in the system, particularly in the 5 and 10 µm gap rows, along with minimal debris. Figure 3.16.B is representative of pan-cytokeratin staining and results show that the majority of the cells are cytokeratin positive and thus display an epithelial phenotype. Further analysis suggests that cells present in the 20 and 15 µm gap rows, particularly those with round and dense cytoplasm cells as well as cell aggregates, exhibit a clear epithelial phenotype due to the intensity of the signal detected. Interestingly, fluorescence labelling intensity decreases when moving further from the 20 µm rows, and is only significant for some isolated cells.

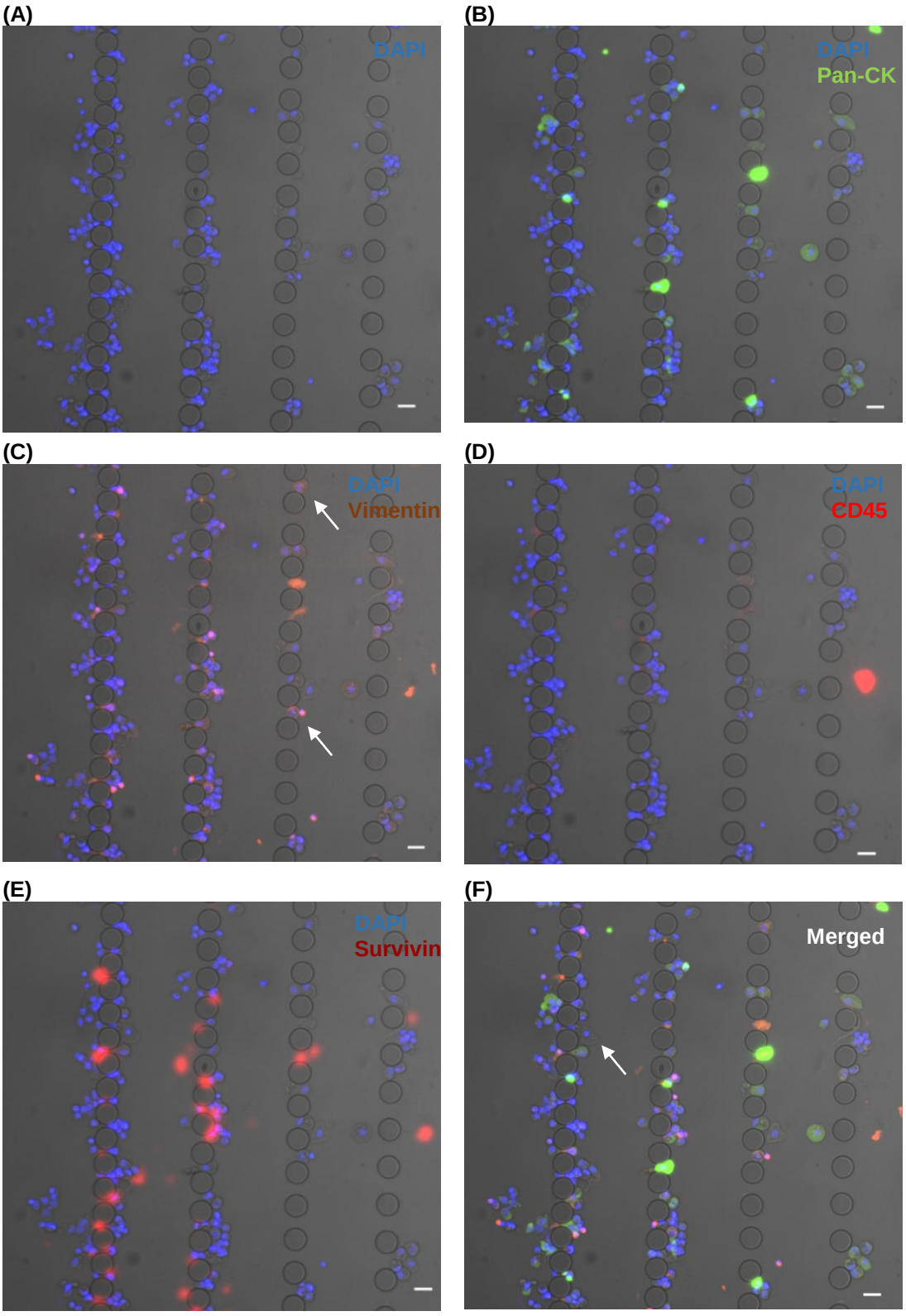

Figure 3.16. Bright Field and split fluorescence channels of one section of the bladder wash device of patient 6. Scale bar: 20 µm

In these micrographs the line of posts that appear from left to right are relative to the 5, 10, 15 and 20 µm gaping. **(A)** Immunocytochemistry performed with DAPI for a clear observation of the nucleus. **(B)** Epithelial phenotype represented by pan-cytokeratin expression **(C)** Mesenchymal phenotype by vimentin and DAPI expression **(D)** CD45 expression for the target of leukocytes **(E)** Survivin immunostaining for the visualisation of tumourigenic cells **(F)** Merged channels for DAPI, pan-cytokeratin, and vimentin.

When assessing mesenchymal marker expression (Figure 3.16.C) it is possible to observe that the majority of cells express vimentin, however the signal intensity is not as strong as the green signal. Even though expression seems to be stronger in cells trapped in the 5 and 10 µm rows, two additional cells located in the 15 µm gap row (indicated with arrows) also appear to have significant vimentin expression. To rule out these cells as lymphocytes, CD45 labelling was assessed (Figure 3.16.D) and no significant expression was found. This suggests that these cells have more mesenchymal-like characteristics.

Finally, survivin immunostaining indicative of malignancy was investigated. As shown in Figure 3.16.E, the intensity of the signal obtained was faint, most probably due to technical constrains, as only 30% of the light can be detected at this wavelength by the camera. It should be noted though that this was the only possible fluorophore that could be combined with the other biomarkers. To improve the detection capacity, as the light focus directly on the cell of interest, analysis at a higher magnification (60x) was performed.

Figure 3.16.F is a merged image of different channels (blue-DAPI, green-pan-cytokeratin, orange-vimentin) showing, in the last row of posts, a cell (indicated by the arrow), that, remarkably, is negative for all biomarkers tested. This suggests that other cell subpopulations not investigated herein, like CSC, might be present, highlighting the relevance of evaluating other biomarkers or analysing genetic alterations on isolated cells.

Strikingly, as illustrated in Figure 3.17, a survivin positive cell was detected in the bladder wash sample from patient 6, along with the pan-cytokeratin and vimentin, indicating that this cell might be undergoing an EMT process.

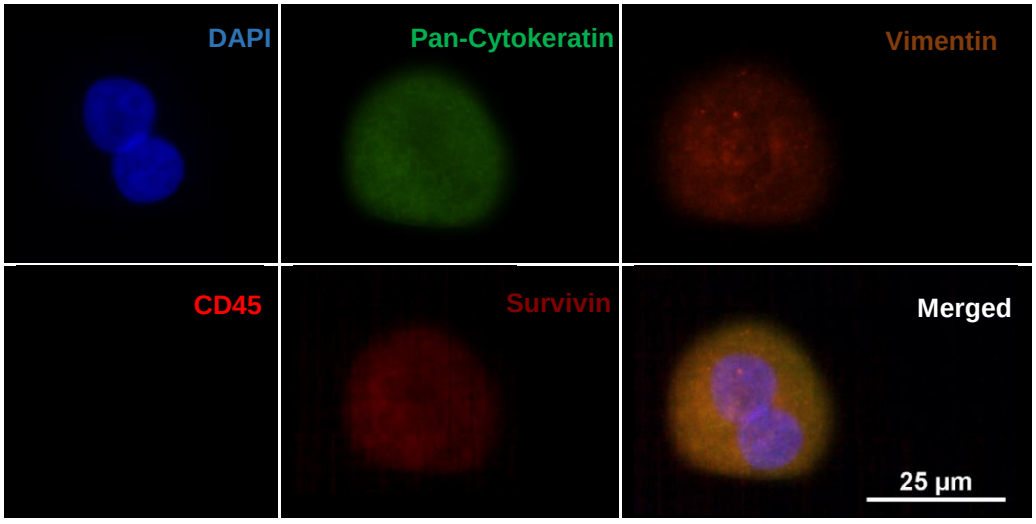

Figure 3.17. Survivin-positive cell isolated in the bladder wash microfluidic device of patient 6.

A very interesting aspect of this cell is not only its survivin expression but also its binucleation, evident with the DAPI staining. Notably, binucleation is indicative of mitotic dysfunction and commonly associated with malignancy[54]. In Figure 3.18, cells differently expressing the analysed biomarkers can be seen trapped in the device.

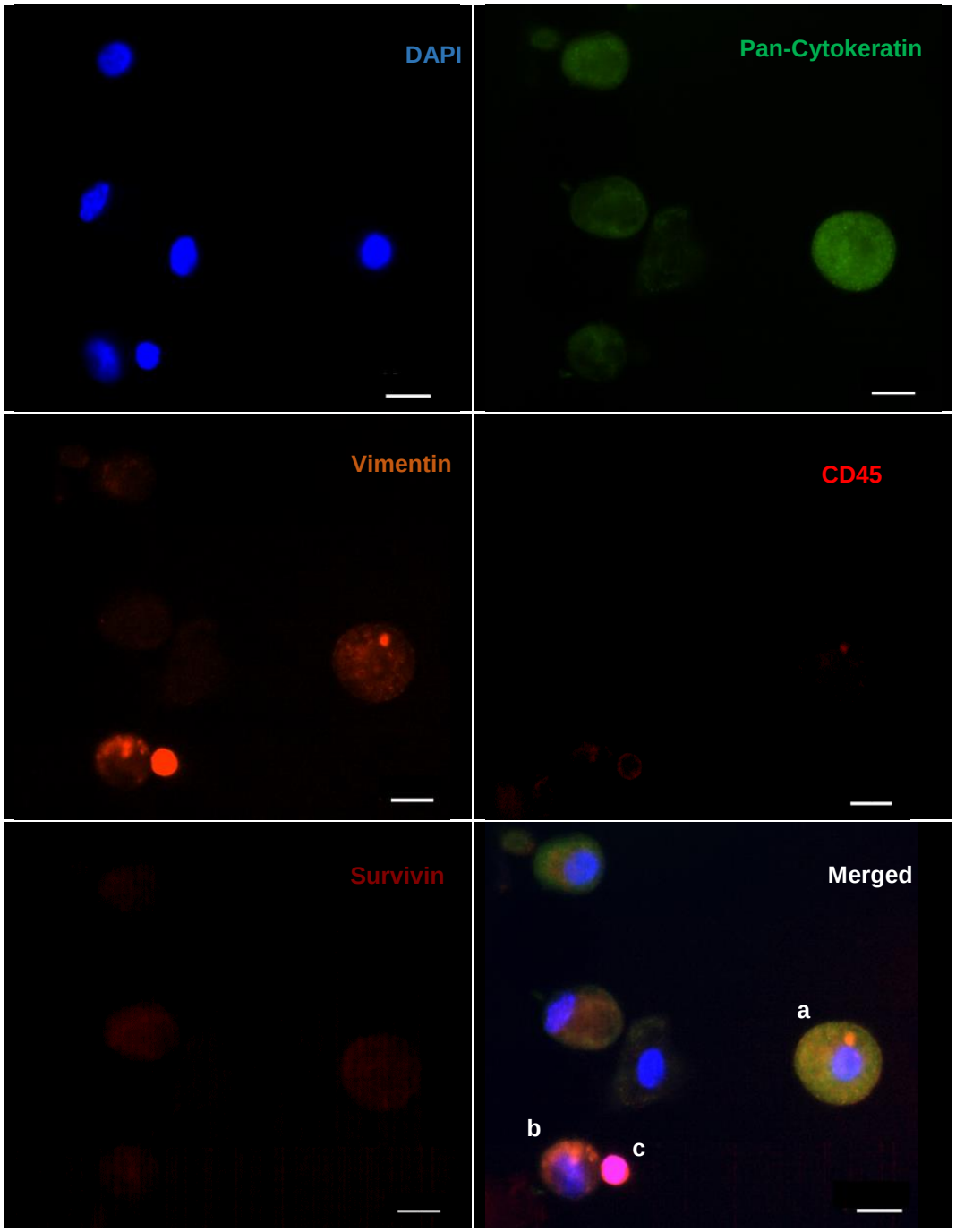

Figure 3.18. Cells present in the bladder wash of patient 6 expressing different phenotypes. Scale bar: 10 µm
A cell expressing high levels of pan-cytokeratin, vimentin and survivin is marked as (a). High vimentin expression is found on a pan-cytokeratin and survivin positive cell (b). Haematological cell expressing vimentin and CD45 is marked as (c) in the merged photomicrograph.

Although these cells are very similar in size, approximately 20 µm diameter, their biomarker expression levels are disparate: the cell on the right (a) for instance, has significant expression of both pan-cytokeratin and vimentin. On the other hand, one of the cells in the left (b) expresses relatively low levels of pan-cytokeratin while displaying significant vimentin expression as well as an irregular nucleus with small cytoplasm. Importantly, both cells were survivin positive, indicating that these are likely cancerous cells. In addition, a cell (c) with increased nucleus-to-cytoplasm ratio, no expression of

epithelial markers and an intense expression of vimentin could also be found. Its reduced size together with CD45 positivity and lack of survivin expression suggests that this cell is most likely a lymphocyte.

Contrarily to patient 6, analysis of microfluidic isolated cells from patient 1 was not so successful most likely due to the large amounts of debris present. Still, cells positive for pan-cytokeratin and vimentin expression were found (Figure 3.19). Nevertheless, vimentin expression in cells from patient 1 was lower than that detected in cells from patient 6, particularly in the case of multinucleated cells. No survivin positive cells were observed for patient 1, in contrast to patient 6. This difference may be related to the disease state of the patients or alternatively to sample processing conditions that were not ideal for this patient.

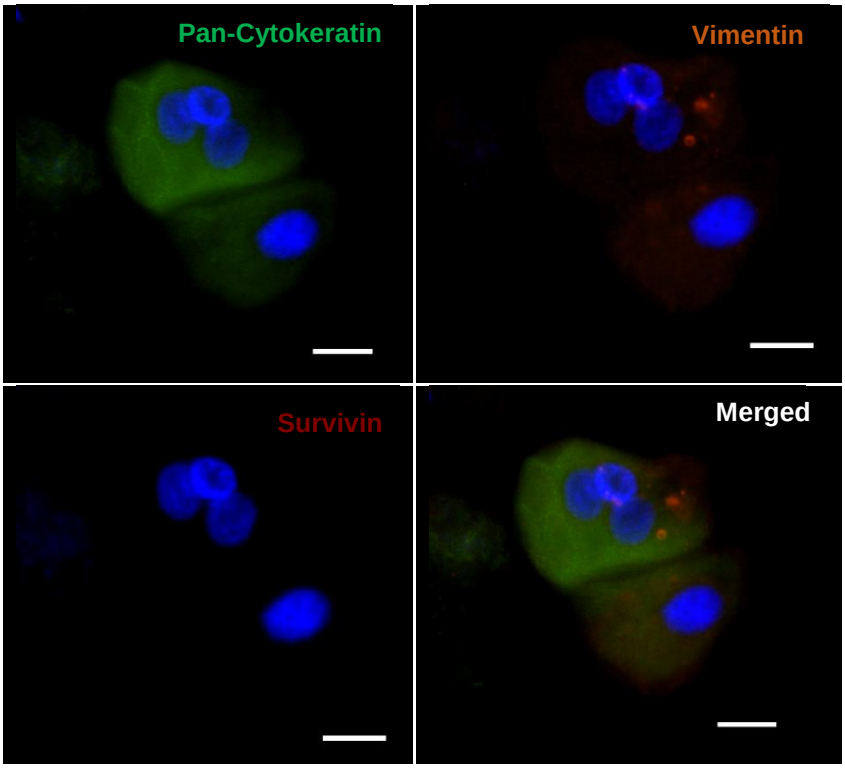

Figure 3.19. Potential cancer cell isolated from the bladder wash of patient 1. Scale bar: 10 μm

3.5.2. Urine analysis

Cell morphology in urine samples was remarkably similar to that of bladder wash samples, as observed in Figure 3.20.A. This was somehow expected since urine was collected though a catheter, thus cells present in the specimen should only be derived from the bladder. In voided urine though other cells from the ureter or urethra should also be present in the specimen[12]. The main difference observed between the two samples was the presence of larger cell debris in non-voided urine, possibly due to a long presence of urine in the bladder.

Figure 3.20.B illustrates cell heterogeneity found after urine processing of patient 6, which was equivalent to that of bladder wash samples (Figure 3.14).

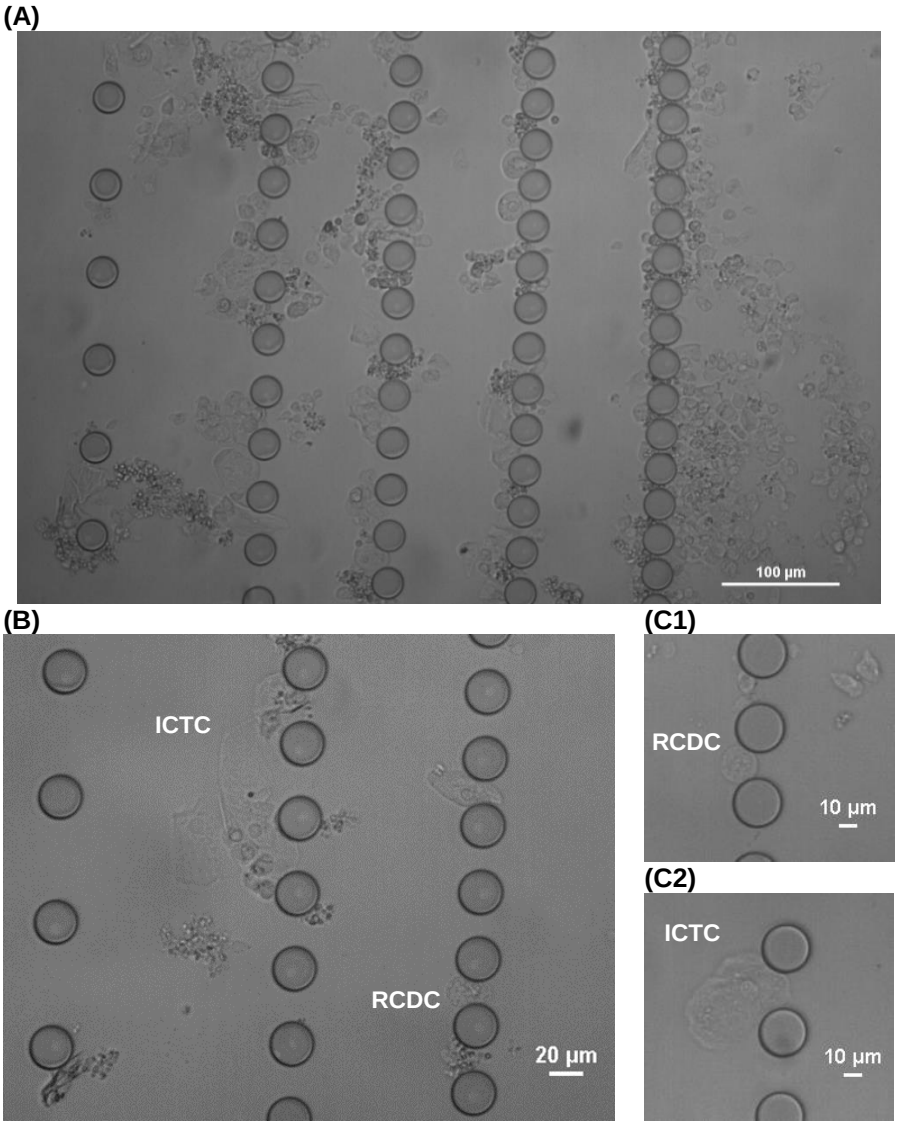

Figure 3.20. Different cell morphologies observed in the urine of patient 6.
(A) Representative image of one section of the microdevice **(B)** Distinct morphologies of cells isolated in the microfluidic system. **(C)** Focus on different morphologies and sizes of cells isolated in the 20 µm gap row of posts in the device. **(C1)** Circular cell with a regular shape and approximately 25 µm of diameter **(C2)** Cell with an irregular shape and large size, small nucleus-to-cytoplasm ratio and apparent high deformability. (ICTC – Irregular cells with translucent cytoplasm; RCDC – Round cells with dense cytoplasm; ICDC – Irregular cells with dense cytoplasm)

Interestingly, after 20 minutes of sample processing inside the device, cell distribution varied with cell characteristics (Figure 3.21), with large irregular cells and cell clusters being entrapped in the

20 µm posts and with the possibility of squeezing to the next row, while smaller cells with a greater nucleus-to-cytoplasm ratio were retained in the 4th row of posts (10 µm).

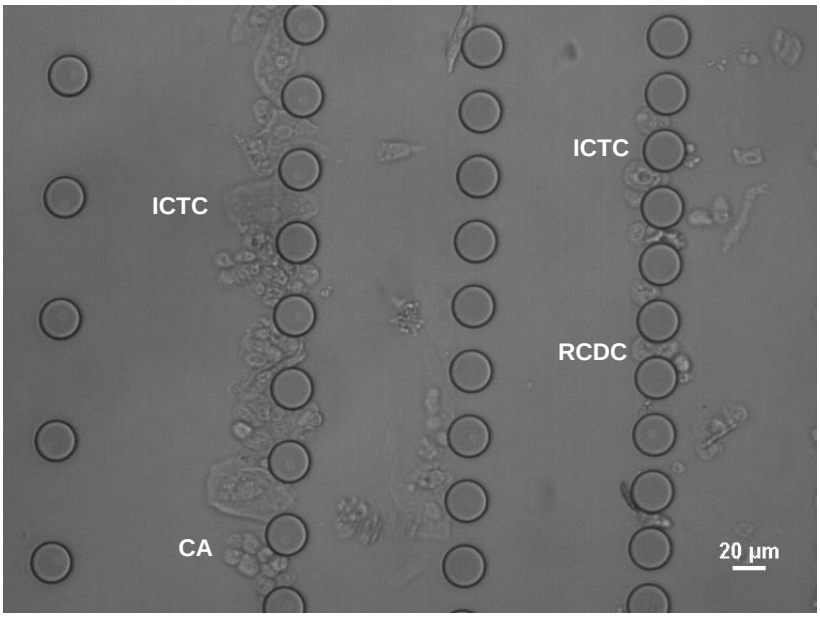

Figure 3.21. Isolation pattern of different cell morphologies after 20 minutes of urine processing in the device for patient 6.
(ICTC – Irregular cells with translucent cytoplasm; RCDC – Round cells with dense cytoplasm; ICDC – Irregular cells with dense cytoplasm; CA – Cell aggregates)

After phenotypically characterising isolated cells from bladder washes, the same approach was conducted for urine samples. Considering solely the expression of pan-cytokeratin (Figure 3.22), cells with an epithelial phenotype were found throughout the device, although when clustered they are predominantly located in the 50 and 20 µm gap rows. Conversely, the epithelial cells retained in the 10 and 5 µm gap rows are in single cell form.

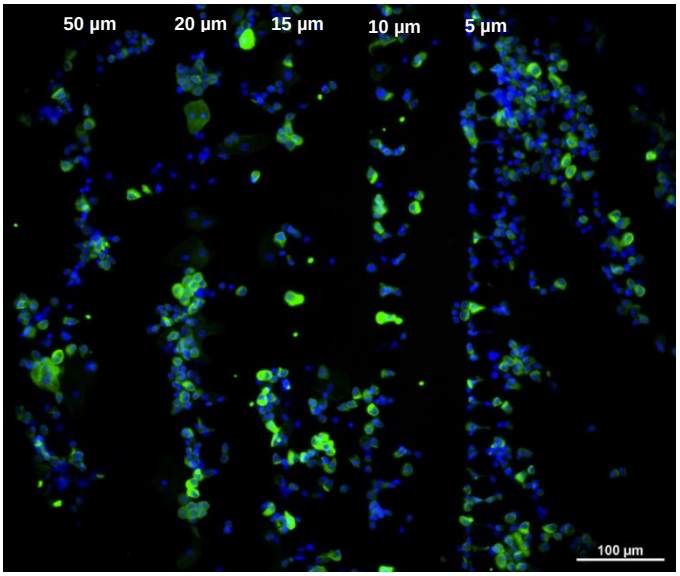

Figure 3.22. Pan-cytokeratin immunostaining of the processed urine of patient 6 on the microfluidic device.

A more detailed analysis at the single cell level revealed the presence of cell expressing pan-cytokeratin, vimentin and, remarkably, also survivin (Figure 3.23). Of note, this cell is also binucleated, similarly to another cell found in the bladder wash sample collected from this patient (Figure

3.17). This extraordinary finding shows that a correlation between data from bladder washes and urine can be established. More importantly, it demonstrates that cancer cells can be targeted in urine.

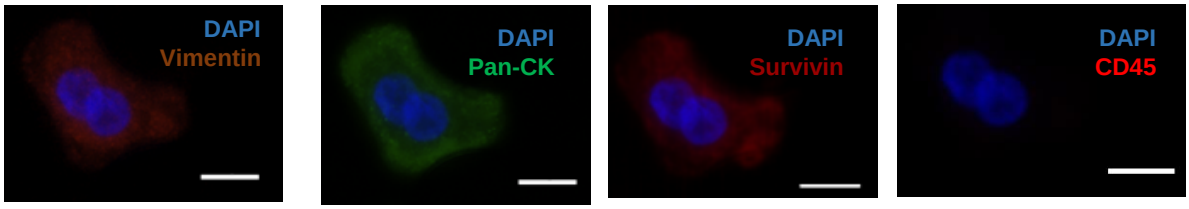

Figure 3.23. Photomicrograph of a survivin positive cell isolated in the urine of patient 6. Scale bar: 10 µm

In addition, cells with different characteristics were found in the same row of posts (Figure 3.24).

Survivin expression was obtained for some pan-cytokeratin^{+}, vimentin^{+} cells (Figure 3.24, merged panel, indicated as a). However, high survivin expression was also detected for some vimentin^{+}, CD45^{+} cells (Figure 3.24, merged panel, indicated as b). This is consistent with previous studies reporting survivin expression by haematological cells[27].

In some areas of the device single-cell isolation in height was not so successful, as evidenced in Figure 3.24, highlighting the need for critical evaluation of the data when interpreting results.

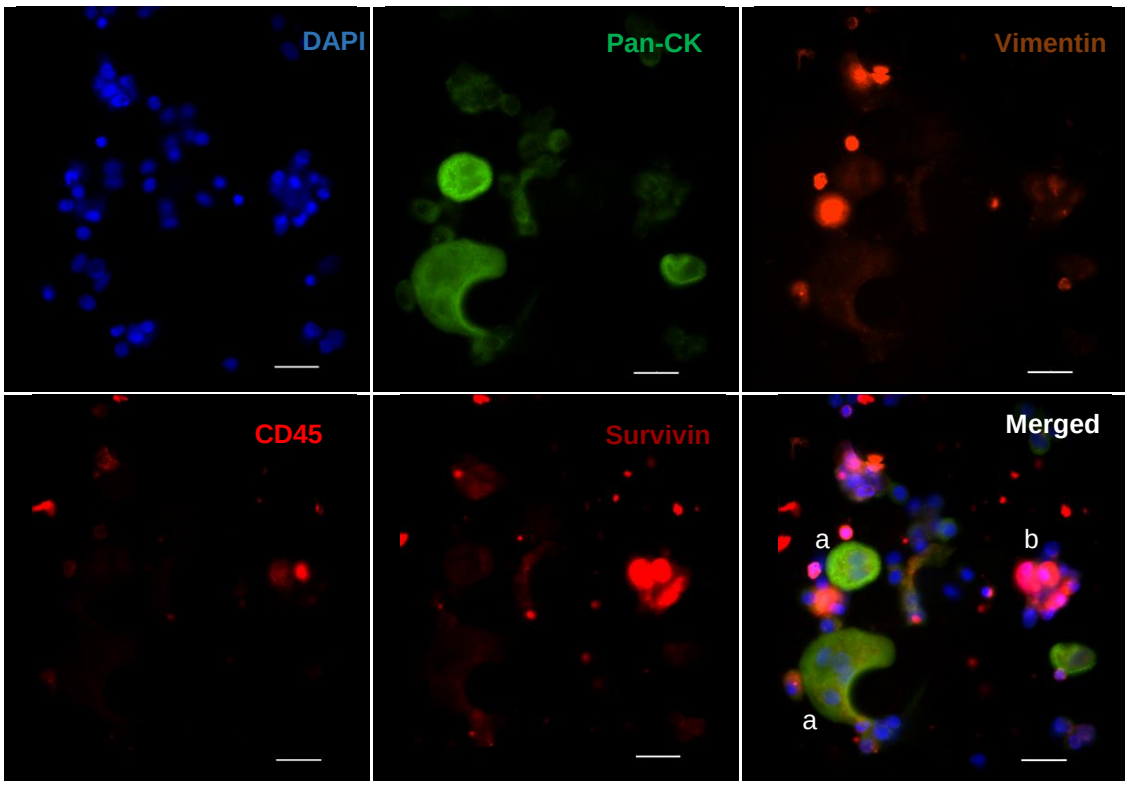

Figure 3.24. Different cell phenotypes present in the urine of patient 6. Scale bar: 20 µm
Cells expressing survivin, pan-cytokeratin and vimentin are marked as (a), representing cancerous cells present in urine. Haematological cells expressing survivin, vimentin and CD45 are marked as (b) in the merged photomicrograph.

When analysing the urine sample from patient 1, vast amounts of cellular debris were found (Figure 3.25), although at much lesser extent than its bladder wash counterpart (Figure 3.15). This was most likely due to the pre-processing protocol optimisation.

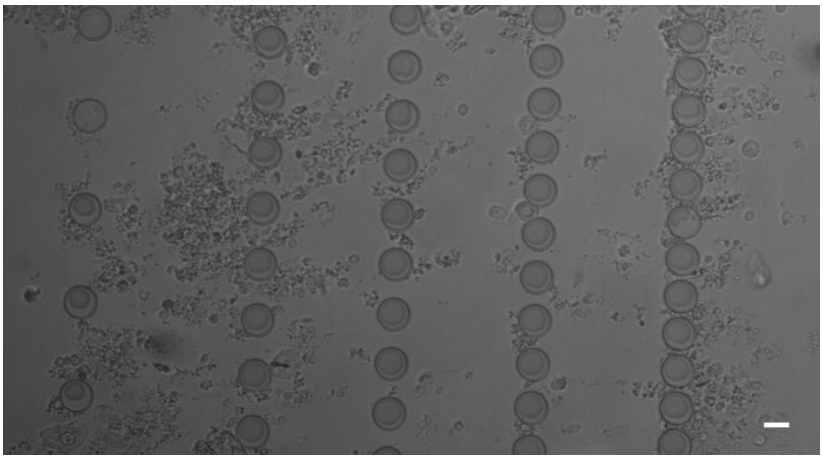

Figure 3.25. Cells isolated from the urine of patient 1 on the device. Scale bar: 20 µm.

In contrast to patient 6 samples, no significant vimentin expression was detected in samples from patient 1. Also, multinucleated cells were particularly checked for survivin expression, as previously found for patient 6. As shown in Figure 3.26, this binucleated cell exhibited high levels of pan-cytokeratin expression and no expression of vimentin or survivin.

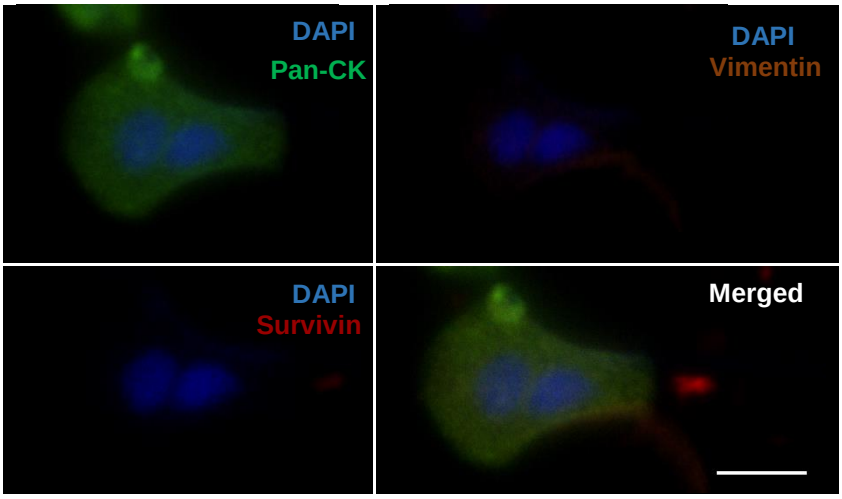

Figure 3.26. Multinucleated cell without vimentin or survivin expression isolated from the urine of patient 1. Scale bar: 10 µm.

This may be indicative of the presence of a superficial urothelial cell (umbrella cell) which possesses round and frequently multiple nuclei[12]. Still, further studies are required, ideally including additional markers and a larger patient cohort.

3.5.3. Pathology Results and Final Remarks

After sample processing and subsequent phenotypic analysis, the laboratory results were crosschecked with data kindly provided by the pathology unit of CHP-HSA. Table 3.3 summarises the main findings obtained for bladder washes and urine using the microfluidic platform as well as the pathology diagnostic.

Table 3.3. Demographic characteristics and biomarkers in bladder wash and urinary cells from patients with transitional cell bladder tumours in TURBT

Patient ID	Gender/Age	Pathology	Biomarkers					Result
			DAPI	Pan-CK	Vimentin	Survivin	CD45	
6	F/57	Stage Ta High-grade	+	+	-	-	-	Normal urothelial cell
			+	+	-	+	-	Epithelial cancer cell
			+	+	+	-	-	Cell in EMT
			+	+	+	+	-	Cancer cell in EMT
			+	-	+	-	-	Mesenchymal cell
			+	-	+	+	-	Mesenchymal cancer cell
			+	-	+	-	+	Haematologic cell
			+	-	+	+	+	Haematologic cell
1	M/78	Stage Ta Low-grade	+	+	-	-	-	Normal urothelial cell
			+	+	+	-	-	Cell in EMT
			+	-	+	-	+	Haematologic cell

F – Female
M – Male

According to the medical evaluation, both patients have non-invasive papillary carcinoma (stage Ta), however there are important differences among them that must be considered: Patient 6 has a high-grade tumour, which is usually poorly differentiated and indicative of a poor prognosis. On the other hand, patient 1 has a low-grade tumour, which has less risk of recurrence and invasiveness.

Taking into account the pathology report, this project provides some interesting results. The low number of vimentin$^+$ cells in patient 1 and of those, the reduced expression levels observed are consistent with low-grade tumours. In addition, these cells are highly differentiated, exhibiting an epithelial phenotype. Moreover, no detection of survivin may be related with the low-stage and low-grade of the tumour. Nonetheless, survivin expression in some cells cannot be ruled out, as only 30% of survivin signal is detected by the microscope used, due to technical constrains.

In contrast, for patient 6 distinct and varied cell phenotypes are observed. The patient samples were positive for survivin staining, indicating that those isolated cells are most likely malignant. This is further corroborated by the pathology report (patient 6: high-grade vs patient 1: low-grade) and by the disparate results observed for patient 1 (no survivin expression), which may be related to tumour aggressiveness. Furthermore, the expression of the different biomarkers analysed (pan-cytokeratin, vimentin and survivin) was higher in multinucleated cells. Also, pan-cytokeratin expression was lower in Vimentin$^+$ cells, as compared to pan-cytokeratin$^+$/vimentin$^-$ cells. This downregulation of epithelial

markers and concomitant expression of mesenchymal ones, indicates a possible epithelial-to-mesenchymal transition, a process associated with tumour progression. Likewise, it is interesting to note that, in this patient, vimentin^{+}/survivin^{+} cells lacking pan-cytokeratin expression were detected. These are typically mesenchymal-like cells which likely underwent EMT. Together, these observations are relevant and if further validated have an impact for therapeutic reasoning and patient follow-up.

In addition to the provided pathology results, which establish a diagnosis based on the immunohistochemical evaluation of the resected tumour, it would be interesting to compare our results with the bladder wash cytology performed at the hospital. Thus performing a direct comparison between the sensitivity achieved with the microfluidic platform and conventional cytology.

4. Conclusion and Future work

The goal of this thesis was to isolate and characterise rare cancer cells from body fluids of bladder cancer patients using a size-based microfluidic device. The microdevice previously designed by the group intends for cancer cell isolation based on cell size and deformability. Cancer cells are generally larger than their normal counterparts and those with higher metastatic potential are more deformable. Size-based isolation ensures that all cells are captured, independently of their phenotype. This is particularly relevant as tumour cells have been shown to exhibit distinct intermediate states in the epithelial-mesenchymal axis, which may likely correspond to a higher malignant phenotype and so be prognostically more relevant. Thus, it is crucial to identify different tumour cell subpopulations to better understand their biological and clinical significance.

Using HT1376 bladder cancer cell line as a model system, the performance of the microfluidic device in terms of cell isolation efficiency and enrichment ratio was investigated and found to be 50% and 22 in spiking experiments, respectively. This indicates that the platform is capable of retaining cells of interest in a heterogeneous sample. In addition, a panel of distinct biomarkers was evaluated and validated for adequate phenotypic characterisation of bladder cancer cells. For clinical sample analysis, improvement and optimisation of specimen pre-processing was necessary, given its complexity. Thus, the processed volume had to be reduced by half and a quantitative analysis of the trapped cells was hindered by the large amounts of debris present.

Nevertheless, interesting results were obtained. In one of the patients analysed (patient 6), cells expressing survivin concomitantly with epithelial and mesenchymal markers were retained by the microfluidic system, whereas for another patient (patient 1), survivin staining could not be detected and vimentin expression was negligible in most cells. Since samples were collected at the initial stage of the TURBT, correlation of microfluidic results and patient's clinical pathological data can be established. Both patients were diagnosed with non-muscle invasive papillary tumours. Interestingly however, patient 6 carcinoma was of high grade, and malignant cells with diverse phenotypes (only epithelial, only mesenchymal and both) were detected for this patient in the microfluidic device in both bladder wash and urine. On the other hand, patient 1 was diagnosed with low-grade carcinoma, and impressively the majority of the cells found were of epithelial-like. Further experiments with optimised sample pre-processing, large cohort of patients and additional biomarkers are necessary to validate these results.

Also, in future studies, normal human bladder urothelium cells or processed urine from healthy individuals should be used for a better mimicking of the sample and a more accurate characterisation. Analysis of specific mutations could also be performed *in situ* by FISH or after cell lysis to obtain DNA content. Recovery of isolated cells by reversing the flow or the creation of lateral channels for cell retrieval from independent rows would also be relevant for further functional characterisation of captured cells. Overall, these preliminary results are very exciting, with the proposed experiments contributing to a better understanding of the clinical significance of isolated cells and paving the way for early and non-invasive detection of bladder cancer using point-of-care microfluidic-based systems.

5. References

1. Cancer Research UK. Bladder cancer incidence statistics. at <http://www.cancerresearchuk.org/health-professional/cancer-statistics/statistics-by-cancer-type/bladder-cancer/incidence#heading-Eight>
2. Cancer of the Urinary Bladder - SEER Stat Fact Sheets. at <http://seer.cancer.gov/statfacts/html/urinb.html>
3. Bladder Cancer Staging: TNM Classification for Bladder Cancer. at <http://emedicine.medscape.com/article/2006834-overview>
4. Knowles, M. A. & Hurst, C. D. Molecular biology of bladder cancer: new insights into pathogenesis and clinical diversity. *Nat. Rev. Cancer* **15,** 25–41 (2014).
5. National Comprehensive Cancer Network. NCCN Guidelines Version 2.2014 for Bladder Cancer. (2014). at <https://www.nccn.org>
6. PDQ Adult Treatment Editorial Board. *Bladder Cancer Treatment (PDQ®): Patient Version*. *PDQ Cancer Information Summaries* (2002). at <http://www.ncbi.nlm.nih.gov/pubmed/26389479>
7. Mitra, A. P. Urine Cytologic Analysis : Special Techniques for Bladder Cancer Detection. *Connection* 169–177 (2010).
8. Lamm, D. L. & Torti, F. M. Bladder cancer, 1996. *CA. Cancer J. Clin.* **46,** 93–112
9. Diaz, L. A. *et al.* The molecular evolution of acquired resistance to targeted EGFR blockade in colorectal cancers. *Nature* **486,** 537–40 (2012).
10. Gerlinger, M. *et al.* Intratumor Heterogeneity and Branched Evolution Revealed by Multiregion Sequencing. *N. Engl. J. Med.* **366,** 883–892 (2012).
11. van der Meijden, A. *et al.* Significance of bladder biopsies in Ta,T1 bladder tumors: a report from the EORTC Genito-Urinary Tract Cancer Cooperative Group. EORTC-GU Group Superficial Bladder Committee. *Eur. Urol.* **35,** 267–71 (1999).
12. Sullivan, P. S., Chan, J. B., Levin, M. R. & Rao, J. Urine cytology and adjunct markers for detection and surveillance of bladder cancer. *Am. J. Transl. Res.* **2,** 412–40 (2010).
13. Flezar, M. S. Urine and bladder washing cytology for detection of urothelial carcinoma: standard test with new possibilities. *Radiol. Oncol.* **44,** 207–214 (2010).
14. Brock, G., Castellanos-Rizaldos, E., Hu, L., Coticchia, C. & Skog, J. Liquid biopsy for cancer screening, patient stratification and monitoring. *Transl. Cancer Res.* **4,** 280–290 (2015).
15. Smith, Z. L. & Guzzo, T. J. Urinary markers for bladder cancer. *F1000Prime Rep.* **5,** 21 (2013).
16. Greene, K. L., Berry, A. & Konety, B. R. Diagnostic Utility of the ImmunoCyt/uCyt+ Test in Bladder Cancer. *Rev. Urol.* **8,** 190–7 (2006).
17. Têtu, B., Tiguert, R., Harel, F. & Fradet, Y. ImmunoCyt/uCyt+ improves the sensitivity of urine cytology in patients followed for urothelial carcinoma. *Mod. Pathol.* **18,** 83–9 (2005).
18. Priolo, G. *et al.* Bladder tumor antigen assay as compared to voided urine cytology in the diagnosis of bladder cancer. *Clin. Chim. Acta* **305,** 47–53 (2001).
19. BTA stat Test (bladder cancer test). at <http://www.btastat.com/searchform.html>
20. Raitanen, M.-P. & Group, T. F. The role of BTA stat Test in follow-up of patients with bladder

cancer: results from FinnBladder studies. *World J. Urol.* **26,** 45–50 (2008).

21. Tritschler, S. *et al.* Validation of the Diagnostic Value of NMP22® BladderChek® Test as a Marker for Bladder Cancer by Photodynamic Diagnosis. *Eur. Urol.* **51,** 403–408 (2007).
22. Protocol, C. Fluorescence in situ hybridization. *Nat. Methods* **2,** 237–238 (2005).
23. Placer, J., Espinet, B., Salido, M., Solé, F. & Gelabert-Mas, A. Clinical Utility of a Multiprobe FISH Assay in Voided Urine Specimens for the Detection of Bladder Cancer and its Recurrences, Compared with Urinary Cytology. *Eur. Urol.* **42,** 547–552 (2002).
24. Schlomer, B. J., Ho, R., Sagalowsky, A., Ashfaq, R. & Lotan, Y. Prospective validation of the clinical usefulness of reflex fluorescence in situ hybridization assay in patients with atypical cytology for the detection of urothelial carcinoma of the bladder. *J. Urol.* **183,** 62–7 (2010).
25. Kirkali, Z. *et al.* Bladder cancer: Epidemiology, staging and grading, and diagnosis. *Urology* **66,** 4–34 (2005).
26. Chen, Y., Tu, J. J., Kao, J., Zhou, X. K. & Chen, Y.-T. Survivin as a useful adjunct marker for the grading of papillary urothelial carcinoma. *Arch. Pathol. Lab. Med.* **132,** 224–31 (2008).
27. Margulis, V., Lotan, Y. & Shariat, S. F. Survivin: a promising biomarker for detection and prognosis of bladder cancer. *World J. Urol.* **26,** 59–65 (2008).
28. Moussa, O. *et al.* Evaluation of survivin reverse transcriptase-polymerase chain reaction for noninvasive detection of bladder cancer. *J. Urol.* **175,** 2312–6 (2006).
29. Shariat, S. F. *et al.* Urine detection of survivin is a sensitive marker for the noninvasive diagnosis of bladder cancer. *J. Urol.* **171,** 626–30 (2004).
30. Gradilone, A. *et al.* Prognostic significance of survivin-expressing circulating tumour cells in T1G3 bladder cancer. *BJU Int.* **106,** 710–5 (2010).
31. Lamouille, S., Xu, J. & Derynck, R. Molecular mechanisms of epithelial-mesenchymal transition. *Nat. Rev. Mol. Cell Biol.* **15,** 178–96 (2014).
32. Plaks, V., Kong, N. & Werb, Z. The cancer stem cell niche: how essential is the niche in regulating stemness of tumor cells? *Cell Stem Cell* **16,** 225–38 (2015).
33. Yu, Z., Pestell, T. G., Lisanti, M. P. & Pestell, R. G. Cancer stem cells. *Int. J. Biochem. Cell Biol.* **44,** 2144–2151 (2012).
34. Craene, B. De & Berx, G. Regulatory networks defining EMT during cancer initiation and progression. *Nat. Rev. Cancer* **13,** 97–110 (2013).
35. Liu, C.-Y., Lin, H.-H., Tang, M.-J. & Wang, Y.-K. Vimentin contributes to epithelial-mesenchymal transition cancer cell mechanics by mediating cytoskeletal organization and focal adhesion maturation. *Oncotarget* **6,** 15966–83 (2015).
36. Mendez, M. G., Kojima, S.-I. & Goldman, R. D. Vimentin induces changes in cell shape, motility, and adhesion during the epithelial to mesenchymal transition. *FASEB J.* **24,** 1838–51 (2010).
37. Baumgart, E. *et al.* Identification and prognostic significance of an epithelial-mesenchymal transition expression profile in human bladder tumors. *Clin. Cancer Res.* **13,** 1685–94 (2007).
38. Franzen, C. A. *et al.* Urothelial cells undergo epithelial-to-mesenchymal transition after exposure to muscle invasive bladder cancer exosomes. *Oncogenesis* **4,** e163 (2015).
39. Andersson, E., Dahmcke, C., Steven, K., Larsen, L. & Guldberg, P. Filtration Device for On-Site

Collection, Storage and Shipment of Cells from Urine and Its Application to DNA-Based Detection of Bladder Cancer. *PLoS One* **10,** 15 (2015).

40. Sackmann, E. K., Fulton, A. L. & Beebe, D. J. The present and future role of microfluidics in biomedical research. *Nature* **507,** 181–9 (2014).
41. Stott, S. L. *et al.* Isolation of circulating tumor cells using a microvortex-generating herringbone-chip. *Proc. Natl. Acad. Sci. U. S. A.* **107,** 18392–7 (2010).
42. Mohamed, H., Murray, M., Turner, J. N. & Caggana, M. Isolation of tumor cells using size and deformation. *J. Chromatogr. A* **1216,** 8289–8295 (2009).
43. Tan, S. J., Yobas, L., Lee, G. Y. H., Ong, C. N. & Lim, C. T. Microdevice for the isolation and enumeration of cancer cells from blood. *Biomed. Microdevices* **11,** 883–892 (2009).
44. Campo, A. del *et al.* SU-8: a photoresist for high-aspect-ratio and 3D submicron lithography. *J. Micromechanics Microengineering* **17,** R81–R95 (2007).
45. Bhushan, B. *Springer Handbook of Nanotechnology*. (Springer Berlin Heidelberg, 2010). doi:10.1007/978-3-642-02525-9
46. Glass, N. R., Tjeung, R., Chan, P., Yeo, L. Y. & Friend, J. R. Organosilane deposition for microfluidic applications. *Biomicrofluidics* **5,** 36501–365017 (2011).
47. Mazutis, L. *et al.* Single-cell analysis and sorting using droplet-based microfluidics. *Nat. Protoc.* **8,** 870–891 (2013).
48. Xiong, L., Chen, P. & Zhou, Q. Adhesion promotion between PDMS and glass by oxygen plasma pre-treatment. *J. Adhes. Sci. Technol.* **28,** 1046–1054 (2014).
49. Murphy, D. B. & Davidson, M. W. *Fundamentals of Light Microscopy and Electronic Imaging*. (John Wiley & Sons, Inc., 2012). doi:10.1002/9781118382905
50. Semrock. Transmission profile of the BrightLine® Sedat filter set, optimised for DAPI, FITC, TRITC, Cy5 & Cy7 and other like fluorophores. at <https://www.semrock.com/SetDetails.aspx?id=2931>
51. Mescher, A. L. *Junqueiras's Basic Histology Text and Atlas*. (McGraw-Hill Education, 2013).
52. Wang, S. Y., Mak, K. L., Chen, L. Y., Chou, M. P. & Ho, C. K. Heterogeneity of human blood monocyte: two subpopulations with different sizes, phenotypes and functions. *Immunology* **77,** 298–303 (1992).
53. Covey, T. M. *et al.* Single cell network profiling assay in bladder cancer. *Cytom. Part A* **83 A,** 386–395 (2013).
54. Krajcovic, M. *et al.* A non-genetic route to aneuploidy in human cancers. *Nat. Cell Biol.* **13,** 324–330 (2011).

Appendix

A. Control experiments data

Table A 1. Number of HT1376 bladder cancer cells retained in the microfluidic platform for the tested inlet pressure differentials (mbar).

	Inlet pressure	
Experiment	**200 mbar**	**300 mbar**
#1	373	143
#2	457	19
#3	251	213
#4	404	290

Table A 2. Number of PBMCs retained in the microfluidic platform for the tested inlet pressure differentials (mbar).

	Inlet pressure	
Experiment	**200 mbar**	**300 mbar**
#1	454	56
#2	367	72
#3	343	78

Table A 3. Number of HT1376 bladder cancer cells and PBMCs retained in the microfluidic platform for spiking experiments at 200 mbar inlet pressure.

	Cell type	
Experiment	**HT1376**	**PBMCs**
#1	595	221
#2	401	122
#3	503	848

B. Clinical Sample processing photomicrographs

Patient 2

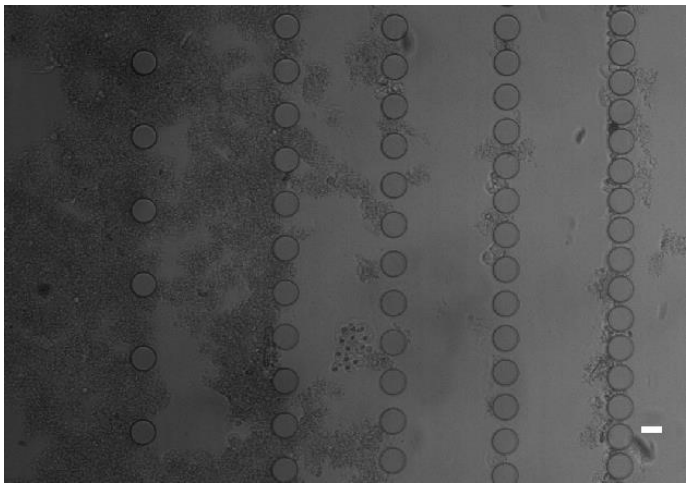

Figure.A 1. Bladder wash processing of patient 2 with visible extent of debris and presence of apparent papillary tumours. Scale bar: 20 μm

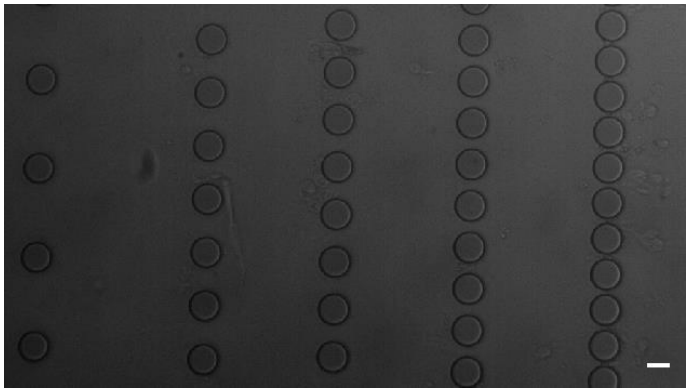

Figure.A 2. Urine sample processed for patient 2. Cell clusters are isolated on the 15 μm gap rows. Scale bar: 20 μm

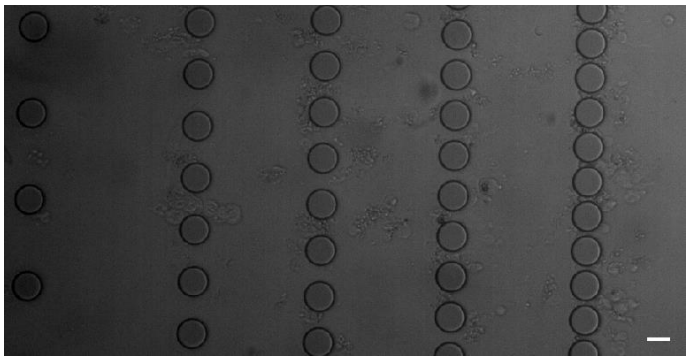

Figure.A 3. Different section of the processed urine device of patient 2. Larger extent of debris is visible, along with the isolation of cell clusters in the 20 µm gap row. Scale bar: 20 µm

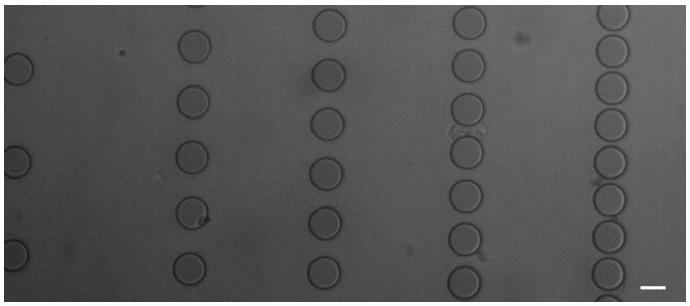

Figure.A 4.Single cell isolated in one region of the processed urine device of patient 2. Scale bar: 20 µm

Patient 3

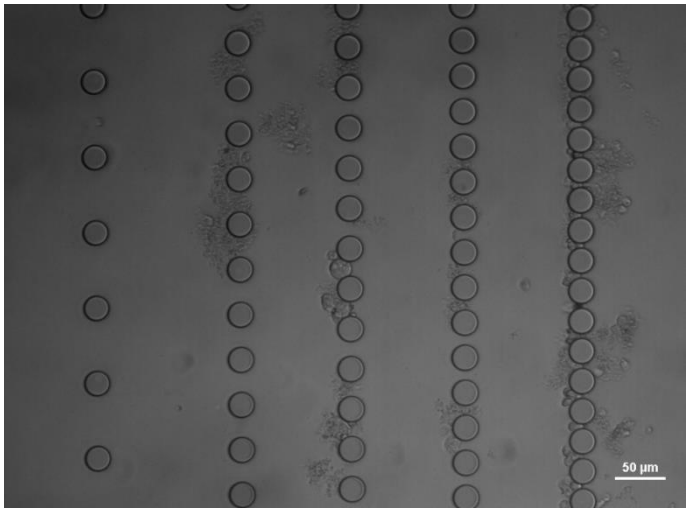

Figure.A 5. Representative image of one section of the processed bladder wash device of patient 3. Single cells with approximately 20-25 µm are isolated in the 15 µm gap rows. Scale bar: 20 µm

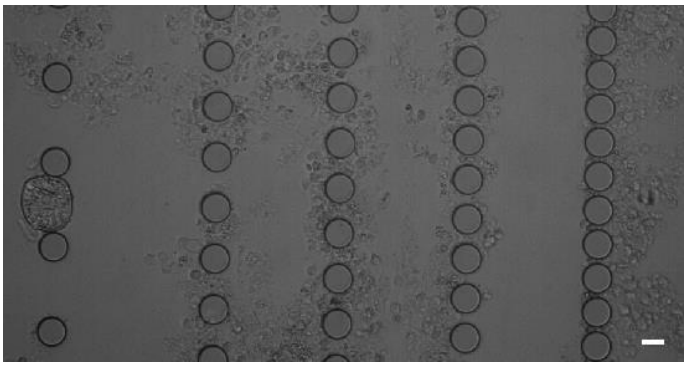

Figure.A 6. Section of the processed urine device of patient 3. Apparent cell is retained in the 50 µm gap row. The device presents an elevated extent of debris. Scale bar: 20 µm

Patient 4

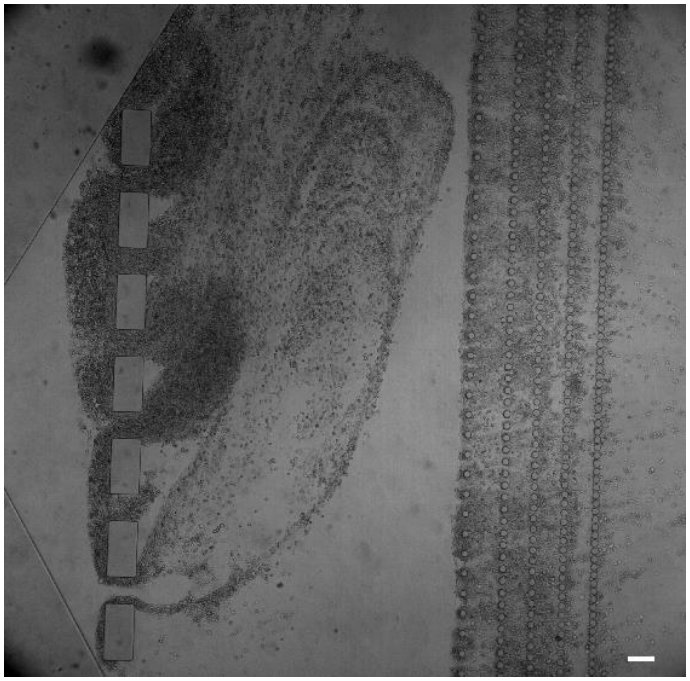

Figure.A 7. Representative image of one section of the bladder wash device of patient 4. Elevated cell number is retained in the system, which is responsible for post obstruction. At this point, TryPLE reagent was added. Scale bar: 100 µm

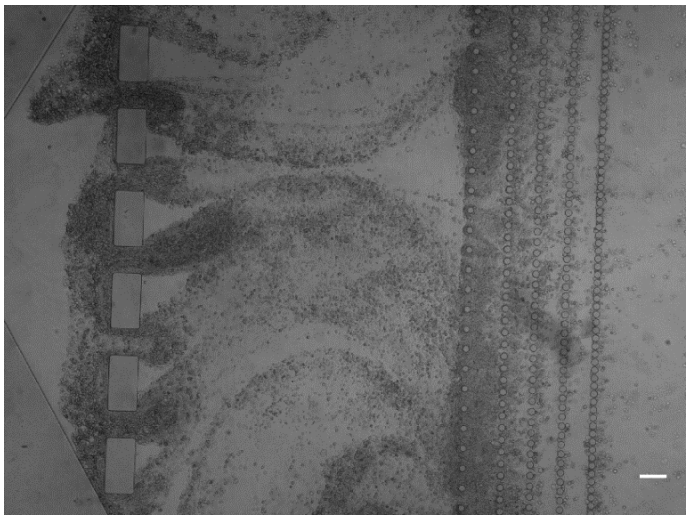

Figure.A 8. Behaviour of retained cells in the bladder wash device of patient 4 after TryPLE reagent actuation and washing. Scale bar: 100 µm

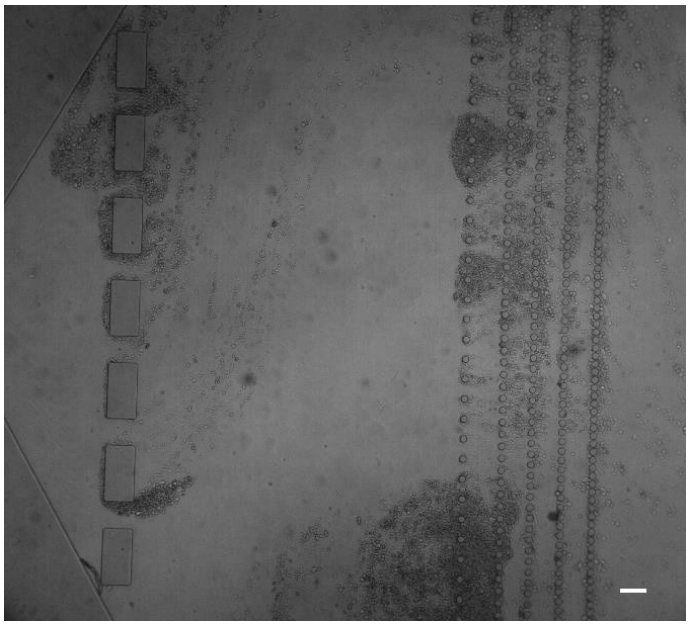

Figure.A 9. Different region of the bladder wash device of patient 6 after TryPLE reagent actuation. Scale bar: 100 µm

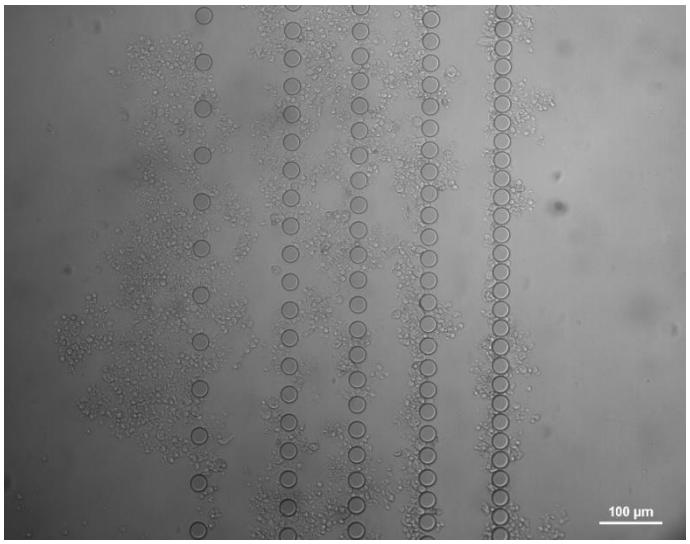

Figure.A 10. Processed urine device of patient 4 with visible obstruction of the microposts and aggregate formation. Sample processing had to be interrupted.

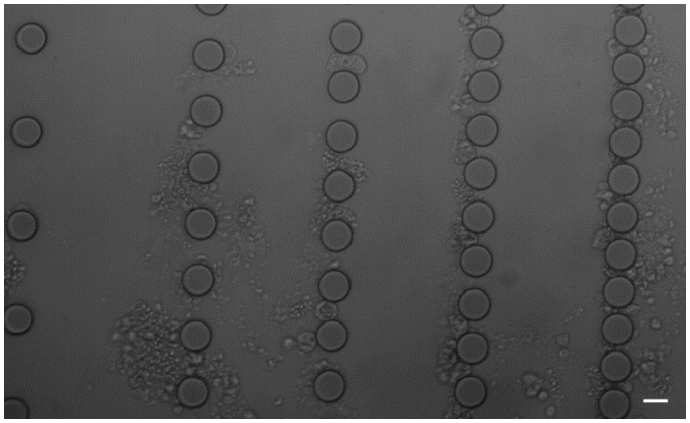

Figure.A 11. Representative image of one section of the new urine device of patient 4 after the adjustment of the sample pre-processing protocol. Scale bar: 20 µm

Patient 5

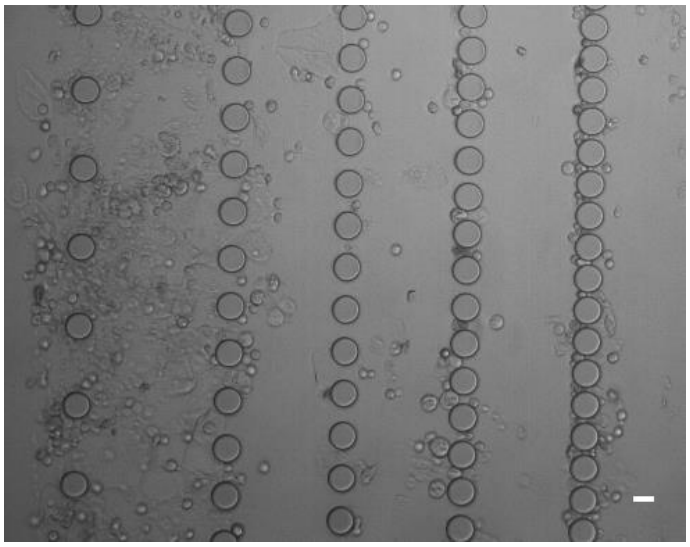

Figure.A 12. Bladder Wash device of patient 5. Different cell morphologies are clearly isolated by the system. Scale bar: 20 µm

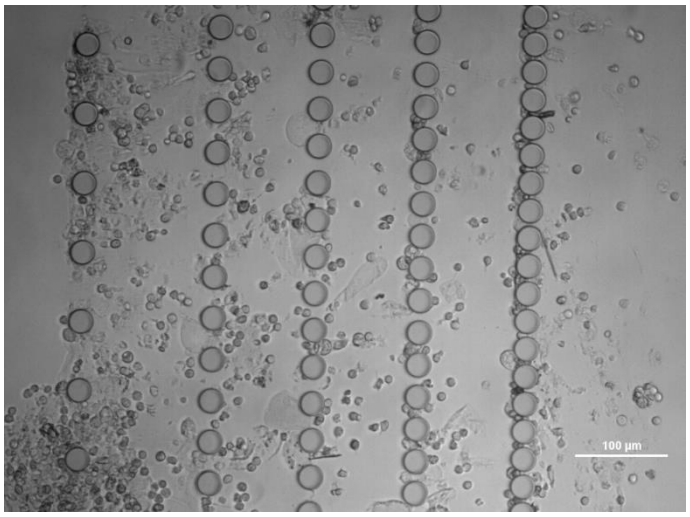

Figure.A 13. Different section of the bladder wash device of patient 5. Visible existence of large potential cancer cells and elevated cell number. Scale bar: 100 µm

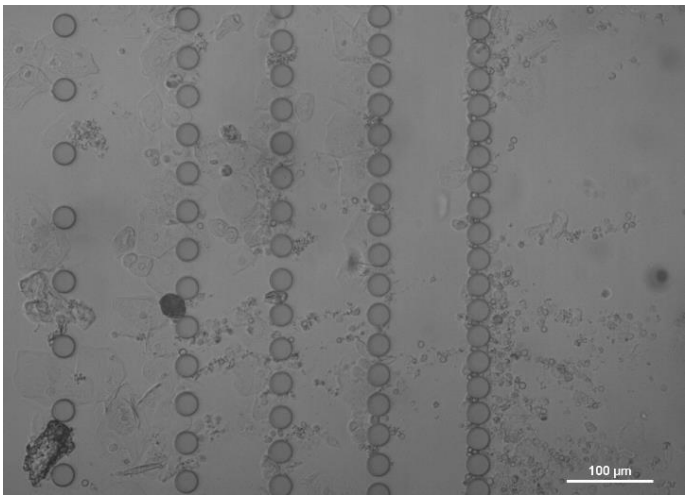

Figure.A 14. Urine device of patient 5. The system has able to isolate cells with different morphologies and in an elevated cell number without clogging of the device. Scale bar: 100 µm